Improvement of Winter Oilseed Rape Resistance to *Verticillium longisporum*

– Assessment of Field Resistance and Characterization of Ultrastructural Plant Responses

Dissertation

zur Erlangung des Doktorgrades

der Fakultät für Agrarwissenschaften

der Georg-August-Universität Göttingen

vorgelegt von

Jessica Knüfer

geboren in Wiesbaden

Göttingen, Juli 2011

D 7

1. Referent: Prof. Dr. Andreas von Tiedemann

2. Korreferent: Prof. Dr. Petr. Karlovsky

Tag der mündlichen Prüfung: 21. Juli 2011

Contents

1. General Introduction

1.1 Oilseed rape

Winter oilseed rape (OSR) is the main crop cultivated in Germany, with cultivation areas of 1.47 M ha in 2010 (Eurostat, 2011). For additional information about winter OSR cultivation, including the plant protection practice, the reader is referred to Friedt and Christen (2007).The rapidly increasing demand of oil from winter OSR has led to a marked increase of production areas. Oil of winter OSR is used in the food industry as well as in other industries where it finds applications in hydraulic oils or as biodiesel fuel (Heale and Karapapa, 1999). The increased demand for winter OSR and the resulting increase in cultivation area are accompanied by a foreshortening of crop rotations. These short crop rotations can cause phytosanitary problems by promoting the spread of fungal diseases. Apart from *Sclerotinia sclerotiorum*, causing stem rot, and *Phoma lingam* (anamorph of *Leptosphaeria maculans*), which is the causal agent of stem canker and blackleg, *Verticillium longisporum* is one of the major diseases of OSR.

1.2 *Verticillium longisporum*

Verticillium species are soil-borne vascular plant pathogens with a wide host range of more than 200 plant species, including tomato, potato, eggplant, cotton and OSR as well as important tree crops such as olive, pistachio and avocado (Fravel and Larkin, 1997). The species *V. longisporum* differs from other *Verticillium* species by not causing wilt symptoms but, rather, inducing premature ripening (Hornig, 1987). In contrast to *S. sclerotiorum* and *P. lingam*, which mainly cause infection by penetration of plant tissues above the soil surface, *V. longisporum* infects the rapeseed plants via the roots and is therefore referred to as soil-borne. Although *V. longisporum* is widely acknowledged as an independent species, there is a persisting controversy of the evolutionary origin of *V. longisporum* and its discrimination from *V. dahliae*. The existence of *Verticillium* isolates on crucifers different from *V. dahliae* was first reported by Stark (1961), who isolated a *V. dahliae* strain from horseradish with significantly longer conidia and accordingly denominated the isolates *Verticillium dahliae* var. *longisporum*. Karapapa *et al*. (1997) intensively investigated the long-spored isolates and compared them to short-spored isolates. Ample evidence based on differences concerning morphological features such as conidia size, shape of microsclerotia (or microsclerotia appearance) and phialide organization, differences on the molecular level such as enzyme properties, phylogenetic variations and differences in genome size (1.75 fold increase in nuclear DNA content of long spored isolates), as well as in the degree of pathogenicity led to

the proposition of the new species *V. longisporum* comb. nov. With respect to the taxonomic classification, Karapapa *et al*. (1997) proposed that the `near diploid` *V. longisporum* species is a hybrid originating from parasexual hybridization of *V.albo-atrum* and *V. dahliae*. This classification has been controversially discussed in the successive years. While some concurred with this classification (Zeise and Tiedemann, 2001, 2002 a, Fahleson *et al*., 2004), others challenged this argumentation and continued to use the name *V. dahliae* var. *longisporum* (Collins *et al*., 2003). Several investigations revealed that long-spored isolates are isolated almost exclusively from cruciferous plants (Zeise and Tiedemann, 2001, Collins *et al*., 2003). Based on randomly amplified polymorphic DNA (RAPD)-PCR of different *Verticillium* isolates, long-spored isolates were grouped into the two distinct classes lsp and lsp* (Zeise and Tiedemann, 2002b). Complementary data from amplified fragment length polymorphisms (AFLP) revealed two similar groups, termed α and β (Collins et al., 2003; Barbara and Clewes, 2003). Additional studies suggested *V. longisporum* to be an amphihaploid interspecific hybrid between a *V. dahliae*-like and an unknown species (Clewes *et al*., 2008). Quite recently Inderbitzin *et al*. (2011) presented a detailed study of the evolutionary origin of *V. longisporum*. In an extensive study of a total of 203 *V. longisporum*, *V. dahliae*, *V. albo-atrum* and related species the authors show that (a) *V. longisporum* is a diploid species and (b) evolution of this hybrid proceeded along four different lineages: According to the authors, the common ancestor of all hybrids, A1 (unknown taxon), formed a hybrid with either of the species D1 (unknown taxon), D2 (*V*. *dahliae*) or D3 (*V. dahliae*). This thorough study based on analysis of seven nuclear loci helps to understand the phylogenetic relationship among closely related *Verticillium* species. Building on these results, further research is needed to provide information about the pathogenicity of the investigated isolates and to discover potential relationships between aggressiveness and geographic origin of the *V. longisporum* lineages.

1.3 Life cycle of *V. longisporum*

A characteristic of *V. longisporum* and other *Verticillium* species such *as V. dahliae* and *V. albo-atrum* is a change in life style during the life cycle of the fungus. Dependent on the environmental conditions, *V. longisporum* can be in a dormant, parasitic or saprophytic phase (Eynck, 2008; Gao *et al*., 2010). In the dormant phase the fungus produces resting structures, called microsclerotia, which are melanized aggregates of swollen hyphae. Microsclerotia have a survival time of more than 10 years and can therefore cause a long lasting contamination of the soil (Heale and Karapapa, 1999). Microsclerotia start to germinate when attracted by root exudates of the plant (Schnathorst, 1981). Previous studies

have demonstrated that microsclerotia can be stimulated not only by host, but also by non-host exudates (Schnathorst, 1981; Mol and Riessen, 1995; Gödecke, 2007). Exudates released by root cells diffuse into the rhizosphere, which results in an exudate gradient (Olsson and Nordbring-Hertz, 1985). This gradient induces the movement of hyphae towards the root and the parasitic phase of the fungus is initialized by a direct penetration of the root epidermal cells (Zhou *et al*., 2006; Eynck *et al*., 2007). During the penetration process it has never been observed that hyphae formed appressoria-like structures. Entering of epidermal cells rather occurred by formation of slight swellings in the hyphal tip and formation of a thin penetration peg. Crossing of the root cortex was observed to occur intra- and intercellularly before xylem vessels were colonized (Eynck *et al*., 2007). In the vascular system, systemic spread occurs in the central root cylinder and in the vascular bundles of the stem. During this phase a new generation of conidia is produced. With the beginning of plant senescence, the pathogen leaves the xylem vessels and enters the parenchymatic cells. This transition designates the saprophytic phase of the fungal life cycle and leads to the formation of microsclerotia. In the field, first symptoms of the disease occur relatively late with the beginning of plant ripening. Early symptoms can be discolorations of stems, such as one-sided brownish stripes along the stem and, later on, microsclerotia become visible beneath the epidermis, in the pith and also in the root tissue (Figure 1.1). *V. longisporum* infection is further accompanied by premature ripening, but unlike in other *Verticillium* diseases wilt symptoms are not observed. After decomposition of plant material microsclerotia are released into the soil.

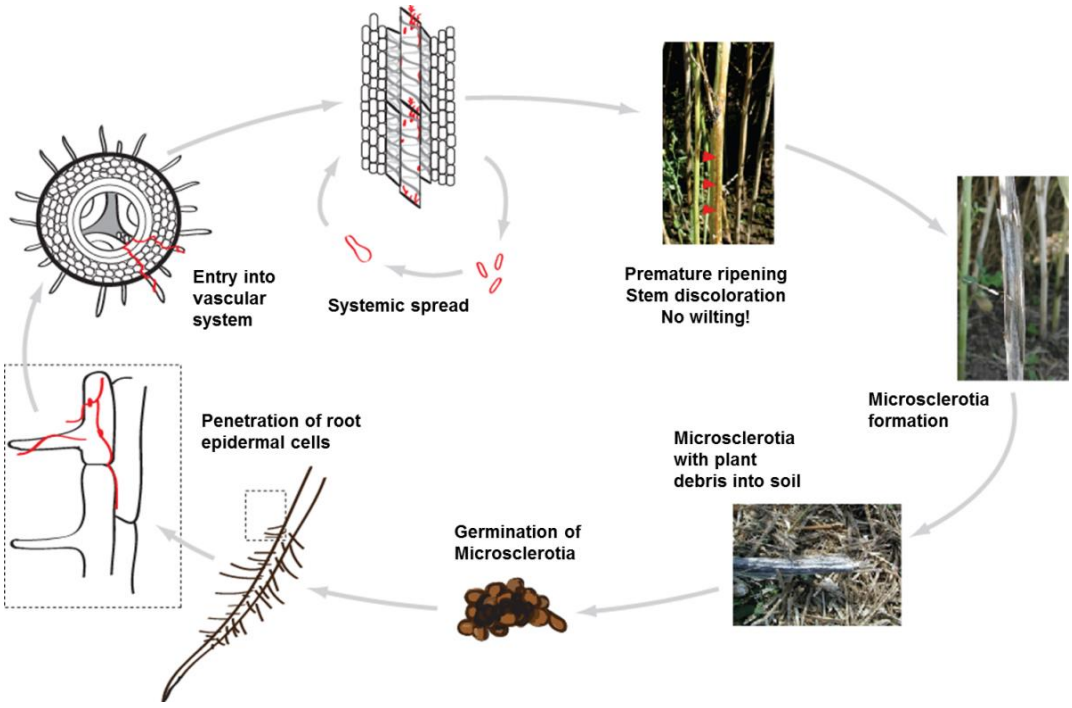

Figure 1.1 Life cycle of *V. longisporum*

1.4 Aim of the thesis

Winter oilseed rape is the most important oil crop in Europe. The intensified cultivation of winter OSR, together with the favorable climatic conditions have rendered *V. longisporum* a major threat to OSR production in Northern Europe. At present, infestation of OSR with *V. longisporum* is difficult to control owing to the absence of efficient fungicides. As a consequence the breeding of resistant cultivars remains of central importance to secure agronomic performance of OSR and forestall further spread of the disease. In a collaborative effort with the Institute of Plant Breeding of the Justus-Liebig-University Gießen and the German Federation of Private Plant Breeders (GFP), one objective of the present thesis was the identification of *B. napus* accessions with improved resistance against *V. longisporum* by phenotypisation in the greenhouse (chapter 2).

A robust screening for resistance needs to consider the unique environmental conditions that winter OSR is exposed to in the field. This thesis aims to complement the currently used screening methods for field experiments with a sensitive diagnostic method for evaluation of disease severity that permits the early-stage detection of the pathogen in plant tissue and supports a robust and accurate classification with respect to resistance levels (chapter 3).

Since breeding of resistant cultivars currently is the most promising option to control the disease, a detailed understanding of the plant-pathogen interaction is of prime importance to support the breeding efforts. Another objective of the present work therefore were histological investigations of infected plant tissue with the aim to characterize, on an ultrastructural level, the resistance structures induced upon infection with *V. longisporum*. Based on investigations of resistant and susceptible OSR genotypes, the hypocotyl part was previously identified as an important tissue in this pathosystem (Eynck, 2008). Using transmission electron microscopy, our studies seek to identify characteristic differences of structures involved in mediating pathogen resistance in the vascular tissue of the hypocotyl (chapter 4).

Previous studies suggested that OSR responds to pathogen invasion with the formation of vascular occlusions (Eynck, 2008). Since the physical restriction of fungal structures by occluded vessel elements will likely also affect water transport in the plant, resistant plants may be more sensitive to environmental and climatic conditions that induce limited water supply. This work therefore aims at a systematic comparison of the effects of *V. longisporum* infection and simultaneous water shortage on the performance of resistant and susceptible genotypes in terms of disease parameters, physiological status and agronomic traits (chapter 5).

2. Evaluation of winter oilseed rape resistance to *V. longisporum* under greenhouse and field conditions

2.1 Introduction

Verticillium longisporum is a soil-borne fungal pathogen causing premature ripening on oilseed rape (Hornig, 1986). An increase in areas with oilseed rape (OSR) cultivation and relatively short crop rotation cycles has intensified the importance of the disease in Europe. The disease is especially prominent in Sweden (Steventon *et al.*, 2002) and in other Northern European countries. Areas with a disease incidence above 60% together with favorable climatic conditions represent a significant yield damage potential (Dunker *et al.*, 2008). The resting structures of *V. longisporum*, the microsclerotia, can remain in the soil for several years and lead to long-term contamination of the soil (Heale and Karapapa, 1999). Since there are no fungicides available until today (Dunker et al, 2008) breeding for resistance remains a major goal in minimizing the disease. Resistance to *Verticillium* spp. is not expressed in complete immunity. Rather, the level of symptom expression defines the level of resistance, since also cultivars with high resistance are at least partially colonized by the pathogen (Pegg and Brady, 2002; Eynck *et al*., 2009).

Sources of resistance to *V. longisporum* have been found in *B. oleracea* and *B. rapa* genotypes (Happstadius *et al*., 2003; Dixelius *et al*. 2005). In recent studies improvement of *B. napus* resistance was achieved by breeding resynthesized (RS) lines generated from hybridization of resistant zero erucic acid *B. oleracea* genotypes with *B. rapa* lines (Rygulla et al, 2007a). For the development of molecular markers, resistant RS-lines are combined with elite high oleic acid content OSR cultivars to generate a segregating population of double haploid (DH) lines (Rygulla, 2008). First quantitative trait loci (QTL) for resistance to *V. longisporum* have been identified in a population of double haploid (DH) lines (Rygulla *et al*., 2008). Within the framework of this current project, continuing efforts aim at the development and improvement of molecular markers for breeding of resistant cultivars.

Here, we evaluate the resistance level of *B. napus* accessions based on greenhouse assays over the years 2004 until 2009 and investigate selected accessions under field conditions at different locations in an attempt to compare greenhouse and field data.

2.2 Material and Methods

2.2.1 Plant material for greenhouse trials

A greenhouse screening for evaluation of *B. napus* resistance to *V. longisporum* was established at the University of Göttingen in 2004 (Eynck, 2008). To date, a total of roughly 1500 accessions (breeding lines) of *B. napus* supplied by eight plant breeding companies have been tested from 2004 to 2009. Collaborating breeding companies have been Dr. h.c. CARSTEN Pflanzenzucht (DM), Bad Schwartau, Germany; Deutsche Saatveredelung AG (DSV), Lippstadt, Germany; KWS Saat AG (KWS), Einbeck, Germany; Limagrain GmbH (NICK), Edemissen, Germany; Lantmännen SW Seed GmbH (SEM), Hadmersleben, Germany; Syngenta Seeds GmbH (SYN), Bad Salzuflen, Germany; Raps GbR Saatzucht Lundsgaard (SRG), Grundhof, Germany; Norddeutsche Pflanzenzucht Hans-Georg Lembke KG (NPZ), Hohenlieth, Germany; W. von Borries-Eckendorf GmbH & Co.KG (WVB), Leopoldshöhe, Germany. Furthermore, a total of 380 double haploid (DH) *B. napus* lines produced by the cooperating partners (Department of Plant Breeding at the Justus-Liebig-University of Gießen and division of Plant Breeding at the University of Göttingen, as well as plant breeding companies of the Association of German Plant Breeders e. V., GFP) have been tested, partially in duplicate (data not shown). DH-lines were derived from a cross between a resistant line R53 (resynthesized from kale, *B. oleracea* var. *acephala* and chinese cabbage, *B. rapa* var. *pekinensis*) and the moderately resistant cultivar Express 617. For comparison of resistance responses of the various tested accessions, two reference cultivars were used, the susceptible cultivar ‘Falcon’ and the moderately resistant cultivar ‘Express’ (Norddeutsche Pflanzenzucht, NPZ, Hans-Georg Lembke KG, Hohenlieth, Germany).

Figure 2.1 Setup of the greenhouse screening of *Brassica* genotypes for resistance against *V. longisporum*. Ten pots containing two plants each are arranged in trays.

2.2.2 Preparation of inoculum and root-dip inoculation of the seedlings

A mix of two *V. longisporum* isolates, VL40 and VL43, isolated from *B. napus* in Northern Germany (Zeise and Tiedemann, 2001; Zeise and Tiedemann, 2002a; Zeise and Tiedemann, 2002b) was used for inoculation. Stock cultures of these isolates were produced by complementing conidial suspensions in Czapek-Dox medium with 25% glycerol and storage at -80°C. For preparation of fungal cultures, 500 µl stock solution was transferred to 150 ml potato extract glucose broth (Roth, Karlsruhe, Germany) and grown on a rotary shaker at 100 rpm and 23°C. After incubation of about 7 days mycelium was filtered through a sieve, spore concentration was determined with a Thoma haemocytometer and adjusted to a final concentration of 10^6 conidia/ml (Eynck, 2008)

Seeds were surface-sterilized with 70% ethanol, subsequently washed with tap water and grown in silica sand for approximately 10 days under day/night conditions of 16 h/8 h at 20°C. After one week, seedlings were carefully removed from the sand and roots cleaned under running tap water. Root tips were cut with scissors and placed in a conidial suspension of VL43 for a period of 30 min. Roots of control plants were equally cut and incubated in tap water for the same time. Subsequently, 20 inoculated and control seedlings each were transferred to pots containing a mixture of sand, peat and compost (1:1:2), resulting in 2 plants per container (Figure 2.1). Plant cultivation conditions were as described above.

2.2.3 Greenhouse Screening

The development of symptoms was recorded weekly in a time period from 7 to 28 dpi with a 1 to 9 score scale (Table 2.1) according to Eynck (2008; modified from Zeise, 1992). Disease severity was assessed by calculating area under the disease progress curve (AUDPC) values according to the formula (Shaner and Finney, 1977, Campbell and Madden, 1990):

$$\text{AUDPC} = \sum_{i=1}^{n} (y_i + y_{i+1}\ /2) * (t_{i+1} - t_i)$$

In which n = number of observations, $_i$ = time point of observation, y_i = disease severity value at i*th* observation, and t_i = time (days) at the i*th* observation.

The obtained AUDPC values were corrected by calculating the difference between the AUDPC value of the inoculated plants and the respective control plants (Eynck, 2008). These `net AUDPC values` take senescence alterations including yellowing of leaves into account. Furthermore, the AUDPC value of each cultivar was normalized with the AUDPC values of the cultivars 'Falcon' and 'Express' in order to consider fluctuations between different screenings. These normalized AUDPC values ($AUDPC_{norm}$) were calculated according to Eynck (2008).

Table 2.1 Assessment key for the evaluation of the disease severity of *B. napus* plants infected by *V. longisporum* (according to Eynck (2008; modified from Zeise, 1992)).

Score	Symptom development
1	No symptoms
2	Weak symptoms on the oldest leaf (yellowing, black veins)
3	Weak symptoms on the next younger leaves
4	About 50% of the leaves have symptoms
5	> 50% of the leaves have symptoms
6	Up to 50% of the leaves are dead
7	> 50% of the leaves are dead
8	Only apex is still alive
9	The plant is dead

2.2.4 Experimental design of field trials and screening of stubbles

Apart from experiments under controlled conditions, screening for resistance to a pathogen also requires trials under field conditions. Selected accessions from greenhouse screening were therefore tested at different locations in Northern Germany and Southern Sweden from 2008 to 2010. In the season 2008/09 36 field accessions of the collaborating breeders (in the season 2009/10 16 field accessions of breeders and 20 DH-lines) and four reference cultivars, were sown in a field near Göttingen, Lower-Saxony (Germany). Similar to the greenhouse trials the susceptible cultivar 'Falcon', the moderately resistant cultivar 'Express', the susceptible cultivar 'Laser' and the moderately resistant cultivar 'Oase' served as the reference cultivars. Additional field trials in Germany were located in Fehmarn (Schleswig-Holstein) and Rostock (Mecklenburg-West Pomerania) as well as in Svalöv in Southern Sweden (Skåne County). In Göttingen, an enhanced inoculation was achieved by incorporation of microsclerotia into the soil. Directly before sowing 15 g of microsclerotia infested stubbles per m^2 were evenly distributed manually and subsequently incorporated in the upper soil layers. The plots were arranged randomly with two replicates in 2008/09 and four replicates in the following season. Standard cultural practices, including the spraying of fungicides against *Phoma lingam* and *Sclerotinia sclerotiorum* at the adequate stages of plant growth were performed at the location Göttingen (Appendix Table A 1, A 2). At the other three locations field experiments were conducted in naturally infested soils. Plots were also randomly organized in 2 replicates. Disease incidence (DI) and disease severity (DS) in the field experiments were evaluated visually by scoring 25 stubbles randomly sampled from each plot after harvest (GS 97). In the season 2009/10 the sample number in Göttingen was reduced to 15 stubbles per plot in favor of an increased number of replicates (4). Microsclerotia formed at the stems beneath the epidermis and in the pith tissue, and in the roots were recorded by light microscopy and DS was quantified using a 1 to 4 assessment key according to Eynck (2008) (Table 2.2).

Table 2.2 Assessment key for the evaluation of the disease severity of *B. napus* stubbles infected by *V. longisporum* (according to Eynck (2008)).

Score	Symptom development
1	No microsclerotia visible in tissue
2	Low abundance of microsclerotia
3	High abundance microsclerotia
4	Tissue heavily infested with microsclerotia, epidermis is peeling off from the stubble

Based on this scoring, a disease index was calculated according to Eynck (2008):

$$\text{Disease Index} = \frac{(1 \times N_1) + (2 \times N_2) + (3 \times N_3) + (4 \times N_4)}{n}$$

where N_n = number of plants in the respective class, 1-4 = score numbers and n = total number of given scores.

2.2.5 Statistical analysis

The Software STATISTICA for Windows Version 9.1 (Statsoft 2010, Tulsa, USA) was used for statistical analysis. Spearman rank correlations were used to correlate disease severity parameters obtained in field trials and AUDPC values.

Frequency distributions of either $AUDPC_{norm}$ values or DI (%) were represented in box-whisker plots for analysis and comparison of median values.

2.3 Results

2.3.1 Greenhouse experiment

Under greenhouse conditions typical *Verticillium* symptoms developed at 14 dpi on susceptible plants such as 'Falcon' and 'Laser'. A characteristic partial yellowing and necrotisation of the oldest leaves were observed (Figure1). Black veins on leaves were also often visible and associated with a *V. longisporum* infection. A stunting effect was measurable starting at 14 dpi, but became more pronounced at 28 dpi.

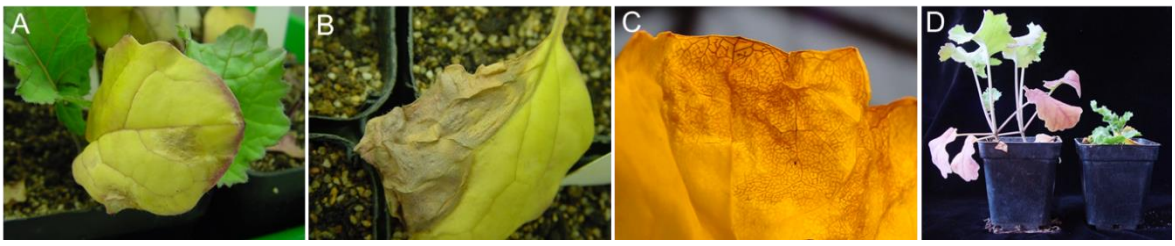

Figure 2.2 *V. longisporum* disease symptoms in the greenhouse. Yellowing of leaves (A-C), developing of black veins (C) and necrotic leaves in older stages of disease (B). A typical stunting of infected plants is only observed under controlled conditions as in the greenhouse (D, left hand plant, VL-infected; right hand plant, control plant).

In the first project period from 2004 to 2007, 20 independent screenings with *B. napus* accessions were conducted (for review: graphs with AUDPC values are found in Eynck (2008; see also Appendix, Figure A 2, A 4 to A 16, A 18, A 21 to A 25). In 2008 and 2009 four additional screenings were run with *B. napus* accessions from collaborating breeders (Appendix Figure A 1 to A 4). Besides the screening of these accessions, around 380 DH *B. napus* breeding lines originating from the Institutes of Plant Breeding of the Justus-Liebig-University of Gießen and Göttingen and the Association of German Plant Breeders e.V. (GFP) were screened from 2008 to 2011, partially within two independent screenings (data not shown).

Greenhouse screenings of *B. napus* accessions conducted in the years 2004-2009 showed a broad distribution of resistance levels with AUDPC values varying from 0.02 to 3.2 (Figure 2.3). For analysis of the frequency distribution of the $AUDPC_{norm}$ values obtained from the 24 screenings in the period 2004 to 2009, a total of six screenings were grouped into one class. The borders of the boxes in Figure 2.3 represent the 25% and 75% quartiles, meaning that 50% of all observed values are found within the box, while the whiskers mark the values between 0 and 25% and 75 and 100%. The median is slightly decreasing during the investigated period, suggesting that the overall resistance level of the tested *B. napus* accessions is increasing throughout the course of the screening period, which is expressed in lower $AUDPC_{norm}$ values. The median of the first class (i.e. first six screenings) has a value of 0.91 while the last performed screenings, represented by class 4, show a significantly lower median of 0.59.

For evaluation of the resistance levels, reference cultivars were consistently included in each screening run. AUDPC values of the moderately resistant cv. ‘Express’ were always lower compared to AUDPC values of susceptible cv. ‘Falcon’. Mean $AUDPC_{norm}$ values of all 24 screenings are 0.74 and 1.28 for the reference cv. ‘Express’ and ‘Falcon’, respectively (Table 2.3).

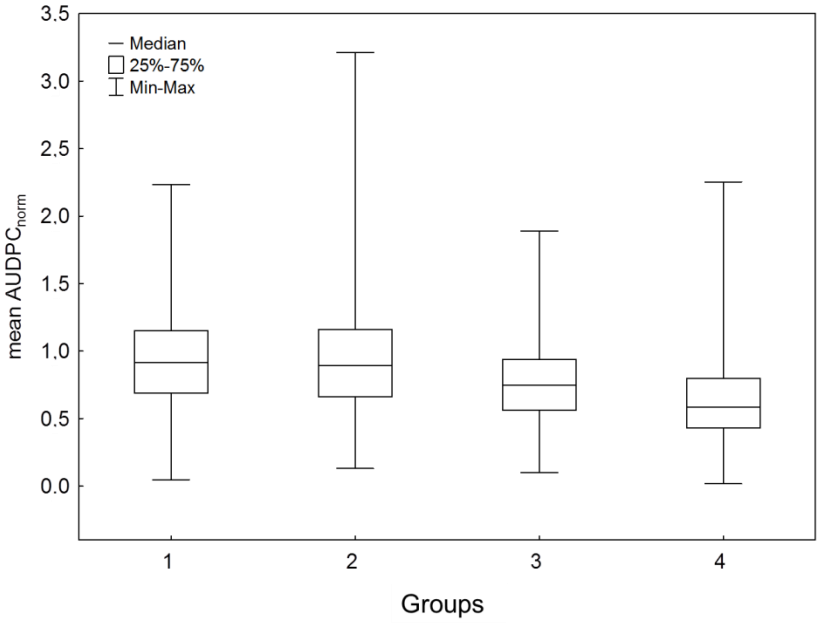

Figure 2.3 Frequency distribution of mean AUDPC$_{norm}$ values obtained from greenhouse screenings conducted from 2004 to 2009. Data show Box-Whisker-Plots and median. Borders of boxes represent 25% and 75% quartiles. Data of 24 screenings are grouped into four classes, i.e. one class represents AUDPC$_{norm}$ values of 6 screenings each; first group contains values obtained in the year 2004 and 2005 (n = 347); group 2 contains data of the following 6 screenings performed in the year 2005 (n = 360), group 3 includes screenings conducted in the years 2005, 2006 and 2007 (n = 425) and group 4 contains data of the years 2007, 2008 and 2009 (n = 374).

Table 2.3 Mean AUDPC$_{norm}$ values (derived from 24 screenings) of *B. napus* plants (cultivar 'Express' and 'Falcon') inoculated with *V. longisporum*.

AUDPC$_{norm}$	
Express	Falcon
0.74	1.28

2.3.2 Field trials

For evaluation of field resistance selected breeding lines were chosen by breeders in the seasons 2008/09 and 2009/10, and tested at the different locations. Additionally, the complete set of field accessions was screened again in the greenhouse for direct comparison of the breeding line performance. For field scoring, stubbles were sampled directly after harvest and subsequently scored for microsclerotia abundance to record DI and DS. Symptom expression in the field occurred relatively late in the plant development. First symptoms of infection consisted of half-sided brown stripes on rapeseed stems (Figure 2.4, left). The definite identification of *Verticillium* disease was based on the detection of microsclerotia. Figure 2.4 (right) shows a heavily infested field in Sweden as an example. In

Göttingen, disease levels in the two following years, 2009 and 2010, were extremely variable (Figure 2.5). While the DI in 2009 was in a range from 22% (SEM SW 2-09) to 80% (‘Falcon’), DI in 2010 did not exceed 24% and ranged between 0% (DH 8-10, DH 9-10) and 23.3% (DH 6-10, Table 2.6 and 2.8). Correspondingly, DS in 2009 varied from 1.2 (SEM SW 2-09) to 2.04 (‘Falcon’) and 1.0 (DH 8-10, DH 9-10) to 1.31 (DH 6-10) in 2010. DI and DS for both years and all locations strongly correlated as indicated by spearman rank correlation coefficients ranging between r_s = 0.85 and r_s = 0.96 (Table 2.4 and 2.5). For reasons of argumentative clarity the following discussion will therefore be based on only one of these parameters (DI). In Fehmarn and Svalöv, mean DI was higher compared to Göttingen (Figure 2.5). The DI in Fehmarn ranged from 60 to 100%, of which 80% of the accessions showed a DI >80% in 2009 (Table 2.6). The following year, DI was slightly lower with values between 52% and 100%, of which more than 60% exhibited values higher than 80% (Table 2.8). In Svalöv, disease levels were in similar ranges to those in Fehmarn (Figure 2.5). Here, DI varied from 54% to 100% of which 52% were higher than 80% in 2009 (Table 2.6). In 2010 disease values were comparable with the previous year (Table 2.8). In contrast, disease levels in Rostock were relatively low compared to the other locations (Figure 2.5). In 2009 DI exhibited values between 2% and 48% (Table 2.6) and in 2010 infestation levels were slightly higher with values ranging from 6% to 64% (Table 2.8).

In 2009, the reference cultivars ‘Express’ and ‘Oase’ in Göttingen, Fehmarn and Svalöv showed disease values similarly low and comparable to the other accessions, whereas DI of ‘Express’ was 6 times higher in Rostock (Table 2.6). Notably, DI of these moderately resistant cultivars was relatively high in Fehmarn with values of 88% and 84%, respectively (Table 2.6). The susceptible cultivars ‘Falcon’ and ‘Laser’ were always located in the group with the highest DI. In 2010, ‘Oase’ showed low values in Göttingen and Svalöv, while ‘Express’ showed disease values identical to ‘Falcon’ at Göttingen (Table 2.8). These results demonstrate that the resistance ranking of the reference cultivars is not always identical to the ranking obtained from the greenhouse screenings.

Figure 2.4 *V. longisporum* symptoms in the field. Early symptoms such as one sided brown discoloration on stems at the beginning of maturity (left) and heavily infested field shortly after harvest in Svalöv (Sweden, right).

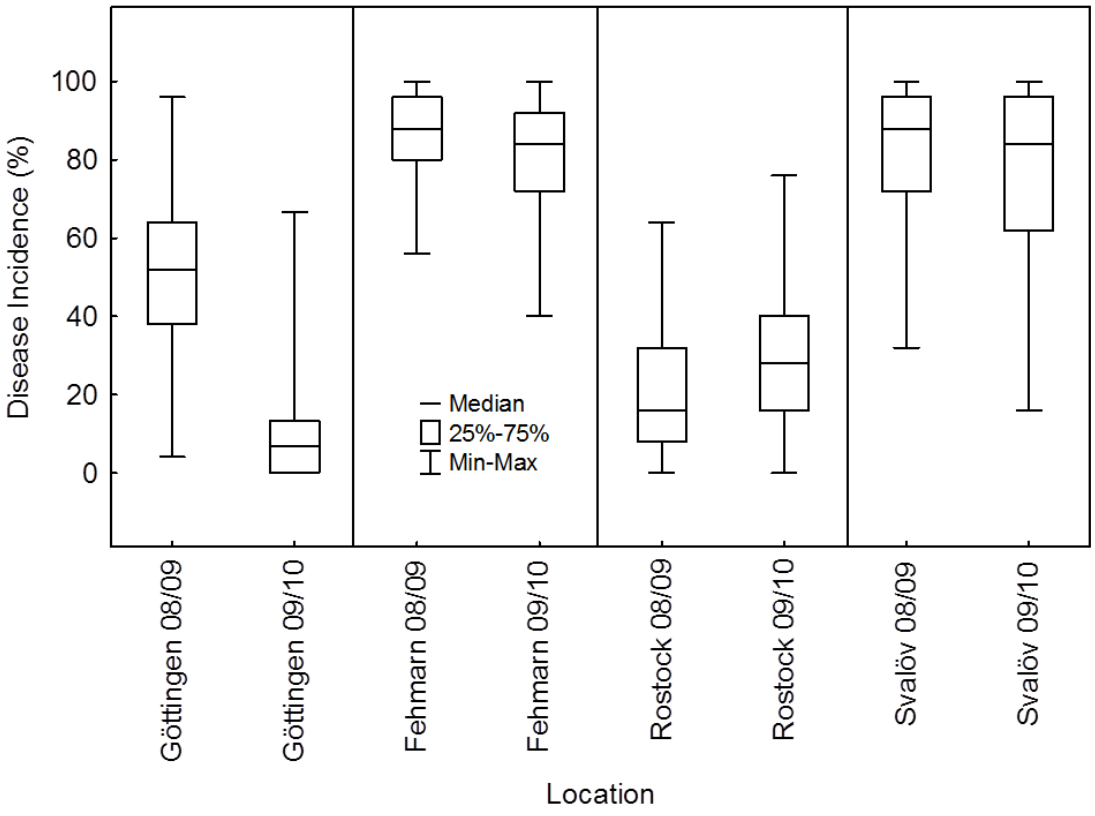

Figure 2.5 Frequency distribution of the disease incidence (%) at different locations and years (2008/09 and 2009/10). Data show Box-Whisker-Plots with median values. Borders of boxes represent 25% and 75% quartiles, thus boxes contain 50% of observed values. Each Box-Whisker-Plot contains disease incidence values of 40 (n = 2 x 25, Göttingen 09/10: n = 4 x 15) different field accessions. Boxes represent 25-75% of the data and whiskers contain outliers and extreme values.

2.3.3 Correlation of greenhouse and field screening data

The Spearman rank correlations between greenhouse data ($AUDPC_{norm}$) and disease values (DI and DS) obtained from the field trial in Göttingen 2009 were relatively low with correlation coefficients of r_s = 0.260 ($AUDPC_{norm}$ vs. DI) and r_s = 0.253 ($AUDPC_{norm}$ vs. DS, Table 2.4). Analysis of greenhouse and field data from the other locations showed a moderate but significant correlation of $AUDPC_{norm}$ vs. DI (r_s = 0.372) and $AUDPC_{norm}$ vs. DS (r_s = 0.422) in Svalöv. Field data determined for Fehmarn and Rostock did not correlate with greenhouse values. In 2010 correlation between greenhouse data and field scoring data of Göttingen was also not significant with r_s-values of 0.291 ($AUDPC_{norm}$ vs. DI) and 0.162 ($AUDPC_{norm}$ vs. DS, Table 2.5). None of the field data obtained from other locations showed significant correlations with greenhouse data. Nevertheless single accessions could be identified which displayed moderate to good levels of resistance under greenhouse and field conditions in 2008/09 (Table 2.6 and 2.7). In 2009/2010, four DH-lines performed well under greenhouse and field conditions with remarkably lower DI < 40% at the Svalöv site (Table 2.8).

Table 2.4 Spearman rank correlation analysis between the disease values (disease incidence (DI) and disease severity (DS)) derived from field resistance tests in Göttingen, Fehmarn, Svalöv and Rostock and the normalized area under the disease progress curve values ($AUDPC_{norm}$) from greenhouse screenings in the season 2008/09. Data highlighted in red represent significant differences at $p \leq 0.05$, (n = 40 accessions).

		Göttingen		Fehmarn		Svalöv		Rostock	
		DI	DS	DI	DS	DI	DS	DI	DS
$AUDPC_{norm}$		0.260	0.253	0.146	0.199	0.372	0.422	0.244	0.136
Göttingen	DI		0.891	0.303	0.314	0.011	0.142	0.164	0.144
	DS			0.343	0.382	0.090	0.221	0.180	0.138
Fehmarn	DI				0.853	0.261	0.298	0.265	0.200
	DS					0.386	0.416	0.319	0.249
Svalöv	DI						0.934	0.496	0.469
	DS							0.551	0.519
Rostock	DI								0.937
	DS								

Table 2.5 Spearman rank correlation analysis between the disease values (disease incidence (DI) and disease severity (DS)) derived from field resistance tests in Göttingen, Fehmarn, Svalöv and Rostock and the normalized area under the disease progress curve values ($AUDPC_{norm}$) from greenhouse screenings in the season 2009/10. Data highlighted in red represent significant differences at $p \leq 0.05$ (n = 40 accessions).

		Göttingen		Fehmarn		Svalöv		Rostock	
		DI	DS	DI	DS	DI	DS	DI	DS
$AUDPC_{norm}$		0.291	0.162	0.220	0.231	0.126	0.096	0.298	0.317
Göttingen	DI		0.920	0.122	0.049	0.559	0.587	0.168	0.147
	DS			0.108	-0.029	0.404	0.503	0.011	0.018
Fehmarn	DI				0.867	-0.040	-0.047	-0.031	-0.043
	DS					0.072	0.053	0.001	-0.008
Svalöv	DI						0.945	0.356	0.319
	DS							0.344	0.329
Rostock	DI								0.957
	DS								

Table 2.6 Rating of *Verticillium* resistance of 36 *B. napus* accessions and 4 reference cultivars expressed as normalized area under the disease progress curve ($AUDPC_{norm}$) and disease incidence (DI). $AUDPC_{norm}$ values are obtained from greenhouse experiments and DI is derived from field trials at four different locations in the season 2008/09. Data are means of 20 replicates ($AUDPC_{norm}$) or 2 replicates (DI) with standard deviations (in brackets). Data highlighted in green represent accessions with enhanced resistance in the greenhouse and field.

Accession	$AUDPC_{norm}$		DI Göttingen (%)		DI Fehmarn (%)		DI Svalöv (%)		DI Rostock (%)	
Falcon	**1.23**	(± 0.66)	**80.00**	(±22.63)	**98.00**	(± 2.83)	**90.00**	(± 8.49)	**18.00**	(± 2.83)
Express	**0.78**	(± 0.30)	**54.00**	(±25.46)	**88.00**	(± 0.00)	**72.00**	(±11.31)	**36.00**	(±28.28)
Laser	**0.84**	(± 0.42)	**76.00**	(± 5.66)	**86.00**	(± 8.49)	**94.00**	(± 8.49)	**24.00**	(±11.31)
Oase	**0.28**	(± 0.23)	**58.00**	(± 2.83)	**84.00**	(± 5.66)	**62.00**	(±42.43)	**6.00**	(± 8.49)
DM 1-09	0.60	(± 0.27)	52.00	(± 0.00)	100.00	(± 0.00)	92.00	(±11.31)	36.00	(± 5.66)
DM 2-09	0.88	(± 0.44)	64.00	(±22.63)	100.00	(± 0.00)	92.00	(± 0.00)	14.00	(±14.14)
DM 3-09	0.74	(± 0.42)	64.00	(± 5.66)	98.00	(± 2.83)	80.00	(±11.31)	16.00	(±11.31)
DM 4-09	0.88	(± 0.37)	70.00	(±25.46)	100.00	(± 0.00)	84.00	(±22.63)	32.00	(±11.31)
DSV 1-09	0.37	(± 0.33)	56.00	(±16.97)	86.00	(± 2.83)	76.00	(± 5.66)	12.00	(± 0.00)
DSV 2-09	0.53	(± 0.24)	54.00	(± 8.49)	88.00	(±11.31)	78.00	(±19.80)	14.00	(±19.80)

Continuing from previous page (**Table 2.6**)

DSV 3-09	0.46	(± 0.26)	52.00	(±16.97)	72.00	(±22.63)	70.00	(± 8.49	18.00	(± 8.49)
DSV 4-09	0.78	(± 0.38)	62.00	(± 8.49)	74.00	(± 8.49)	84.00	(±22.63)	2.00	(± 2.83)
KWS 1-09	0.32	(± 0.21)	36.00	(±16.97)	96.00	(± 5.66)	80.00	(±22.63)	6.00	(± 8.49)
KWS 2-09	0.17	(± 0.10)	36.00	(±22.63)	82.00	(± 2.83)	94.00	(± 8.49)	16.00	(± 5.66)
KWS 3-09	0.62	(± 0.34)	48.00	(±11.31)	80.00	(±16.97)	98.00	(± 2.83)	30.00	(±14.14)
KWS 4-09	0.48	(± 0.19)	48.00	(±22.63)	100.00	(± 0.00)	100.00	(± 0.00)	44.00	(±11.31)
NICK 1-09	1.27	(± 0.40)	60.00	(± 5.66)	76.00	(± 5.66)	92.00	(± 0.00)	32.00	(±22.63)
NICK 2-09	0.39	(± 0.26)	36.00	(±11.31)	86.00	(± 2.83)	78.00	(±19.80)	16.00	(±16.97)
NICK 3-09	0.69	(± 0.25)	66.00	(± 2.83)	96.00	(± 5.66)	96.00	(± 0.00)	48.00	(±22.63)
NICK 4-09	0.73	(± 0.25)	38.00	(± 2.83)	90.00	(±14.14)	98.00	(± 2.83)	20.00	(±16.97)
NICK 5-09	0.40	(± 0.25)	34.00	(± 2.83)	84.00	(± 5.66)	100.00	(± 0.00)	36.00	(±28.28)
NPZ 1-09	0.68	(± 0.41)	66.00	(± 8.49)	82.00	(±14.14)	90.00	(± 8.49)	24.00	(±16.97)
NPZ 2-09	0.57	(± 0.18)	56.00	(±11.31)	82.00	(± 8.49)	72.00	(±16.97)	28.00	(±11.31)
NPZ 3-09	0.70	(± 0.32)	44.00	(±16.97)	88.00	(± 5.66)	94.00	(± 8.49)	42.00	(±25.46)
SEM SW 1-09	0.47	(± 0.25)	50.00	(± 8.49)	88.00	(± 0.00)	62.00	(±25.46)	4.00	(± 5.66)
SEM SW 2-09	0.58	(± 0.36)	22.00	(±14.14)	64.00	(±11.31)	80.00	(±22.63)	2.00	(± 2.83)
SEM SW 3-09	0.65	(± 0.30)	34.00	(± 2.83)	82.00	(± 8.49)	78.00	(±19.80)	4.00	(± 5.66)
SEM SW 4-09	0.95	(± 0.30)	28.00	(±33.94)	82.00	(± 2.83)	98.00	(± 2.83)	18.00	(±14.14)
SRG 1-09	0.44	(± 0.16)	48.00	(± 5.66)	86.00	(±14.14)	78.00	(± 8.49)	14.00	(± 2.83)
SRG 2-09	0.70	(± 0.26)	46.00	(±19.80)	94.00	(± 8.49)	86.00	(±19.80)	28.00	(± 5.66)
SRG 3-09	0.66	(± 0.34)	36.00	(±16.97)	76.00	(± 5.66)	70.00	(±25.46)	24.00	(±22.63)
SRG 4-09	0.26	(± 0.15)	36.00	(± 0.00)	82.00	(± 2.83)	54.00	(±14.14)	18.00	(±19.80)
SYN 1-09	0.74	(± 0.40)	54.00	(±14.14)	98.00	(± 2.83)	100.00	(± 0.00)	34.00	(±19.80)
SYN 2-09	0.51	(± 0.30)	58.00	(±14.14)	92.00	(± 5.66)	76.00	(± 0.00)	14.00	(± 2.83)
SYN 3-09	0.91	(± 0.41)	38.00	(±14.14)	82.00	(± 8.49)	64.00	(±16.97)	2.00	(± 2.83)
SYN 4-09	0.53	(± 0.26)	46.00	(± 2.83)	90.00	(± 2.83)	92.00	(± 5.66)	10.00	(± 8.49)
WVB SQ1-09	0.38	(± 0.33)	58.00	(±42.43)	84.00	(± 5.66)	78.00	(± 2.83)	22.00	(± 8.49)
WVB SQ 2-09	0.59	(± 0.40)	64.00	(±22.63)	100.00	(± 0.00)	86.00	(± 8.49)	22.00	(±25.46)
WVB SQ 3-09	0.29	(± 0.16)	58.00	(±14.14)	90.00	(± 8.49)	60.00	(± 0.00)	18.00	(±14.14)
WVB SQ 4-09	0.36	(± 0.31)	78.00	(± 8.49)	80.00	(± 5.66)	84.00	(± 0.00)	16.00	(± 5.66)

Table 2.7 Rating of *Verticillium* resistance tests of 36 *B. napus* accessions and 4 reference cultivars expressed as normalized area under the disease progress curve values ($AUDPC_{norm}$) and disease severity (DS). $AUDPC_{norm}$ values are obtained from greenhouse experiments and DS values are derived from field trials at four different locations in the season 2008/09. Data are means of 20 replicates ($AUDPC_{norm}$) or 2 replicates (DS) with standard deviations (in brackets). Data highlighted in green represent accessions with enhanced resistance in the greenhouse and field.

Accession	$AUDPC_{norm}$		DS Göttingen		DS Fehmarn		DS Svalöv		DS Rostock	
Falcon	**1.23**	(± 0.66)	**2.04**	(±0.36)	**3.02**	(±0.03)	**2.73**	(±0.44)	**1.15**	(±0.06)
Express	**0.78**	(± 0.30)	**1.50**	(±0.29)	**2.36**	(±0.43)	**2.36**	(±0.34)	**1.53**	(±0.41)
Laser	**0.84**	(± 0.42)	**1.74**	(±0.12)	**2.09**	(±0.07)	**2.83**	(±0.12)	**1.35**	(±0.09)
Oase	**0.28**	(± 0.23)	**1.70**	(±0.18)	**2.05**	(±0.14)	**2.10**	(±0.84)	**1.04**	(±0.06)
DM 1-09	0.60	(± 0.27)	1.47	(±0.04)	3.26	(±0.07)	2.82	(±0.12)	1.29	(±0.14)
DM 2-09	0.88	(± 0.44)	1.62	(±0.44)	3.09	(±0.41)	2.67	(±0.23)	1.09	(±0.10)
DM 3-09	0.74	(± 0.42)	1.85	(±0.15)	2.89	(±0.65)	2.53	(±0.29)	1.13	(±0.02)
DM 4-09	0.88	(± 0.37)	1.82	(±0.41)	3.00	(±0.19)	2.53	(±0.55)	1.20	(±0.04)
DSV 1-09	0.37	(± 0.33)	1.51	(±0.13)	2.50	(±0.42)	2.27	(±0.01)	1.21	(±0.12)
DSV 2-09	0.53	(± 0.24)	1.51	(±0.12)	2.43	(±0.31)	2.28	(±0.51)	1.15	(±0.22)
DSV 3-09	0.46	(± 0.26)	1.49	(±0.19)	2.06	(±0.33)	2.05	(±0.03)	1.26	(±0.18)
DSV 4-09	0.78	(± 0.38)	1.61	(±0.02)	2.00	(±0.13)	2.69	(±0.63)	1.01	(±0.01)
KWS 1-09	0.32	(± 0.21)	1.49	(±0.54)	2.71	(±0.39)	2.34	(±0.65)	1.06	(±0.08)
KWS 2-09	0.17	(± 0.10)	1.44	(±0.28)	2.15	(±0.19)	2.81	(±0.35)	1.16	(±0.13)
KWS 3-09	0.62	(± 0.34)	1.65	(±0.02)	2.39	(±0.02)	2.81	(±0.15)	1.28	(±0.09)
KWS 4-09	0.48	(± 0.19)	1.59	(±0.48)	2.89	(±0.47)	3.06	(±0.10)	1.65	(±0.11)
NICK 1-09	1.27	(± 0.40)	1.52	(±0.21)	1.94	(±0.27	2.62	(±0.22)	1.52	(±0.36)
NICK 2-09	0.39	(± 0.26)	1.26	(±0.10)	2.13	(±0.55)	1.93	(±0.48)	1.19	(±0.25)
NICK 3-09	0.69	(± 0.25)	1.86	(±0.18)	2.68	(±0.49)	2.76	(±0.06)	1.60	(±0.28)
NICK 4-09	0.73	(± 0.25)	1.42	(±0.18)	2.59	(±0.84)	3.00	(±0.00)	1.25	(±0.29)
NICK 5-09	0.40	(± 0.25)	1.24	(±0.09)	2.11	(±0.21)	3.06	(±0.12)	1.63	(±0.41)
NPZ 1-09	0.68	(± 0.41)	1.81	(±0.11)	1.87	(±0.02)	2.85	(±0.32)	1.27	(±0.22)
NPZ 2-09	0.57	(± 0.18)	1.53	(±0.08)	2.18	(±0.37)	2.29	(±0.28)	1.30	(±0.14)
NPZ 3-09	0.70	(± 0.32)	1.47	(±0.25)	2.47	(±0.59)	2.95	(±0.17)	1.55	(±0.25)
SEM SW 1-09	0.47	(± 0.25)	1.55	(±0.03)	2.09	(±0.41)	1.71	(±0.25)	1.06	(±0.08)
SEM SW 2-09	0.58	(± 0.36)	1.21	(±0.12)	1.67	(±0.10)	2.21	(±0.24)	1.01	(±0.01)
SEM SW 3-09	0.65	(± 0.30)	1.46	(±0.03)	2.13	(±0.25)	2.37	(±0.48)	1.05	(±0.07)
SEM SW 4-09	0.95	(± 0.30)	1.26	(±0.29)	2.30	(±0.18)	2.79	(±0.01)	1.19	(±0.22)
SRG 1-09	0.44	(± 0.16)	1.37	(±0.00)	2.19	(±0.59)	2.11	(±0.17)	1.10	(±0.08)
SRG 2-09	0.70	(± 0.26)	1.47	(±0.31)	2.69	(±0.31)	2.53	(±0.44)	1.28	(±0.02)
SRG 3-09	0.66	(± 0.34)	1.39	(±0.28)	1.85	(±0.07)	1.84	(±0.36)	1.22	(±0.14)
SRG 4-09	0.26	(± 0.15)	1.39	(±0.01)	1.83	(±0.21)	1.68	(±0.08)	1.17	(±0.23)
SYN 1-09	0.74	(± 0.40)	1.79	(±0.23)	2.81	(±0.17)	3.00	(±0.15)	1.63	(±0.41)

Continuing from previous page (**Table 2.7**)

SYN 2-09	0.51	(± 0.30)	1.62	(±0.08)	2.70	(±0.63)	2.33	(±0.10)	1.13	(±0.01)
SYN 3-09	0.91	(± 0.41)	1.49	(±0.17)	1.95	(±0.29)	1.91	(±0.41)	1.01	(±0.01)
SYN 4-09	0.53	(± 0.26)	1.41	(±0.16)	2.14	(±0.50)	2.52	(±0.13)	1.07	(±0.08)
WVB SQ1-09	0.38	(± 0.33)	1.61	(±0.49)	2.29	(±0.12)	2.17	(±0.08)	1.23	(±0.08)
WVB SQ 2-09	0.59	(± 0.40)	1.63	(±0.41)	2.95	(±0.01)	2.60	(±0.28)	1.29	(±0.36)
WVB SQ 3-09	0.29	(± 0.16)	1.57	(±0.00)	2.26	(±0.63)	1.91	(±0.09)	1.25	(±0.23)
WVB SQ 4-09	0.36	(± 0.31)	1.81	(±0.27)	2.22	(±0.37)	2.49	(±0.07)	1.17	(±0.09)

Table 2.8 Rating of *Verticillium* resistance tests of 36 *B. napus* accessions (inclusive 20 *B. napus* DH-lines) and 4 reference cultivars expressed as normalized area under the disease progress curve values ($AUDPC_{norm}$) and disease incidence (DI). $AUDPC_{norm}$ values are obtained from greenhouse experiments and DI is derived from field trials at four different locations in the season 2009/10. Data are means of 20 replicates ($AUDPC_{norm}$) or 2 replicates (DI) at locations Fehmarn, Svalöv and Rostock with standard deviations (in brackets). DI values from location Göttingen are means of 4 replicates with standard deviations (in brackets). Data highlighted in green represent accessions with enhanced resistance in the greenhouse and field.

Accession	**$AUDPC_{norm}$**		**DI Göttingen**		**DI Fehmarn**		**DI Svalöv**		**DI Rostock**	
Falcon	**1.44**	(± 1.06)	**11.67**	(±19.15)	**80.00**	(±11.31)	**98.00**	(± 2.83)	**54.00**	(± 8.49)
Express	**0.56**	(± 0.57)	**11.67**	(± 6.38)	**64.00**	(±28.28)	**80.00**	(± 5.66)	**44.00**	(±11.31)
Laser	**0.98**	(± 0.74)	**15.00**	(±19.15)	**70.00**	(±19.80)	**92.00**	(± 5.66)	**20.00**	(±22.63)
Oase	**0.24**	(± 0.29)	**1.67**	(± 3.34)	**78.00**	(±14.14)	**46.00**	(±14.14)	**16.00**	(± 5.66)
DH 1-10	0.66	(± 0.48)	1.67	(± 3.34)	78.00	(±31.11)	80.00	(± 5.66)	60.00	(±22.63)
DH 2-10	1.07	(± 0.56)	5.00	(± 3.34)	66.00	(±36.77)	78.00	(± 2.83)	42.00	(±25.46)
DH 3-10	1.02	(± 0.50)	6.67	(±13.34)	90.00	(±14.14)	60.00	(±11.31)	44.00	(±28.28)
DH 4-10	1.36	(± 0.56)	1.67	(± 3.34)	90.00	(± 8.49)	64.00	(±11.31)	48.00	(±39.60)
DH 5-10	1.26	(± 0.78)	5.00	(± 6.38)	88.00	(±11.31)	96.00	(± 0.00)	42.00	(±19.80)
DH 6-10	0.47[1]	(± 0.20)	23.34	(±30.06)	92.00	(± 0.00)	90.00	(± 2.83)	24.00[2]	(± 5.66)
DH 7-10	0.31[1]	(± 0.20)	3.34	(± 3.85)	66.00	(±25.46)	26.00	(±14.14)	16.67[3]	(±23.57)
DH 8-10	0.85	(± 0.45)	0.00	(± 0.00)	78.00	(± 8.49)	32.00	(± 5.66)	16.50	(±12.02)
DH 9-10	0.79	(± 0.56)	0.00	(± 0.00)	84.00	(±16.97)	30.00	(± 8.49)	22.00	(±25.46)
DH 10-10	0.89	(± 0.66)	1.67	(± 3.34)	66.00	(±25.46)	78.00	(±14.14)	36.00	(± 0.00)
DH 11-10	1.05	(± 0.44)	8.33	(± 6.38)	100.00	(± 0.00)	86.00	(± 2.83)	64.00	no s.d.
DH 12-10	0.94	(± 0.55)	6.67	(± 5.44)	90.00	(± 8.49)	82.00	(± 2.83)	18.00	(±14.14)
DH 13-10	0.71[1]	(± 0.24)	5.00	(± 6.38)	80.00	(±22.63)	36.00	(±22.63)	6.00[4]	(± 8.49)
DH 14-10	0.68	(± 0.43)	3.34	(± 3.85)	76.00	(±22.63)	88.00	(± 5.66)	34.00	(± 8.49)
DH 15-10	1.19	(± 1.12)	18.33	(±11.38)	80.00	(± 5.66)	98.00	(± 2.83)	42.00	(±19.80)
DH 16-10	0.89	(± 0.57)	3.33	(± 6.67)	82.00	(±19.80)	80.00	(±11.31)	30.00	(±25.46)
DH 17-10	0.54	(± 0.30)	5.00	(±10.00)	64.00	(± 5.66)	96.00	(± 0.00)	24.00	(±22.63)
DH 18-10	0.98	(± 0.42)	10.00	(±12.77)	88.00	(±11.31)	62.00	(±14.14)	36.00	(± 5.66)

Continuing from previous page (**Table 2.8**)

DH 19-10	0.70	(± 0.44)	5.00	(± 6.38)	86.00	(±14.14)	70.00	(± 2.83)	20.00	(± 5.66)
DH 20-10	0.06	(± 0.20)	6.67	(± 9.43)	92.00	(± 0.00)	40.00	(± 5.66)	10.00	(± 2.83)
DIE 1-10	n.i.	n.i.	10.00	(± 3.85)	58.00	(±19.80)	77.50	(±19.09)	32.00	(±11.31)
DIE 2-10	n.i.	n.i.	18.34	(±20.64)	86.00	(± 2.83)	100.00	(± 0.00)	38.00	(± 8.49)
DSV 1-10	0.75	(± 0.40)	8.33	(±16.67)	88.00	(±11.31)	98.00	(± 2.83)	36.00	(±28.28)
DSV 2-10	0.57	(± 0.28)	5.00	(± 6.38)	82.00	(±14.14)	66.00	(± 8.49)	10.00	(± 2.83)
KWS 1-10	0.98	(± 0.68)	16.67	(±17.64)	70.00	(±19.80)	100.00	(± 0.00)	46.00	(±25.46)
NICK 1-10	1.83	(± 0.87)	11.67	(±11.39)	96.00	(± 0.00)	60.00	(± 5.66)	24.00	(±11.31)
NICK 2-10	0.78	(± 0.53)	11.67	(± 8.39)	68.00	(±11.31)	96.00	(± 0.00)	30.00	(± 2.83)
NPZ 1-10	0.64	(± 0.32)	1.67	(± 3.34)	84.00	(± 0.00)	82.00	(± 2.83)	38.00	(±31.11)
NPZ 2-10	1.23	(± 0.69)	15.00	(±11.39)	80.00	(±22.63)	98.00	(± 2.83)	8.00	(±11.31)
SRG 1-10	0.68	(± 0.41)	5.00	(± 3.34)	90.00	(± 2.83)	94.00	(± 2.83)	16.00	(±16.97)
SRG 2-10	0.88	(± 0.43)	5.00	(± 6.38)	80.00	(± 0.00)	96.00	(± 0.00)	36.00	(±16.97)
SW 1-10	1.24	(± 1.06)	1.67	(± 3.34)	88.00	(± 0.00)	36.00	(± 5.66)	16.00	(±11.31)
SYN 1-10	0.88	(± 0.29)	15.00	(±21.34)	92.00	(± 5.66)	90.00	(± 2.83)	32.00	(±11.31)
SYN 2-10	0.88	(± 0.40)	3.33	(± 6.67)	82.00	(± 2.83)	90.00	(± 8.49)	38.00	(±25.46)
WVB 1-10	0.74	(± 0.45)	10.00	(± 8.61)	88.00	(± 5.66)	82.00	(±14.14)	44.00	no s.d.
WVB 2-10	0.89	(± 0.40)	6.67	(± 5.44)	52.00	(±16.97)	66.00	(±19.80)	38.00	(± 2.83)

[1] data obtained in another screening; [2]value for accession SW 2-10; [3]value for accession NPZ 3-10; [4]value for accession KWS 2-10; n.i.: not investigated

Table 2.9 Rating of *Verticillium* resistance tests of 36 *B. napus* accessions (including 20 *B. napus* DH-lines) and 4 reference cultivars expressed as normalized area under the disease progress curve values ($AUDPC_{norm}$) and disease severity (DS). $AUDPC_{norm}$ values are obtained from greenhouse experiments and DS are derived from field trials at four different locations in the season 2009/10. Data are mean values of 20 replicates ($AUDPC_{norm}$) or 2 replicates (DS) at locations Fehmarn, Svalöv and Rostock with standard deviations (in brackets). DS values from location Göttingen are means of 4 replicates with standard deviations (in brackets). Data highlighted in green represent accessions with enhanced resistance in the greenhouse and field.

Accession	$AUDPC_{norm}$		DS Göttingen		DS Fehmarn		DS Svalöv		DS Rostock	
Falcon	**1.44**	(± 1.06)	1.15	(±0.27)	2.20	(±0.28)	2.49	(±0.01)	1.91	(±0.29)
Express	**0.56**	(± 0.57)	1.13	(±0.07)	1.95	(±0.78)	1.93	(±0.01)	1.67	(±0.29)
Laser	**0.98**	(± 0.74)	1.22	(±0.28)	2.05	(±0.17)	2.45	(±0.10)	1.28	(±0.32)
Oase	**0.24**	(± 0.29)	1.04	(±0.08)	2.13	(±0.23)	1.44	(±0.21)	1.21	(±0.14)
DH 1-10	0.66	(± 0.48)	1.01	(±0.01)	2.51	(±0.51)	2.11	(±0.02)	2.18	(±0.50)
DH 2-10	1.07	(± 0.56)	1.03	(±0.03)	2.06	(±0.61)	1.89	(±0.14)	1.87	(±0.58)
DH 3-10	1.02	(± 0.50)	1.04	(±0.08)	2.65	(±0.47)	1.48	(±0.23)	1.70	(±0.61)
DH 4-10	1.36	(± 0.56)	1.01	(±0.01)	2.58	(±0.31)	1.53	(±0.09)	1.82	(±0.61)
DH 5-10	1.26	(± 0.78)	1.02	(±0.03)	2.42	(±0.22)	2.14	(±0.03)	1.63	(±0.52)

Continuing from previous page (**Table 2.9**)

DH 6-10	0.47[1]	(± 0.20)	1.31	(±0.41)	2.38	(±0.10)	2.50	(±0.31)	1.36[2]	(±0.02)
DH 7-10	0.31[1]	(± 0.20)	1.04	(±0.05)	1.99	(±0.46)	1.15	(±0.07)	1.13[3]	(±0.18)
DH 8-10	0.85	(± 0.45)	1.00	(±0.00)	2.21	(±0.37)	1.37	(±0.09)	1.31	(±0.35)
DH 9-10	0.79	(± 0.56)	1.00	(±0.00)	2.37	(±0.15)	1.19	(±0.10)	1.29	(±0.34)
DH 10-10	0.89	(± 0.66)	1.01	(±0.01)	2.15	(±0.52)	1.89	(±0.26)	1.62	(±0.05)
DH 11-10	1.05	(± 0.44)	1.06	(±0.06)	2.69	(±0.04)	1.92	(±0.11)	1.85	no s.d.
DH 12-10	0.94	(± 0.55)	1.08	(±0.10)	2.57	(±0.44)	2.16	(±0.08)	1.23	(±0.23)
DH 13-10	0.71[1]	(± 0.24)	1.08	(±0.13)	2.36	(±0.34)	1.20	(±0.04)	1.11[4]	(±0.15)
DH 14-10	0.68	(± 0.43)	1.02	(±0.03)	2.32	(±0.32)	2.07	(±0.09)	1.51	(±0.14)
DH 15-10	1.19	(± 1.12)	1.19	(±0.09)	2.39	(±0.01)	2.53	(±0.07)	1.68	(±0.47)
DH 16-10	0.89	(± 0.57)	1.04	(±0.09)	2.24	(±0.40)	2.01	(±0.12)	1.38	(±0.39)
DH 17-10	0.54	(± 0.30)	1.06	(±0.11)	2.19	(±0.02)	2.52	(±0.30)	1.39	(±0.35)
DH 18-10	0.98	(± 0.42)	1.17	(±0.21)	2.37	(±0.23)	1.91	(±0.23)	1.69	(±0.20)
DH 19-10	0.70	(± 0.44)	1.06	(±0.09)	2.42	(±0.14)	1.79	(±0.05)	1.27	(±0.09)
DH 20-10	0.06	(± 0.20)	1.07	(±0.12)	2.50	(±0.03)	1.21	(±0.02)	1.15	(±0.08)
DIE 1-10	n.i.	n.i.	1.16	(±0.08)	2.02	(±0.50)	1.99	(±0.25)	1.51	(±0.20)
DIE 2-10	n.i.	n.i.	1.21	(±0.29)	2.55	(±0.01)	2.77	(±0.12)	1.55	(±0.19)
DSV 1-10	0.75	(± 0.40)	1.16	(±0.31)	2.46	(±0.22)	2.73	(±0.08)	1.63	(±0.49)
DSV 2-10	0.57	(± 0.28)	1.04	(±0.05)	2.34	(±0.61)	1.63	(±0.05)	1.08	(±0.00)
KWS 1-10	0.98	(± 0.68)	1.21	(±0.31)	2.15	(±0.15)	2.80	(±0.00)	1.69	(±0.50)
NICK 1-10	1.83	(± 0.87)	1.16	(±0.19)	2.83	(±0.29)	1.79	(±0.13)	1.29	(±0.02)
NICK 2-10	0.78	(± 0.53)	1.15	(±0.13)	2.20	(±0.38)	2.41	(±0.13)	1.36	(±0.06)
NPZ 1-10	0.64	(± 0.32)	1.01	(±0.01)	2.36	(±0.02)	2.03	(±0.02)	1.45	(±0.52)
NPZ 2-10	1.23	(± 0.69)	1.10	(±0.07)	2.41	(±0.49)	2.19	(±0.25)	1.13	(±0.19)
SRG 1-10	0.68	(± 0.41)	1.03	(±0.02)	2.71	(±0.12)	2.07	(±0.22)	1.18	(±0.20)
SRG 2-10	0.88	(± 0.43)	1.02	(±0.03)	2.37	(±0.14)	2.09	(±0.24)	1.45	(±0.26)
SW 1-10	1.24	(± 1.06)	1.03	(±0.07)	2.55	(±0.05)	1.36	(±0.04)	1.27	(±0.25)
SYN 1-10	0.88	(± 0.29)	1.21	(±0.37)	2.69	(±0.08)	2.46	(±0.16)	1.43	(±0.18)
SYN 2-10	0.88	(± 0.40)	1.03	(±0.06)	2.39	(±0.36)	2.24	(±0.13)	1.52	(±0.15)
WVB 1-10	0.74	(± 0.45)	1.16	(±0.12)	2.23	(±0.08)	1.96	(±0.30)	1.72	no s.d.
WVB 2-10	0.89	(± 0.40)	1.06	(±0.05)	1.73	(±0.26)	1.85	(±0.44)	1.49	(±0.01)

[1] data obtained in another screening; [2] value for accession SW 2-10; [3] value for accession NPZ 3-10; [4] value for accession KWS 2-10; n.i.: not investigated

2.4 Discussion

With the lack of suitable fungicides, resistant cultivars remain the most important method to control *V. longisporum* diseases in OSR. One of the prime challenges in OSR breeding programs is therefore the screening for resistant genotypes. To aid the identification of resistant lines, a broad greenhouse screening for phenotyping of *B. napus* accessions has been set up and applied over several years. A selection of the most promising breeding lines was subsequently tested under field conditions.

The screening of a large number of different accessions is only feasible under greenhouse conditions. With the established greenhouse screening a total of up to 100 different accessions in 20 replicates can be screened within five weeks under controlled and constant conditions. The set of screenings conducted from 2004 to 2009 with *B. napus* accessions was analyzed in terms of reproducibility and robustness. In all screenings the cv. 'Express' and 'Falcon' served as reference cultivars and were used for normalization of the values of tested breeding lines. $AUDPC_{norm}$ values of cv. 'Express' were lower compared to values of cv. 'Falcon' in all but one of the investigated screenings. While the mean $AUDPC_{norm}$ values of 'Express' (0.74) were near the 25% quartile, mean values of 'Falcon' (1.28) were close to the 75% quartile. These data demonstrate the overall reproducibility of the individual greenhouse screenings required to classify and compare resistant levels of new breeding lines.

When comparing the performance of all tested accessions it becomes apparent that the frequency distribution of the $AUDPC_{norm}$ values is very narrow, implying that many accessions differ only marginally in terms of their resistance levels. This could be due to the fact that *V. longisporum* resistance is inherited in a polygenic way (Rygulla *et al*., 2007b, Rygulla *et al*., 2008) i. e. the phenotypes are determined by regulation of several genes, which may result in small quantitative differences in resistance levels (Lindhout, 2002) rather than abrupt qualitative resistance leaps. The difficulty to clearly differentiate between the phenotypes can contribute to the fact that repeated screenings with the same accessions do not show a strong correlation, i.e. identical ranking orders. In addition, it is unclear to which degree homogeneity of the tested accessions is indeed valid. Although our data do not support a straightforward matching of rank positions of individual accessions between the various screenings, the frequency distribution of the $AUDPC_{norm}$ data from greenhouse screenings illustrates the overall success of the breeding efforts over several years. This is reflected in the decrease of the $AUDPC_{norm}$ median from 0.91 at the beginning of the resistance screenings to 0.59 in the most recent screening, demonstrating that the greenhouse screening is well suited to score and support ongoing efforts in resistance breeding. Additionally, Eynck (2008), besides *B. napus,* screened *B. rapa* and *B. oleracea* for

Verticillium resistance and confirmed previous findings that the level of resistance is elevated in *B. oleracea* species (Kemmochi *et al*., 2000; Happstadius *et al*., 2003; Debode *et al*., 2005), suggesting that resistance in *B. napus* had been derived from the C genome of *B. oleracea* (Happstadius *et al*., 2003; Rygulla *et al*., 2007b).

Stunting caused by *V. longisporum* infection represents another parameter well suited for scoring of resistance levels and therefore was determined at the last scoring time point (28 dpi). Stunting is a conclusive parameter regarding evaluation of resistance since correlation analysis has shown that plant height is strongly correlated with $AUDPC_{norm}$ values and the degree of fungal colonization of the stem (Eynck, 2008).

The assessment of resistance in selected breeding lines in the field revealed differential results depending on the experimental location. While in Göttingen and Rostock resistance levels were low to moderate (despite for incorporation of additional inoculum into the soil in Göttingen), disease levels in Fehmarn and Svalöv were constantly high in both investigated seasons. In Göttingen, the overall disease level was even lower compared to Rostock in 2009/10. A low infestation level in Göttingen was also found in 2005/06 (Eynck, 2008), indicating that even additional incorporation of inoculum into the soil does not assure a sufficiently high infection pressure. The higher disease pressure identified in Fehmarn is also consistent with previous results of *Verticillium* field resistance screenings conducted by Eynck (2008). In both cases, DI of selected field accessions were similar and ranged from 86% to 100%. Remarkably, in both investigations even the more moderately resistant cultivars ‘Express’ and ‘Oase’, which are characterized by low AUDPC values in the greenhouse and low DI and DS in Göttingen, exhibited high disease values in Fehmarn and Svalöv. In 2009/10, only five accessions displaying DI below 40% were identified in Svalöv, while disease values for Fehmarn were increased throughout.

Although several reasons can explain the discrepancy of the data obtained from different field sites, it shows that genotype-specific resistance is decreased at locations with high disease pressure, thus hampering a differentiation and screening for resistance. One of the main reasons for the high disease pressure is that Fehmarn and Sweden (especially Skåne, the major cultivation area for OSR (Steventon *et al*., 2002; Johansson *et al.*, 2006) have a long tradition in intensive cultivation of rapeseed, which may have led to an enhanced DI in these regions. In Sweden, *Verticillium* infected OSR plants were already reported in the late 1960s (Kroeker, 1970). Since VL microsclerotia can persist in the soil for more than 10 years (Heale and Karapapa, 1999) even after several months of soil temperatures around 0°C (Zielinski and Sadowski, 1998), soil inoculum is markedly accumulated in these rapeseed growing areas leading to high soil infestation.

Besides the soil inoculum density in these locations, several other factors may have been relevant for the observed differences in disease levels. The origin of different *V. longisporum* pathotypes may play an essential role in the extent of infection and colonization of the plant. As shown by pathogenicity tests with nine different *V. longisporum* isolates under greenhouse conditions, a broad range of aggressiveness levels towards *B. napus* exists among the different isolates of different origins (Heseker, 2009). Especially two isolates of Swedish origin elicited stronger disease symptoms on *B. napus* compared to the other tested isolates. While these tests demonstrated a broad spectrum of aggressiveness of nine *V. longisporum* isolates, they did not address the pathogenicity potential for a mixture of different isolates as it will likely be the case under field conditions. However, in our greenhouse trials a mixture of VL40 and VL43 isolates was used to mimic natural conditions. Pathogenicity of both isolates was compared to the isolates of Swedish origin in the above experiment (Heseker, 2009) and confirmed the high aggressiveness of the two isolates (Zeise and Tiedemann, 2002 a, b).

On the other hand, inoculation and screening methods in the greenhouse are not entirely comparable to infection induced by microsclerotia. Based on the assumption that infection in the field occurs already in autumn (Zeise and Seidel, 1990), plant age is comparable with that of greenhouse seedlings. However, roots of seedlings for greenhouse trials are injured and enable conidia to directly enter the vascular system without previous penetration of the root epidermal cells, which is not equivalent to field conditions where roots are mostly intact. Disease progress is therefore retarded under field conditions compared to those applied in greenhouse trials. Apart from inoculum density and the precise nature of the inoculation process, climatic conditions can have a crucial impact on disease development in the field. Keunecke (2009) showed that an increase in soil temperature by about 1°C in autumn can promote *Verticillium* infection in field trials. Laboratory investigations have shown that germination of *V. dahliae* (supposed to be *V. longisporum* on winter OSR) microsclerotia occurs in a broad temperature range from 6°C to 34°C with an optimum temperature of 20°C (Zielinski and Sadowski, 1998), whereas in another study optimum germination rates for *V. dahliae* and *V. longisporum* were found at 24°C (Stadler, 2010). Increased soil temperature caused by mild temperatures in autumn can therefore promote infection through microsclerotia. Similarly, higher air temperatures together with higher soil temperatures around the ripening stages of winter OSR (May to July) were also considered to promote disease development (Dunker *et al.*, 2008).

Another important parameter that has to be included when analyzing differences between controlled and natural screening conditions is the ripening of the plant, which is obviously linked to disease development in the field and can therefore skew scoring results. A novel

approach that circumvents complications in disease scoring due to the degree of ripening is the quantification of fungal DNA in the plants during vegetative growth (chapter 3).

Finally, another potential cause of poor correlation between scoring results from greenhouse and field screenings may be the use of different scoring parameters in the individual disease screenings. The greenhouse screening comprises the screening of whole plants, whereas in the field screening only parts of the plants (stubble) are scored.

Although confirmation of screening results from greenhouse data in field trials is hampered by various influential factors, some breeding lines showed good resistance to the pathogen both in the greenhouse and field (e.g. DSV 1-09, NICK 2-09 and SRG 4-09). Some further lines performed well in the field in 2008/09, although exhibiting higher AUDPC values in the greenhouse (SEM SW 2-09 and SEM SW 3-09). In 2009/10, DH 7-10 showed a low disease severity both under greenhouse and field conditions, while three other DH-lines (DH 8-10, DH 9-10 and DH 13-10) showed increased resistance only in the field.

In general, a combination of different screening approaches will provide unique and complementary information that is decisive at various stages throughout a screening process. Foremost, a rapid screening method to identify best performing genotypes is necessary to test large numbers of accessions. We have demonstrated that our greenhouse approach enables us to screen large numbers of accessions in one screening run within a short time frame. In this context, the combination of greenhouse experiments with field trials is important to further evaluate resistance stability. Obtaining a strong correlation between greenhouse and field experiments is difficult to realize since quantitative resistance is often strongly influenced by environmental conditions (Lindhout, 2002). However, qPCR analysis of fungal DNA in stems of field-grown rapeseed plants and associated greenhouse tests of four cultivars show a significant relationship (see chapter 3). In addition to regular field trials, it is also important to evaluate resistance under additional abiotic stresses, e.g. insufficient water supply or cold temperatures, in order to test the stability of the resistance under extreme conditions. First efforts towards this direction address the stability of resistance under drought stress (chapter 5).

Overall, the present data indicate that our current screening methodology is well suited to classify accessions for resistance if differences between resistance levels are sufficiently large, but is limited in accuracy when resistance levels of accessions are very close. Once resistant genotypes have been identified by rapid greenhouse phenotyping, stability of resistance under external environmental factors has to be further validated by modified greenhouse experiments and field experiments.

3. Assessment of field resistance of *B. napus* to *V. longisporum* by *in planta* quantification of fungal DNA with real-time PCR

3.1 Introduction

The soil-borne fungal pathogen *Verticillium longisporum* is the causal agent of premature ripening in oilseed rape (OSR). The disease is agronomically important in Northern Europe, especially in Sweden (Steventon, 2002; Zhou *et al.*, 2006) and Northern Germany (Daebeler *et al*., 1988; Zeise and Seidel, 1990; Günzelmann and Paul, 1989), but has also been reported from France, Poland, Ukraine (Heale and Karapapa, 1999) and UK (Gladders *et al.*, 2011). Recent field studies showed that *V. longisporum* holds a considerable yield damage potential if disease incidence is high and conditions are favorable (Dunker *et al*., 2008). Infection by *V. longisporum* occurs through the plant roots, followed by the systemic colonization of the host vascular system. Typically, this pathogen forms resting structures, referred to as microsclerotia. These microsclerotia are dormant in the soil unless coming into contact with root exudates, which promote their germination. Root directed movement of the hyphae is promoted by an exudate gradient surrounding the roots (Olsson and Nordbring-Hertz, 1985). Direct penetration of the rhizodermal cells near the root tips or penetration via wounds (Schnathorst, 1981) is followed by intra- and intercellular growth towards the root central cylinder, from which the fungus may enter the shoot vascular system and proceed into upper plant parts by hyphal growth and conidia travelling with the xylem sap (Eynck *et al.*, 2007). In a later stage of the vegetation period when plant senescence is initiated, the pathogen begins to colonize the parenchyma surrounding the vascular tissue and to form microsclerotia. This marks a transition from the parasitic to a saprophytic lifestyle, although this process is not yet well understood. Zeise and Seidel (1990) reported that symptoms are expressed when metabolic processes are changing at the beginning of the ripening phase. Recent studies of *B. napus*/*V. longisporum* interaction under controlled greenhouse conditions suggested the initiation of flowering to be crucial for pathogen spread (Zhou *et al.*, 2006). The formation of microsclerotia in necrotic plant tissue continues with progressing plant senescence and fungal resting structures return to the soil with plant debris (Schnathorst, 1981).

Importantly, a characteristic for the disease development in the field is a long period of latency during which the fungus does not produce symptoms distinguishable from natural senescence of the plants. Only after onset of plant maturity stages, first symptoms may appear as one-sided brownish discoloration of the stem, which however, is not always a conclusive symptom of *Verticillium* infection since insect damage can cause similar effects (Zhou *et al*., 2006; own observation). When the ripening of the crop has progressed, resting

structures are found subepidermally and in the pith (Zeise and Seidel, 1990; Heale and Karapapa, 1999).

So far, conventional screening of winter oilseed rape genotypes for resistance to *V. longisporum* has been performed by quantification of microsclerotia on the OSR stubble after harvest. Although this method helps to obtain a rough estimate of the levels of fungal colonization of the plants, the formation of microsclerotia and the time point of symptom expression obviously depend on the ripening of the crop (own observations; Zeise, 1992; Zeise and Steinbach, 2004). Since the production of microsclerotia inside the plant is promoted when a plant enters the ripening phase, this method is limited in adequately classifying the disease levels of early versus late ripening genotypes, as the latter ones will score artificially low compared to plants that have already further matured. Therefore, these complications interfere with the uniformity and reproducibility of such stubble screening. Moreover, the estimation of disease severity by scoring of fungal resting structures implies that the fungus is in the saprophytic phase of its life cycle. Together with the dependence on the maturity stage of the plant tissue, these are suboptimal conditions for the evaluation of the resistance level of a plant genotype. It would therefore be desirable to have a method available that supports detection of the fungus in the biotrophic phase prior to symptom development in the field. For that purpose a quantitative real-time PCR (qPCR) method was developed that permits sensitive quantification of the fungus in field grown OSR plants. Real-time PCR is a refinement of conventional PCR and is based on monitoring of the PCR product after each amplification cycle by fluorescence emission measurement (Brouwer *et al*., 2003). Amplicon detection can be achieved by chemistries that can be roughly divided into amplicon-independent methods (e.g. SYBR Green I (Morrison *et al*., 1998) or YO-PRO-1 (Ishiguro *et al*., 1995)) or amplicon-specific methods (fluorescence resonance energy transfer (FRET), Cardullo *et al*., 1998) (Schena *et al*., 2004). The main advantages of real-time PCR approaches are its superior sensitivity, rapid performance and versatility (Schena *et al*., 2004). Owing to its sensitivity, real-time PCR holds the potential to detect even minute differences in host resistance or susceptibility (Gayoso *et al*., 2007) and to monitor disease progression (Brouwer *et al*., 2003). Lievens *et al.* (2006) were among the first to apply real-time PCR to the sensitive detection of different *Verticillium* spp. Several other reports exist that describe the detection and quantification of *Verticillium* spp. in plant species by qPCR-based methods. For instance, *V. dahliae* could be successfully quantified in olive trees (Mercado-Blanco *et al*., 2003) and the resistance of olive trees to *Verticillium* pathotypes was quantitatively assessed by qPCR (Markakis *et al.*, 2009). In similar studies, *V. dahliae* colonization of potato was monitored by multiplex real-time PCR (*Atallah* et al., 2007) and real-time PCR was applied to the quantitative assessment of *V. albo-atrum* infestation levels

in alfalfa plants differing in their susceptibility to the fungus (Larsen et al., 2007). Gayoso *et al.* (2007) used a similar approach to study differences in susceptibility of four *C. annuum* cultivars to *V. dahliae* by real-time PCR. One limitation of the technique is the inability to discriminate between viable and non-viable fungal biomass. Therefore complementary methods, e.g plating assays (Markakis *et al*., 2009) or Bio-PCR (Schena *et al*., 2004) are frequently used to confirm viability of the fungus in the plant (Markakis *et al*., 2009).

Here, we evaluate different primer pairs targeting distinct gene loci in *V. longisporum* for their specific and sensitive detection of fungal DNA purified from rapeseed stems and assess this method for its ability to distinguish between susceptible and resistant winter OSR cultivars in field trials and greenhouse experiments. While greenhouse trials provide a rapid screening method to identify resistance in *B. napus* plants to *V. longisporum* and permit to screen large numbers of different genotypes, root-dip-inoculation and controlled greenhouse conditions do not adequately mimic *Verticillium* infection via microsclerotia inoculum under environmental conditions (Eynck, 2008). It is therefore important to augment greenhouse trials with field experiments in order to improve resistance screenings for breeding purposes, which warrants a technique that permits a consistent readout of infestation levels. The alternative method for detection and quantification of VL in field trials presented here provides a tool for classification of resistant genotypes for integration into breeding of elite cultivars and to monitor disease dynamics in the field.

3.2 Material and Methods

3.2.1 Primer design

Primers targeting the multicopy ribosomal internal transcribed spacer (ITS) region gene were designed based on detailed analysis of *Verticillium* ITS sequences (Fahleson *et. al*., 2004, Nazar *et al.*, 1991, Robb *et al*., 1993). Based on these data, four primer pairs were designed and tested, of which the OLG70/OLG71 system showed the best performance.

In addition to previously described primers, a primer pair specifically targeting the ß-tubulin gene from *V. longisporum* isolates was used for qPCR (Table 3.1).

Table 3.1 List of primers used for qPCR-analysis

Name	Direction	Target	Sequence (5´→3´)	PCR product size
OLG 70	Forward	ITS	CAGCGAAACGCGATATGTAG	**261 bp**
OLG 71	Reverse		GGCTTGTAGGGGGTTTAGA	
VlTubF2[a]	Forward	ß-tubulin	GCAAAACCCTACCGGGTTATG	**143 bp**
VlTubR1[a]	Reverse		AGATATCCATCGGACTGTTCGTA	

[a] reference: Debode *et al.*, 2011

3.2.2 Evaluation of primer specificity and sensitivity

3.2.2.1 Fungal isolates

For evaluation of the primer specificity a collection of 49 different fungal pathogens isolated from *B. napus* and various other plant species (Table 3.2) were grown in potato dextrose broth (PDB) or Czapeck Dox medium for 7 to10 days at 23°C and 100 rpm. The mycelium of the fungi was isolated by filtration (0.2 µm), rinsed with tap water and subsequently lyophilized for 24 h (Freeze Dryer, Martin Christ Freeze Dryers, Osterode am Harz, Germany). Mycelium was crushed with a mixer mill (Retsch MM 200, Retsch GmbH, Haan, Germany) and DNA was extracted from 40 to 50 mg of fine mycelium powder with the DNeasy Plant Mini Kit (Qiagen GmbH, Hilden, Germany). The quality of the DNA was verified in an ethidium bromide stained agarose gel and DNA concentration was adjusted to ~100 pg/µl by densitometry as described in 3.2.6.

3.2.2.2 Primer specificity

Primer specificity was tested on a collection of 15 *V. longisporum* isolates, 10 *V. dahliae* isolates, three additional *Verticillium* species and 21 other fungal pathogens of OSR (Table 3.2). QPCR analysis with both primer pairs was performed as described in 3.2.5.3.

Table 3.2 Overview of tested fungal isolates for the evaluation of primer specificity

				qPCR amplification	
Isolate	**Organism**	**Host**	**Origin**	ITS	tubulin
Vl 82	*Verticillium longisporum*	*Brassica napus*	Germany	27.3	N/A
Vl 59	*Verticillium longisporum*	*Brassica oleracea var. botrytis*	USA	15.52	29.11
Vl 18	*Verticillium longisporum*	*Brassica napus*	Germany	15.39	29.89
Vl S2	*Verticillium longisporum*	*Brassica napus*	Sweden	19.04	33.78
Vl S3	*Verticillium longisporum*	*Brassica napus*	Sweden	19.72	34.73
Vl S6	*Verticillium longisporum*	*Brassica napus*	Sweden	17.87	33.63
Vl S29	*Verticillium longisporum*	*Brassica napus*	Sweden	19.17	34.22
Vl 40	*Verticillium longisporum*	*Brassica napus*	Germany	19.70	34.21
Vl 60	*Verticillium longisporum*	*B.oleracea var. botrytis*	USA	18.65	N/A
Vl 84	*Verticillium longisporum*	*Brassica napus*	Germany	18.43	34.40
Vl Eschwege	*Verticillium longisporum*	*Brassica napus*	Germany	21.57	N/A
Bob 70	*Verticillium longisporum*	*Brassica napus*	USA	18.33	33.38
Chalons en Champs	*Verticillium longisporum*	*Brassica napus*	France	18.33	31.27
Vl 83	*Verticillium longisporum*	*Brassica napus*	Germany	22.88[a]	37.35
Vl 43	*Verticillium longisporum*	*Brassica napus*	Germany	16.25	30.73
Vd 13	*Verticillium dahliae*	*Gossypium hirsustum*	Spain	14.37	N/A
Vd 16	*Verticillium dahliae*	*Solanum tuberosum*	Germany	17.74	N/A
Vd 76	*Verticillium dahliae*	*Gossypium sp.*	USA	14.18	27.40
Vd 57	*Verticillium dahliae*	*Fragaria x ananassa*	Germany	14.47	N/A
Vd 49	*Verticillium dahliae*	*Capsicum annuum*	Austria	15.22[a]	N/A
Vd 41	*Verticillium dahliae*	*Brassica rapa*	Germany	18.94	N/A

Continuing from previous page (**Table 3.2**)

Vd 85	*Verticillium dahliae*	*Solanum tuberosum*	Germany	21.06	N/A
Vd 52	*Verticillium dahliae*	*Capsicum annuum*	Austria	18.55	N/A
Vd 3	*Verticillium dahliae*	*Fragaria x ananassa*	Germany	13.12[a]	N/A
Vd 88	*Verticillium dahliae*	*Solanum tuberosum*	Germany	22.24[a]	N/A
V 1.0	*Verticillium albo-atrum*	*Solanum tuberosum*	USA	18.78	N/A
V 1.6	*Verticillium tenerum*	*Vitis*	n.i.	33.06	N/A
V 1.1	*Verticillim chlamydosporium*	n.i.	n.i.	N/A	N/A
FC 34,35,36	*Fusarium culmorum*	*Triticum aestivum*	Germany	N/A	N/A
A 4.6	*Alternaria spp.*	*Helianthus. annuus*	Germany	35.14	N/A
A 4.7	*Alternaria spp.*	*Zea mays*	Germany	32.58	N/A
A 4.1.1	*Alternaria alternata*	*Triticum aestivum*	n.i.	33.86	N/A
A 4.11	*Alternaria spp.*	*Beta vulgaris*	Austria	34.12	N/A
IBCN 30	*Leptosphaeria biglobosa*	*Brassica. napus*	Australia	N/A	N/A
IBCN 64	*Leptosphaeria biglobosa*	*Brassica. napus*	Canada	N/A	N/A
IBCN 3	*Leptosphaeria maculans*	*Brassica. napus*	Germany	N/A	N/A
V 1.1	*Botrytis cinerea*	*Brassica. napus*	Germany	N/A	N/A
B 1.10	*Botrytis cinerea*	*Vitis vinifera*	Germany	28.78[a]	N/A
B 1.12	*Botrytis cinerea*	*Brassica napus*	Germany	N/A	N/A
B 1.13	*Botrytis cinerea*	*Brassica napus*	Germany	N/A	N/A
S. Svalöv 09	*Sclerotinia sclerotiorum*	*Brassica napus*	Sweden	N/A	N/A
S. Fehmarn 09	*Sclerotinia sclerotiorum*	*Brassica napus*	Germany	N/A	N/A
S. Rostock 09	*Sclerotinia sclerotiorum*	*Brassica napus*	Germany	N/A	N/A
S. Göttingen	*Sclerotinia sclerotiorum*	*Brassica napus*	Germany	N/A	N/A
S. Lübeck	*Sclerotinia sclerotiorum*	*Brassica napus*	Germany	N/A	N/A
S. Canada	*Sclerotinia sclerotiorum*	n.i.	Canada	N/A	N/A
S. Indien	*Sclerotinia sclerotiorum*	n.i.	India	N/A	N/A
S. Brasilien	*Sclerotinia sclerotiorum*	n.i.	Brazil	N/A	N/A
Ec1	*Erysiphe cruciferarum*	*Brassica napus*	Germany	N/A	N/A

Amplification was positive if baseline threshold was exceeded and maximum melting temperature was consistent with expected Tm_{max} of the product. n.i. no information; [a] initial fungal DNA concentration for qPCR unknown; N/A = no amplification

3.2.2.3 Primer sensitivity

Genomic DNA of *V. longisporum* isolate VL43 served as the template to determine the sensitivity of both primer pairs for amplification of *V. longisporum* DNA. A 3-fold dilution series consisting of 100 pg, 33.3 pg, 11.1 pg, 3.70 pg, 1.23 pg, 412 fg, 137 fg, 45.7 fg, 15.2 fg, 5.08 fg, 1.69 fg, 0.56 fg and 0.19 fg was produced and amplified in 5 technical replicates on a CFX system as described in 3.2.8.3. The mean threshold cycle (C_T) values of the five replicates were fit by linear regression to derive the template DNA concentration.

Additionally, evaluation of primer sensitivity and specificity was also performed on a different thermocycler (iCycler system, BioRad, Hercules, CA, USA), primarily to detect optimal qPCR conditions such as annealing temperature for tubulin primers. In this case, genomic DNA of five different fungal pathogens including *A. alternata*, *S. sclerotiorum*, *B. cinerea*, *L. biglobosa*, *L. maculans* A1 was used for evaluation of primer specificity (Table 3.3). For DNA extraction, fungal isolates (*B. cinerea*, *L. maculans*, *S. sclerotiorum*) were grown on potato glucose agar (Roth, Karlsruhe, Germany), oatmeal agar (*A. alternata*) or V8 medium

(vegetable juice supplemented with 3 g/L $CaCO_3$, 18 g/L agar and 0.2 g/L streptomycin sulfate; *L. biglobosa*). Mycelium agar plugs from these culture plates were transferred to 150 ml potato extract glucose broth (Roth, Karlsruhe, Germany) in 300 ml Erlenmeyer flask and were grown for 8 days at 20°C (*A. alternata*: 23°C) and 100 rpm. Fungal mycelium was isolated by filtration (0.2 µm), rinsed with tap water and subsequently crushed in liquid nitrogen. According to manufacturer's instructions, DNA was extracted from approximately 100 mg fresh mycelium with the DNeasy Plant Mini Kit (Qiagen GmbH, Hilden, Germany). Quality of genomic DNA was evaluated on a 1.5% agarose gel stained with ethidium bromide and imaged by UV-light on a gel documentation system (Quantity One, Version 4.5.0 Bio-Rad Laboratories, Hercules, USA). Reaction mixtures for qPCR consisted of 100 pg genomic DNA of VL43 and 0.3 µM of each primer in Thermo Scientific PCR Master Mix (Absolute Blue QPCR SYBR Green Fluorescein Mix: 10 nM Fluorescein, 3 mM $MgCl_2$) in a total volume of 25 µl. The PCR-program included an initial denaturation step of 15 min, followed by 40 cycles with a denaturation step (15 s at 95°C), annealing (30 s in a gradient ranging from 54.8°C to 63.5°C) and subsequent extension (20 s at 72°C). Fluorescence was detected after each elongation step and the program was completed with a final elongation step of 5 min at 72.0°C. The melt curve analysis was performed with 95°C for 1 min, followed by a 55.0°C step for 1 min and subsequent measurements within a range of 55°C to 95°C (every 10 s in 0.5°C temperature increments).

Table 3.3 Overview of fungal isolates for the evaluation of primer specificity

				qPCR amplification	
Isolate	**Organism**	**Host**	**Origin**	ITS	tubulin
VL43	*V. longisporum*	*B. napus*	Germany	15.2	26.9
lyophilisate 0048	*A. alternata*	*B. napus*	Germany	N/A	N/A
Ss 1.5	*S. sclerotiorum*	*B. napus*	Germany	N/A	N/A
0865	*B. cinerea*	*B. napus*	Germany	N/A	N/A
NA22	*L. biglobosa*	*B. napus*	Germany	N/A	N/A
T12aD34	*L. maculans A1*	*B. napus*	Germany	N/A	N/A

N/A: no amplification

3.2.3 Amplification of fungal DNA in the presence of non-target DNA

To test for inhibition of PCR amplification by genomic plant DNA a 10-fold serial dilution of genomic fungal DNA (target-DNA) of *V. longisporum* isolate VL43 was supplemented with a 1:10 dilution of genomic plant DNA (non-target DNA, Table 3.4) containing inevitable traces of fungal DNA. Genomic plant DNA was extracted from a field-grown *B. napus* plant as described in paragraph 3.2.5.3. Inhibition assays were performed for both ITS and tubulin

primers. QPCR reactions were performed on a CFX 384 Real-Time PCR system and conditions for qPCR amplifications were the same as described in paragraph 3.2.5.3.

Table 3.4 Setup for preparation of standards supplemented with genomic plant DNA for quantification of *V. longisporum* DNA in field grown *B. napus* stems

Final concentration	100 pg	10 pg	1 pg	0.1 pg	0.01 pg	0.001 pg
Volume VL43 DNA	5 µl (1 ng/µl)	5 µl (100 pg/µl)	5 µl (10 pg/µl)	5 µl (1 pg/µl)	5 µl (0.1 pg/µl)	5 µl (0.01 pg/µl)
Volume Plant ([DNA] ~20 ng/µl)	5 µl	5 µl	5 µl	5 µl	5 µl	5 µl
Buffer (TE 0.5x)	45 µl	45 µl	45 µl	45 µl	45 µl	45 µl

3.2.4 Greenhouse trials

3.2.4.1 Plant material

Four winter oilseed rape cultivars were used for field and greenhouse trials; two susceptible cultivars, ‘Falcon’ (Norddeutsche Pflanzenzucht, NPZ, Hans-Georg Lembke KG, Hohenlieth, Germany) and ‘Laser’ *(*Syngenta Seeds GmbH), as well as two moderately resistant cultivars, ‘Express’ (Norddeutsche Pflanzenzucht, NPZ, Hans-Georg Lembke KG, Hohenlieth, Germany) and ‘Oase’ (Deutsche Saatveredelung Lippstadt Bremen GmbH, DSV).

3.2.4.2 Fungal cultures for greenhouse trials

For inoculation in the greenhouse the *V. longisporum* mixed isolates of VL43 and VL40 originating from *B. napus* from Mecklenburg-West Pomerania (Zeise and Tiedemann, 2001; Zeise and Tiedemann, 2002a; Zeise and Tiedemann, 2002b) were used. Stock cultures were produced by supplementing conidial suspensions in Czapek-Dox medium with 25% glycerol and stored at -80°C. For plant inoculation, fungal cultures were produced by cultivation of 500 µl stock solution in 150 ml potato extract glucose broth (Roth, Karlsruhe, Germany) in 300 ml Erlenmeyer flasks on a rotary shaker at 100 rpm and 23°C. Mycelium was filtered through a sterile fine cloth after 7 to 20 days of cultivation and spore concentration was adjusted to $1*10^6$ conidia/ml with a Thoma haemocytometer (Eynck, 2008).

3.2.4.3 Cultivation of the plants and root dip inoculation

Seeds of the four cultivars were surface sterilized for 1 to 2 min in 70% ethanol and sown into silica sand for cultivation in the greenhouse where they were subjected to day/night conditions of 16 h/8 h at 20°C. After 7 to 10 days seedlings were removed from the silica sand and roots were cleaned under running tap water. The terminal root parts of the seedlings were cut with scissors and injured seedlings were placed in a glass beaker containing the conidial suspension of VL43. The plants were inoculated for about 30 min and control plants were placed in tap water for the same period. Finally, a total of 20 inoculated and control seedlings each were repotted into a soil mixture consisting of sand, peat and compost (1:1:2), resulting in two plants per pot. Plants were grown in the greenhouse under conditions as described above.

3.2.4.4 Evaluation of disease severity in the greenhouse

The development of symptoms was recorded weekly from 7 dpi to 28 dpi (Table 3.5) using an assessment key according to Eynck (2008; modified from Zeise (1992)).

Table 3.5 Assessment key for the evaluation of the disease severity of *B. napus* plants infected by *V. longisporum*.

Score	Symptom development
1	No symptoms
2	Weak symptoms on the oldest leaf (yellowing, black veins)
3	Weak symptoms on the next younger leaves
4	About 50% of the leaves have symptoms
5	> 50% of the leaves have symptoms
6	Up to 50% of the leaves are dead
7	> 50% of the leaves are dead
8	Only apex is still alive
9	The plant is dead

For evaluation of the disease severity area under the disease progress curve (AUDPC) values were calculated according to the formula (Shaner and Finney, 1977, Campbell and Madden, 1990):

$$\text{AUDPC} = \sum_{i=1}^{n} (y_i + y_{i+1}/2) * (t_{i+1} - t_i)$$

where n = number of observations, i = time point of observation, y_i = disease severity value at i*th* observation, and t_i = time (days) at the i*th* observation.

Next, AUDPC values were scaled by calculating the difference between the AUDPC value of the inoculated plant and the respective control plant (Eynck, 2008). These 'net AUDPC values' ($AUDPC_{net}$) consider symptoms that occur in natural senescence such as yellowing of the leaves.
Since *V. longisporum* symptoms include reduced growth, i.e. stunting of the plants, the plant height was measured at 28 dpi from the insertion of the cotyledons to the tip of the shoots.

3.2.5 Field trial

3.2.5.1 Plant material

In the season 2008/09, the four winter oilseed rape cultivars 'Falcon', 'Laser', 'Express' and 'Oase' were sown on 14th of August 2008 in a field near Göttingen, Lower-Saxony (Germany). Seeds were coated with a Cruiser seed coat (Syngenta Agro GmbH) and seeding density was 50 seeds/m^2. Immediately prior to sowing, *Verticillium* inoculum (15 g of infested stubbles per m^2) was evenly distributed on the soil surface by hand and was then incorporated by a rotary harrow into the upper soil layers. The inoculum was prepared by milling dried rapeseed stubbles that were heavily infected with microsclerotia. The plots with a size of 14.7 m^2 (9.8 x 1.5 m) were arranged in a randomized block design with two replicates. Pesticide treatment was performed according to standard cultural practices, including the spraying of fungicides against *Phoma lingam* and *Sclerotinia sclerotiorum* at the adequate stages of plant growth. See Appendix, Table A 1 for an overview of applied cultural practices.

3.2.5.2 Experimental design and evaluation of disease severity in the field by screening of stubbles

For the visual scoring of disease symptoms 25 stubbles of each plot were randomly sampled immediately after harvest (GS 97) and screened for both disease incidence (DI) and disease severity (DS). For estimation of the disease severity the amount of subepidermal microsclerotia (directly beneath the epidermis), microsclerotia in the pith tissue and in the root tissue were determined by binocular microscopy and scored with a 1 to 4 assessment key according to Eynck (2008) (Table 3.6).

Table 3.6 Assessment key for the evaluation of the disease severity of *B. napus* stubbles infected by *V. longisporum*.

Score	Symptom development
1	No microsclerotia visible in tissue
2	Low abundance of microsclerotia
3	High abundance of microsclerotia
4	Tissue heavily infested with microsclerotia, epidermis is peeling off from the stubble

Based on this scoring, a disease index was calculated according to Eynck (2008):

$$\text{Disease Index} = \frac{(1 \times N_1) + (2 \times N_2) + (3 \times N_3) + (4 \times N_4)}{n}$$

where N_n = number of plants in the respective class, 1-4 = score numbers and n = total number of given scores.

3.2.5.3 DNA extraction from field plants and qPCR analysis

In the season 2008/09 five plant samples per plot were randomly harvested at growth stage 65 and 80 (phenological growth stage assessment by BBCH identification key according to Weber and Bleiholder, 1990 and Lancashire *et al*., 1991) and a 10 cm stretch of the stem part was excised in a distance of approx. 5 cm from the root crown (Figure 3.1). The stems were rinsed and stored at -20°C until further preparation. Stem tissue was lyophilized for 96 h (Freeze Dryer Alpha 1-4, Martin Christ Freeze Dryers, Osterode am Harz, Germany) and subsequently crushed with a mill (Retsch KG, Haan, Germany), followed by grinding with a mixer mill (Retsch MM 200, Retsch GmbH, Haan, Germany). The DNA of 1 g plant material (5 pooled stems) was isolated according to a modified CTAB protocol by Brandfass and Karlovsky (2008). Following the CTAB treatment, 400 µl supernatant were transferred to a 1.5 ml reaction tube and 4 µl of RNAse A of the DNeasy Plant Mini Kit (Qiagen GmbH, Hilden, Germany) was added. The DNA extraction was further performed with the kit according to the manual instructions. The quality of the purified DNA was verified in an ethidium bromide stained agarose gel (1% Agarose in TAE buffer) after UV-visualization and imaged by a gel documentation system (Quantity One, Version 4.5.0 Bio-Rad Laboratories, Hercules, USA). For qPCR reactions a CFX 384 Real-Time PCR detection system including a C1000 thermal cycler base with a CFX 384 optical reaction module was used. The ITS primers OLG 70/OLG 71 amplified a 261 bp fragment of the ITS region. The primer pair

VlTub F2/VlTub R1 amplified a 142 bp fragment of the tubulin region (Table 3.1). The reaction mixture of 10 µl consisted of ≈ 5-10 ng purified genomic DNA and 0.3 µM of each primer in Thermo Scientific PCR Master Mix (Absolute Blue QPCR SYBR Green Fluorescein Mix: 10 nM Fluorescein, 3 mM $MgCl_2$). Each DNA-sample was measured in three technical replicates from which mean starting quantity values were calculated. The PCR program consisted of 15 min at 95°C activation step, followed by 40 cycles with 10 s at 95°C, 15 s at 60°C and 15 s at 72°C. Fluorescence was detected after each elongation step and the program was completed with a final elongation step of 2 min at 72.0°C. For evaluation of the amplification specificity, melting curve analysis was performed by an initial denaturation step at 95.0°C for 10 s, followed by a 55.0°C step for 10 s and subsequent measurements within a range of 55°C to 95°C (every 5 s in 0.5°C temperature increments).

Figure 3.1 Sample site of a rapeseed stubble for qPCR analysis.

3.2.6 Preparation of DNA standards for qPCR analysis of field samples

For quantification of fungal DNA concentrations in infected rapeseed tissue, a 10-fold dilution series was run on the same PCR plate. For the standard curve in a range from 1 ng to 0.0001 pg, genomic DNA of the *V. longisporum* isolate VL43 was purified with the DNeasy Plant Mini Kit (Qiagen GmbH, Hilden, Germany) and DNA concentrations of 5 µl aliquots were adjusted by densitometry with ethidium bromide (< 0.0001% (v/v)) stained agarose gels (1% (w/v) in TAE) using Lambda Phage DNA. To quantify unknown DNA concentrations, a standard curve was generated with Lambda Phage DNA concentrations ranging from 10 ng to 50 ng. Because of possible interference of substances such as buffer salts with photometrical readings, DNA concentrations were determined by densitometry and not by photometrical measurements at 260 nm. Gel documentation and analysis was performed with the Multi-Analyst software (Version 1.1, Bio-Rad Laboratories, Hercules, USA).

3.2.7 Comparison of disease incidence, net AUDPC values and DNA content

For comparison of the various methods applied for disease assessment in this study (visual scoring of stubbles, qPCR based quantification of fungal DNA in stems and recording of AUDPC values in the greenhouse), disease incidence (%), fungal DNA content and net AUDPC values of 39 accessions including the four reference cultivars ‘Falcon’, ‘Laser’, ‘Express’ and ‘Oase’ was investigated in the experimental year 2008/09. The experimental setup for the field trial in 2008/09 is explained in paragraph 3.2.5.1, the evaluation of disease severity by screening of stubbles is defined in paragraph 3.2.5.2 and the quantification of fungal DNA in rapeseed stems with ITS primers is described in paragraph 3.2.5.3. The greenhouse screening is explained in paragraph 3.2.4.4. Putative relationships between the obtained screening data were analyzed by Spearman rank correlation analysis.

3.2.8 Statistical analysis

Statistical analysis was performed with STATISTICA for Windows Version 9.1 (Statsoft, Inc. 2010). The mean data of 20 replicates (AUDPC values) was analyzed with analysis of variance (ANOVA). For determination of the least significant difference (LSD) between the mean values a Fisher LSD test was used at $p \leq 0.05$. A Spearman rank correlation between field data (disease incidence (%)), greenhouse values (net AUDPC) and qPCR data (ng *Verticillium* DNA/g dry weight) was calculated by using the mean of 2 (disease incidence and fungal DNA-content in OSR stems) or 20 (net AUDPC) replicates.

3.3 Results

3.3.1 Primer sensitivity tests reveal significant differences between primer pairs

Two different primer pairs (OLG 70/71 and VlTubF2/R1) were evaluated for their specificity and sensitivity in amplification of fungal DNA from rapeseed stems. To compare sensitivity of both primer pairs we produced threefold serial dilutions of fungal DNA and determined C_T values for each concentration. Slopes of the regression curves to mean C_T values obtained for the ITS primers and the β-tubulin primers only marginally differ with values of -3.5 and -4.2, respectively (Figure 3.2). PCR efficiency of ITS and tubulin primers was 92.0% and 70.6%, respectively. The accuracy of the serial dilutions is reflected in the R^2 curves values of 0.99 and 0.97 for the ITS primers and the β-tubulin primers and standard deviations of mean C_T derived from technical replicates are low. The PCR product amplified from 100 pg fungal DNA was already detected at a mean C_T-value of 16 when using ITS primers, whereas tubulin primers required 31 C_T-cycles to detect the same amount of DNA. On average qPCR experiments performed with ITS primers showed C_T-values that were 15 times lower than those obtained with tubulin primers, meaning that ITS primers were about 32,000 times more sensitive (provided a PCR efficiency of 100%). With a maximum of 40 amplification cycles the minimum amount of fungal DNA that could be successfully amplified was 1.23 pg for VlTubF2/ VlTubR1 and 0.19 fg for OLG 70/7, respectively.

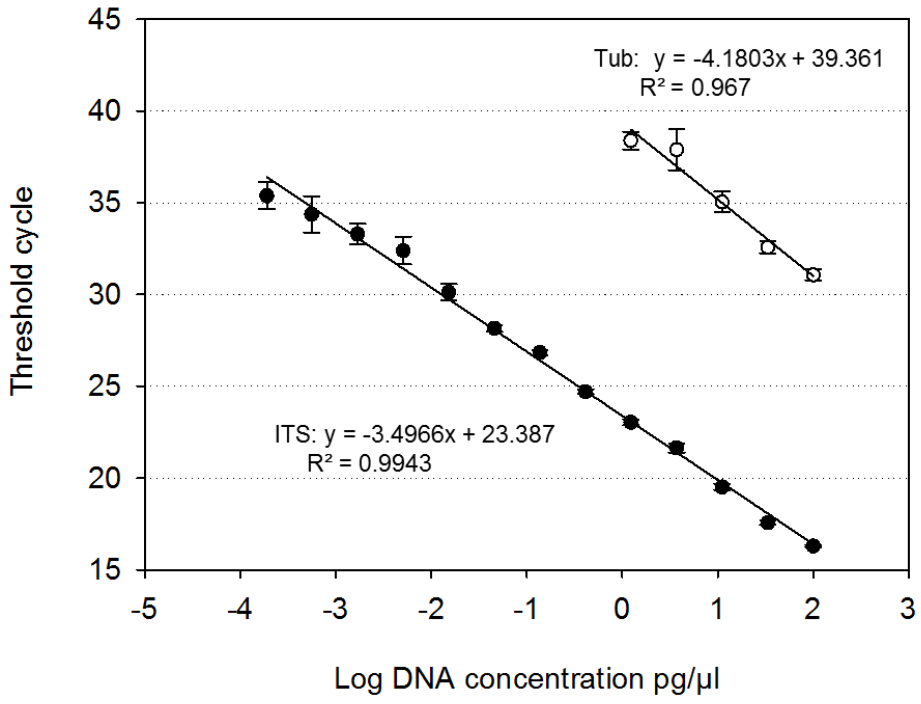

Figure 3.2 Standard curves of 3-fold serial dilution of *V. longisporum* genomic DNA amplified with either ITS primers or tubulin primers. Data are means of 5 replicates (± s.d.).

The melting curves derived for the two different primer pairs are shown in Figure 3.3. While the maximum T_m value for β-tubulin primers is 83.5, ITS primers have a 4°C higher T_m (T_m^{max} =87.5°C).

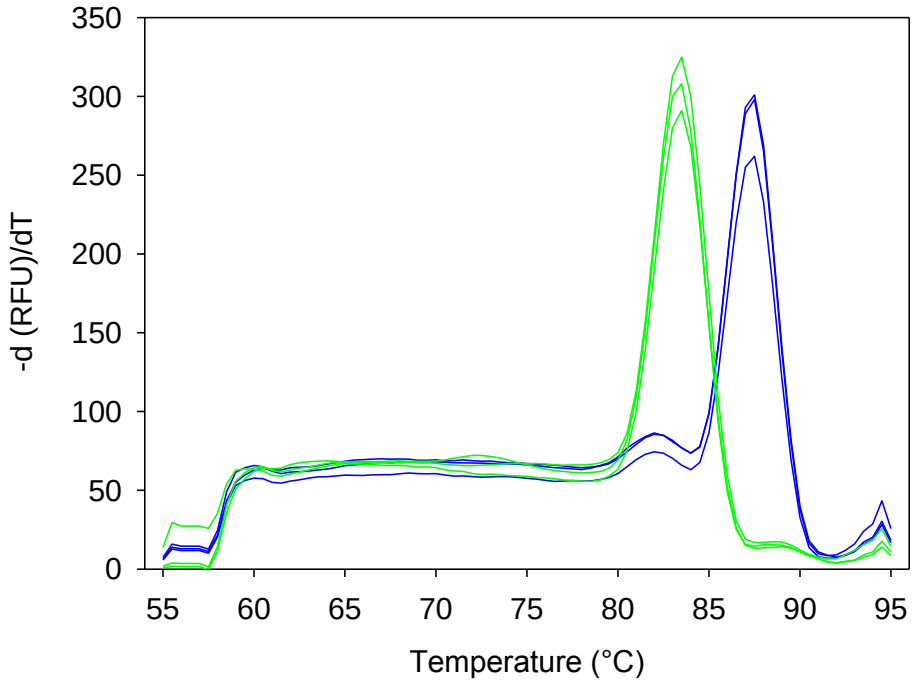

Figure 3.3 Melting curves for qPCR amplification of 100 pg VL43 DNA (n=3) with ITS (blue) and tubulin (green) primer pairs, respectively. –d(RFU)/dT = negative derivative of relative fluorescence with respect to temperature.

3.3.2 Primer specificity

To evaluate specificity of the primers, genomic DNA of a broad range of *V. dahliae* and *V. longisporum* isolates and other fungal rapeseed pathogens was purified and analyzed by quantitative PCR. Tubulin primers revealed high specificity for most of the *V. longisporum* isolates derived from different geographic origins. Interestingly, the three isolates Vl 82, Vl 60 and Vl Eschwege were not detected by the tubulin primers (Table 3.2). DNA of neither *V. dahliae* isolates (with the exception of isolate Vd 76) nor the other isolates of OSR pathogens were targeted by these primers. The ITS primers showed specificity for *Verticillium* isolates but did not distinguish between *V. longisporum and V. dahliae* species. In addition, the ITS primers unspecifically amplified DNA from *Botrytis* and *Alternaria*.

3.3.3 Performance of primer pairs with the iCycler system

Following the characterization of primers on the CFX system, we performed sensitivity and specificity assays on a different thermocycler (iCycler) with five different fungal rapeseed pathogens. In order to optimize our protocol for maximum performance in terms of specificity and sensitivity, we performed a temperature gradient qPCR to determine the optimal annealing temperature for both primer systems with the aim to rationalize the low sensitivity observed for the tubulin primers on the CFX-system. Our data show that both primer pairs specifically amplify fungal DNA of isolate VL43 (Table 3.3) with minimal C_T values at an annealing temperature of 60.4°C and 63.5°C for ITS and tubulin primers, respectively (Figure 3.4). A marked upward shift of 11.5 C_T cycles was observed for the amplification signal of the tubulin primers with respect to the signal from the ITS primers, marking a significant increase in sensitivity for the ITS primer system (Table 3.3). However, the difference in C_T-values was not as high as in the CFX-system (paragraph 3.3.1), where a shift of 15 C_T-values was observed. An increase in annealing temperature to approximately 63°C for the qPCR run in the CFX system may improve tubulin primer performance, but not to such an extent that primer sensitivities are comparably good. Performance of gradient qPCR also shows that amplification with tubulin primers is not stable over a range of different annealing temperatures, i.e. the tubulin based system is sensitive to alterations in PCR sequence such as temperature fluctuations. In contrast, amplification by ITS primers is stable over a wide temperature range.

Concerning specificity, neither of the primer pairs amplified any of the other five tested fungal species. However, melting curve analysis identified some unspecific products, in particular at lower annealing temperatures.

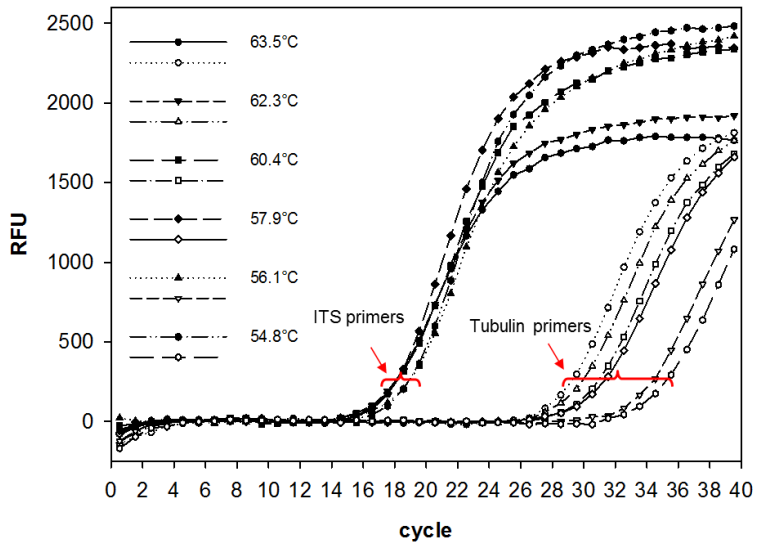

Figure 3.4 Amplification plot showing the accumulation of PCR product amplified with ITS and tubulin primers from of *V. longisporum* VL43 (iCycler system). Symbols indicate corresponding annealing temperatures. RFU = relative fluorescence units.

3.3.4 Plant DNA does not affect PCR amplification of fungal DNA

Recent studies demonstrated that genomic DNA of *B. napus* plants grown in greenhouse did not inhibit amplification of *V. longisporum* DNA (Eynck *et al.*, 2007). However, inhibitory effects of genomic DNA purified from field-grown *B. napus* plants grown in the field have not been evaluated yet. To simulate matrix effects and assess whether plant genomic DNA affects amplification of fungal DNA, we prepared 10-fold dilution series consisting of a mixture of fungal and plant DNA. Accurate estimation of inhibitory effects is complicated by contamination of plant DNA by traces of fungal DNA, which can introduce bias by lowering C_T values. However, we were able to correct for this artifact by calculating the contaminant DNA concentration from standard curves obtained exclusively with genomic VL43 DNA and subtracting this estimate from each step of the dilution series. This allowed us to construct a standard series consisting of fungal genomic DNA and plant-derived matrix DNA next to the established standard series obtained from fungal DNA alone. No inhibitory effect of plant genomic DNA became apparent during amplification with the ITS primer system (Figure 3.5). Both standard curves have similar slopes and excellent R^2 values. Identical experiments performed with tubulin primers did also not show apparent inhibitory effects (data not shown). Since plant genomic DNA does not seem to affect PCR reactions targeting fungal DNA, established fungal DNA standards were used for evaluation of field samples.

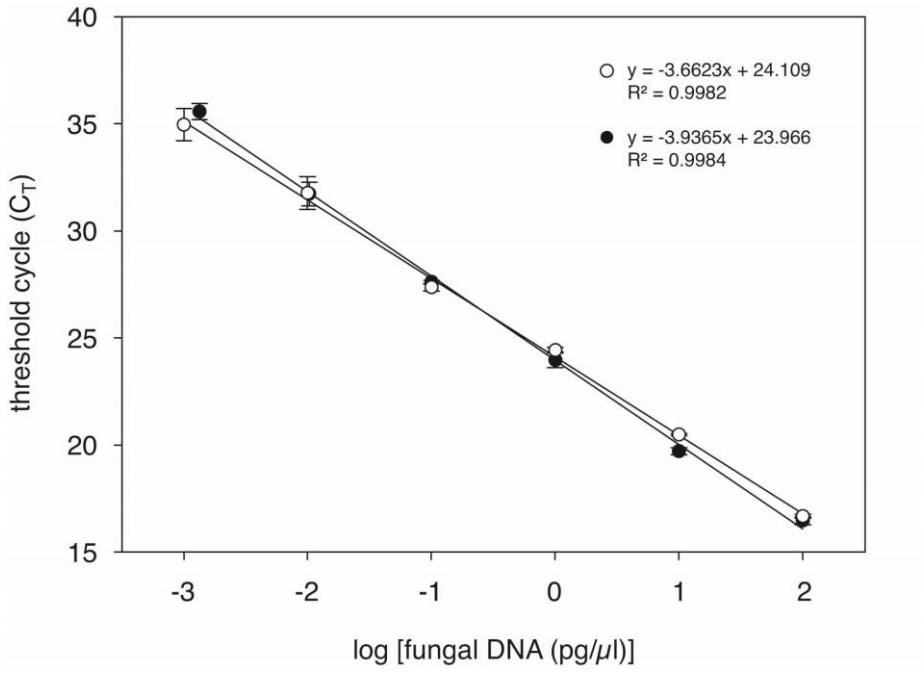

Figure 3.5 Standard curves of a 10-fold serial dilution of *V. longisporum* genomic DNA in the presence (•) or absence (o) of 2 ng plant DNA for the quantification of *V. longisporum* by qPCR with ITS primers. Data shown are means (± s.d.) of 3 replicates.

3.3.5 Comparison of performance of ITS and tubulin-based primers

The result of the performance of the two primer pairs is summarized in Table 3.7. The data show that overall performance of ITS primers is superior compared to the tubulin primer system.

Table 3.7 Comparison of performance of ITS and tubulin-based primers by 3-fold serial dilution of *V. longisporum* genomic DNA

	ITS	tubulin
PCR efficiency	92.0%	70.6%
R^2 of standard curve	0.994	0.967
PCR product size	261 bp	143 bp
Susceptibility for fluctuations of annealing temperature[1]	low	high

[1] tested in iCycler system (see 3.3.3).

3.3.6 Disease development in the greenhouse

Prior to resistance tests in the field, the four winter oilseed rape cultivars were screened for resistance under controlled greenhouse conditions. Disease development in this case is different from the situation found in the field. Typical symptoms such as yellowing of the cotyledons and the oldest leaves or/and the occurrence of black veins were observed in the susceptible cv. 'Falcon' and 'Laser' and developed also in 'Express' already after 14 dpi, while plants of the cv. 'Oase' developed first symptoms only at 21 dpi. This pattern of disease development is expressed in net AUDPC values, which allow for an appropriate estimation of the resistance level of the plant. Cultivar 'Falcon' scored highest on disease level with an AUDPC value of 60.0 (Figure 3.6). Significantly lower AUDPC values were calculated for cv. 'Laser' and 'Express' with net AUDPC values of 41.3 and 38.0 respectively. Plants of cv. 'Oase' showed significantly lower AUDPC ($AUDPC_{net}$ = 13.8) values compared to values of cv. 'Express', 'Laser' and 'Falcon'. The AUDPC values obtained from greenhouse trials rank similarly to the obtained fungal DNA concentrations in the stems of these four cultivars grown in the field (Figures 3.6, 3.7). The AUDPC values are not ranked entirely similar to disease values (disease incidence, disease index) obtained by scoring of microsclerotia on stubbles. Here, the cv. 'Express' exhibited a slightly lower disease level compared to cv. 'Oase'.

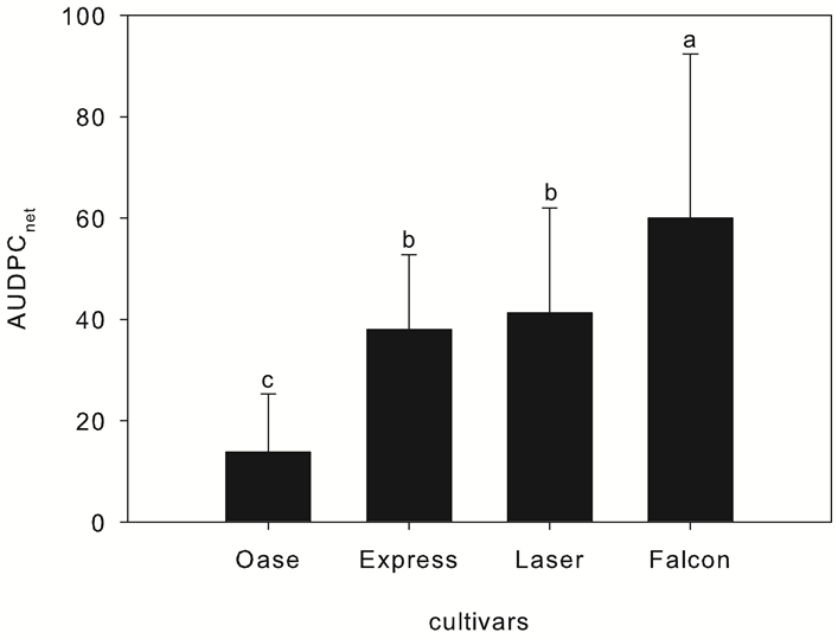

Figure 3.6 Net AUDPC values and standard deviations of four winter rapeseed cultivars inoculated by *V. longisporum* in the greenhouse and screened over a period of four weeks. Values with the same letter do not differ significantly at a level of $p \leq 0.05$ (LSD).

3.3.7 Monitoring of disease progress in the field

3.3.7.1 Sample preparation for qPCR analysis by combined CTAB/Kit method

Total DNA from plant tissue for quantification of fungal DNA was extracted from five plant stems each. Since a representative amount of stem tissue is required for DNA extraction in order to permit comparative analysis, lyophilized stem tissue from five plants was pooled and 1 g of this material was used for DNA extraction. DNA was purified using CTAB and chloroform-isoamyl alcohol extraction according to Brandfass and Karlovsky (2008). In order to obtain uniform yields of total DNA we combined this method with additional purification steps using spin columns (Qiagen GmbH, Hilden, Germany). In our protocol, we did not follow the manufacturer's recommendation of 20 mg initial sample weight, since it has been shown previously that increased sample weight of starting material improves reproducibility of DNA extraction from wheat kernels (Brandfass and Karlovsky, 2008).

3.3.7.2 Quantification of fungal DNA in rapeseed stems prior to symptom development

Following DNA purification from plant material, fungal DNA was detected and quantified by qPCR using ITS primers. As demonstrated in Figure 3.7, this system is able to detect fungal DNA at levels <1 fg. The ITS primer system therefore outperforms the tubulin primers in quantification of fungal DNA during early stages of the disease. On the other hand, specificity tests show that ITS primers amplify DNA of both *V. longisporum* and *V. dahliae*, as well as DNA from distinct species such as *Alternaria spp.* at DNA levels above 100 pg (Table 2).

By using ITS primers, fungal DNA could be detected as early as GS 65-67 in stem material of all tested cultivars (Figure 3.7). At this stage, fungal DNA concentrations in all cultivars are estimated to be approximately 0.1 ng/g dry weight. No detectable symptoms are visible at this time point.

At the second time point (GS 80), which marks initiation of the ripening period, fungal DNA concentrations strongly increase in all tested cultivars. In cv. ‘Falcon’ DNA values were 331.3 ng/g dry weight and ‘Laser’ showed values of 218.8 ng/g dry weight, implying that potentially the fungus has already formed single microsclerotia. Although the duplicate measurements do not allow validation of statistical significance, the moderately resistant cultivars ‘Oase’ and ‘Express’ show a tendency to lower values with DNA concentrations of respectively 9.6 ng and 42.0 ng/g dry weight, suggesting that this time point to be well suited for a reliable classification of the different cultivars. At GS 80, first symptoms such as half-sided stripes of brownish discoloration can appear, but unequivocal identification of *Verticillium* is only possible once microsclerotia are formed in stem tissue during later stages of plant maturation.

Similar DNA concentrations could be verified when using the tubulin primers at GS 80 (Figure 3.8). The DNA concentration at this time point was 442.0 ng/g dry weight for ‘Falcon’ and similarly high DNA concentrations were detected in ‘Laser’ with 378.5 ng/g dry weight. In the cultivars ‘Oase’ and ‘Express’ values with DNA concentrations of respectively 8.3 ng and 42.2 ng/g dry weight were found. These data demonstrate that, in principle, detection of fungal DNA in rapeseed stem tissue is possible with these primers if fungal DNA concentrations are sufficiently high. One advantage of this primer system over the ITS primers is the exclusive specificity towards *V. longisporum*. GS 65 was not evaluated with this system since at this time point only minute concentrations of fungal DNA could be detected by the more sensitive ITS primers.

The classification of cultivars into resistance levels based on quantification of fungal DNA in rapeseed stem tissue is similar to that obtained from conventional scoring of stubbles (Figure 3.9). However, the qPCR data demonstrate that cv. ‘Oase’ is classified as significantly more resistant based on this method.

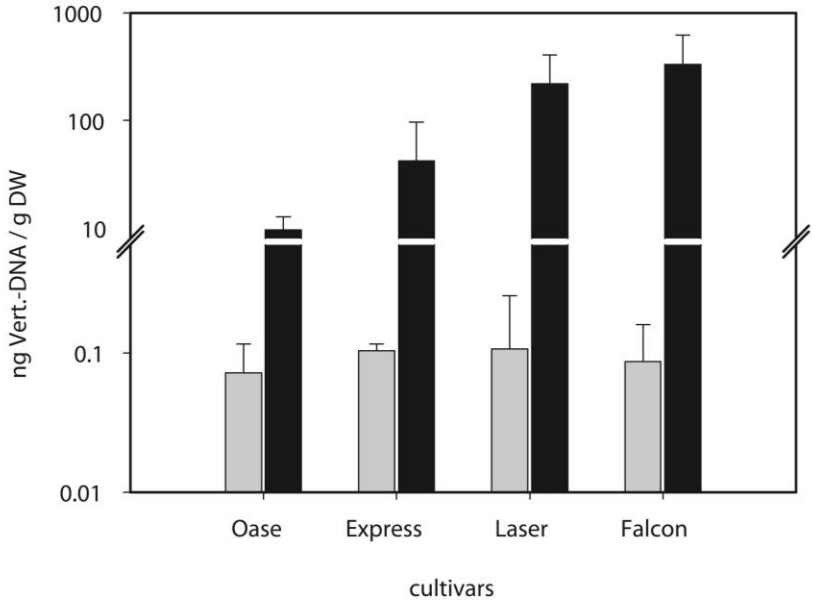

Figure 3.7 Amount of *Verticillium*-DNA detected by qPCR with ITS primers in stem tissue of 4 cultivars at GS 65-67 (2009-05-12, grey bars) and GS 80 (2009-06-29, black bars) showing the disease progress in the field season 2008/09 in Göttingen. Data are means (± s.d.) of two replicates (2 x 5 pooled stems). Significant differences are only observed between different growth stages, but not between the cultivars within one growth stage.

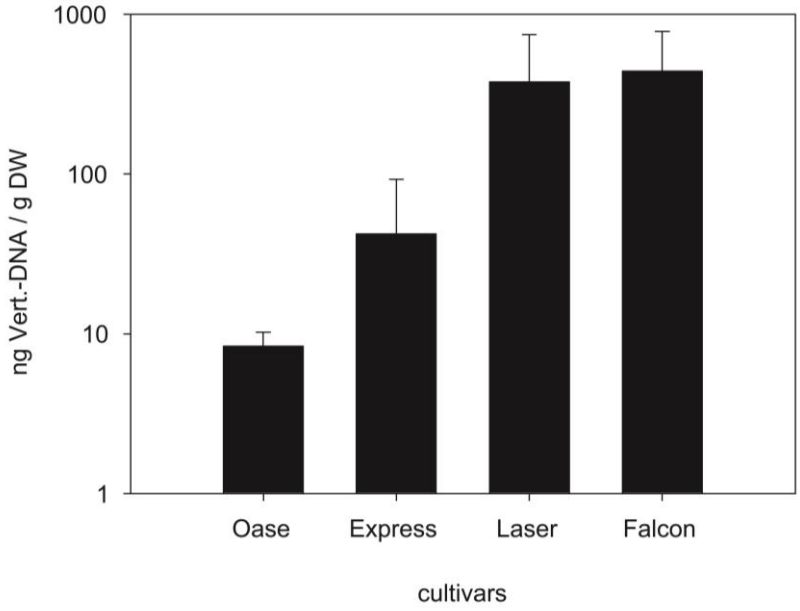

Figure 3.8 Amount of *Verticillium*-DNA detected by qPCR with β-tubulin primers in stem tissue of 4 cultivars at growth stage GS 80 in field season 2008/09 in Göttingen. Data are means (± s.d) of two replicates (2 x 5 pooled stems). There are no significant differences between the cultivars.

3.3.7.3 Evaluation of field resistance by visual scoring of stubbles

Apart from the development of a qPCR method for monitoring disease progress in field trials and detection of the pathogen prior to symptom development, we performed conventional screening of winter oilseed rape stubbles by visually scoring the abundance of microsclerotia in the pith, under the epidermis and in the root for comparison of both methods. In the season 2008/09 a high infestation level with *V. longisporum* was observed at the location Göttingen. Disease incidence ranged from 50% to 80% (Figure 3.9). Disease incidence for the moderately resistant cv. 'Express' and 'Oase' were found to be 54% and 58%, while 'Laser' and 'Falcon' showed values of 76% and 80%. Disease indices are consistent with disease incidence and show lowest values for 'Express' and 'Oase' (1.5 and 1.7), whereas the susceptible cultivars are scored with values of 1.7 and 2.0. Although the limited number of replicates does not permit statistical validation of the differences between the disease values of the four cultivars, cv. 'Oase' and 'Express' show a tendency towards lower disease values.

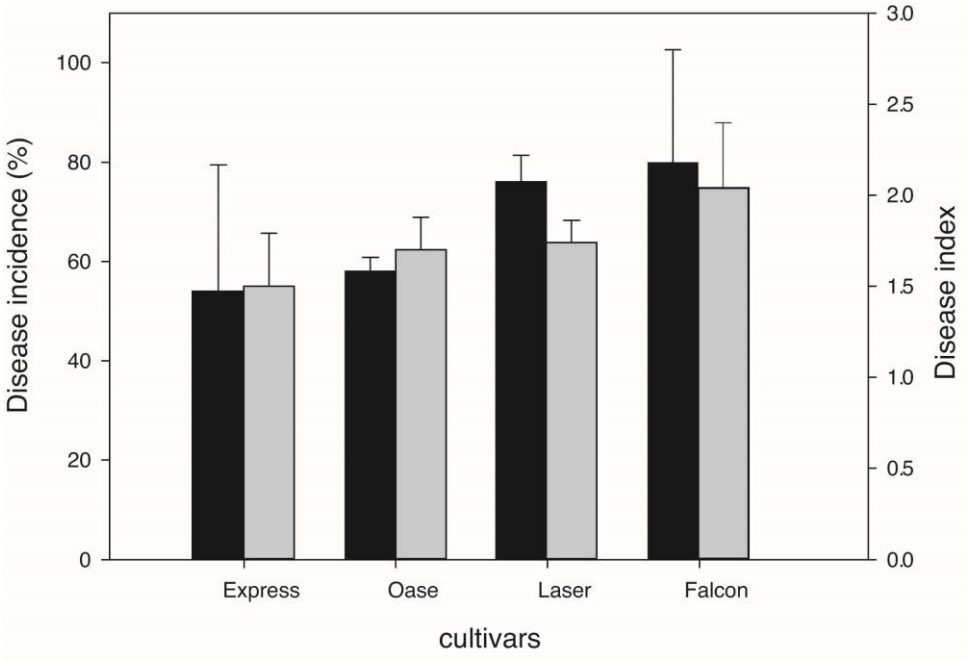

Figure 3.9 Disease index and disease incidence (DI) of winter rapeseed stubbles of 4 cultivars in the season 2008/09 (Göttingen). Samples (n = 2 x 25) were collected shortly after harvest and screened for abundance of microsclerotia. There are no significant differences between the cultivars in terms of the parameter disease index or disease incidence.

3.3.8 Relationship between disease incidence, net AUDPC values and DNA content

Values for disease incidence of the 39 tested accessions in the experimental year 2008/09 ranged from 22 to 80% (Appendix, Figure A 5). Net AUDPC values in the greenhouse were in a range from 8.2 to 62.3 (Appendix, Figure A 6) and fungal DNA concentrations in the rapeseed stems varied from 2 to 800 ng DNA/g dry weight (Appendix, Figure A 7). A comparison of the data obtained by different screening methods showed a slight correlation between the qPCR based screening method and the conventional scoring of stubbles (Table 3.8).

Table 3.8 Spearman rank correlations (n = 39) between the mean DNA content in OSR stems (ITS primers), net AUDPC values and disease incidence (DI). Asterisks label significant differences at a $p \leq 0.05$, n = 39 genotypes.

	qPCR	DI
$AUDPC_{net}$	**0.378***	**0.327***
qPCR		**0.476***

3.4 Discussion

The characteristic latency period of *Verticillium* disease on OSR in the field requires a sensitive method that can detect the fungus prior to symptom development and monitor the disease development in the field. In this study, two primer pairs were evaluated with regard to their specificity and sensitivity for amplification of fungal DNA of *V. longisporum* isolates. The results of the specificity test revealed that ITS primers amplify the target gene of DNA of all tested *Verticillium* isolates (except *V. chlamydosporium*). Specific detection *of V. longisporum* species is therefore not possible with these primers. Since previous studies have shown that *B. napus* stems are not colonized by *V. dahliae* or other known *Verticillium* species (Eynck *et al.*, 2007; Riediger, 2008), application of these primers for detection of *V. longisporum* is still possible provided that stem tissue in some distance from the hypocotyls is used for sampling in order to minimize amplification of unspecific DNA. Specificity tests with ITS primers further demonstrated that most of the fungal isolates that do not belong to *Verticillium* species are not detected by the ITS primers, except for the four *Alternaria* species and a single *Botrytis* isolate. In our study, contamination of the stem material with *Alternaria spp.* could be precluded by an extensive cleaning protocol prior to DNA extraction, because small amounts of *Alternaria* DNA cannot be amplified (amplification of 100 pg *Alternaria spp*. DNA had a corresponding mean C_T-value of 34 (Table 3.2), meaning that

lower DNA concentrations are hard to detect in 40 amplification cycles). As a general recommendation these results suggest to reduce the number of PCR cycles for ITS-based PCR detection of *V. longisporum* DNA in rapeseed tissue to 34 in order to exclude amplification of non-target DNA. Since the number of PCR cycles also determines the minimum of target DNA required for successful amplification, this in turn implies that target DNA concentrations below 0.001 pg cannot be measured. In practice, a balance needs to be defined between the required sensitivity and the risk of amplification of false positives.

In contrast, tubulin primers were highly specific for *V. longisporum* species sampled from different locations, with the exception of Vl 82, Vl 60 and Vl Eschwege that were not detected by the tubulin primers. These outliers should be verified by repeating the specificity test and assessing whether the spore morphology of these species is indeed consistent with long spored isolates. In addition, *V. dahliae* isolate Vd 76 was also detected by these primers. Morevoer, it has to be thoroughly tested if this sample does not contain contaminating traces of *V. longisporum* DNA.

The ability to detect small amounts of fungal biomass in the host plant by sensitive amplification of fungal DNA is one requirement of a suitable primer system for qPCR. Due to the fact that the β-tubulin gene is supposedly only present as a single copy in the fungal genome (Nahimana *et al.*, 2000; Debode *et al*., 2009), it was predictable that β-tubulin primers will have a lower sensitivity compared to the ITS primers. However, the difference in sensitivity (Figure 3.2) observed in the 3-fold dilution series (Figure 3.2) was unexpectedly large. Sensitivity of the ITS primers was approximately 32,000 times higher. It is important to note in this context that the ITS PCR product size is twice as large as the tubulin product, leading to the overestimation of the difference in C_T-values. A difference of ITS and tubulin primer performance was also described by Debode *et al.* (2009). Here, the β-tubulin assay was approximately 66 times less sensitive compared to ITS primers when detecting *Colletotrichum acutatum* in strawberry plants.

It is difficult to prioritize which primer system is most adequate to meet the requirements for detection of *V. longisporum* in field-grown *B. napus* since both systems have individual advantages. Tubulin primers are not suited to detect early stage infections in rapeseed tissue (GS 65-67), but owing to their high specificity are able to distinguish *V. longisporum* from *V. dahliae.* Investigating plant segments in closer proximity to the penetration site of the fungal hyphae, such as the root crown or even the upper root part, could increase the probability to detect elevated fungal DNA concentrations and justify qPCR analysis with tubulin primers for screening of genotypes for their resistance to *V. longisporum.* On the other hand, the high sensitivity of the ITS primers renders this system well suited for early detection and

quantification of infections in upper plant parts if contamination with *Alternaria* or *Botrytis* species can be minimized.

Current screening methods for detection of *V. longisporum* in field trials are based on quantifying the abundance of microsclerotia present in the subepidermal stem tissue, in the pith and in the roots. These methods have the disadvantage to be based on detection of the fungus in its saprophytic life stage. Moreover, the relationship between symptom expression and the individual ripening type of each genotype would require several screenings throughout the season (Zeise, 1992). For adequate classification of resistance levels it is therefore desirable to detect and quantify pathogen colonization at a stage in which plant resistance mechanisms are still present and active. Furthermore, screening of stubbles derived from locations with a high infestation level, e.g. Fehmarn or Svalöv (chapter 2) show that disease severity differs only marginally among the tested genotypes. A method such as qPCR that is able to detect the fungus in the plant at an early stage and during its biotrophic life phase can therefore offer sharper differentiations.

For investigation of the disease development in the field in the year 2008/09, rapeseed stems of four cultivars were investigated by ITS primer-based qPCR. Our results demonstrate that the fungus is already present in low amounts in the plant at growth stage 65, when plants are flowering. At this time no *Verticillium* symptoms were detectable on the plant. Our data show that qPCR with the ITS primer system is sensitive enough to detect the fungus prior to symptoms development**.** In previous studies disease progress in the field was investigated with a direct DAS-ELISA on different genotypes and cultivars including ‘Falcon’, ‘Express’ and ‘Oase’ (Eynck, 2008). Using this method, the earliest time point at which low amounts of *Verticillium* proteins became detectable in roots and stem tissue was at GS 89. Similar results by Keunecke (2009) showed that first *Verticillium* protein concentrations were detectable with ELISA at GS 87 (29^{th} of July 2006). This leads to the conclusion that the described ELISA-based methods allowed for classification of cultivars into different resistance levels but demonstrated that application of these methods is not suited for early stage detection of infection and monitoring of disease progress in the field.

According to Zeise and Seidel (1990) early infections could already occur in autumn. So far, even with our sensitive qPCR method reliable detection of *Verticillium* during the early stages of infection in autumn is not yet possible, since this would imply analysis of root samples. One difficulty in analyses of root samples for infection is that it is not possible to discriminate between fungal hyphae on the root surface and the interior root. Moreover, inhibition of the PCR reaction by root matrix compounds (own observation, data not shown; Bahnweg *et al.*, 1998) or humic acids in soil (Tebbe and Vahjen, 1993) may occur. In addition, quantification

of low amounts of fungal DNA requires the use of sensitive ITS primers, that are indifferent to *V. dahliae* and *V. longisporum* isolates and therefore can not provide reliable estimates of the *V. longisporum* DNA concentration.

In order to compile a robust classification scheme of resistance levels, it is critical to define the optimal time point for field sampling. QPCR analysis of samples collected at GS 65 and GS 80 demonstrated a dramatic increase (3,000 times) of fungal DNA concentrations between the two time points of sampling. These data indicate a considerable spread of the fungus between flowering and early ripeness stages and suggest that first microsclerotia have already formed at this stage (GS 80).

Several factors complicate a consistent choice of sampling time points. For instance, disease incidence at GS 97 was determined as 80% (Figure 2.6) and 12% (Figure 2.8) for the susceptible cultivar 'Falcon' in field trials of the two consecutive years 2008/09 and 2009/10. Since the infection by microsclerotia was the same in both cases and sowing dates differed by only 6 days, the observed variability suggest that climatic conditions play a role in disease development. A similar relation between climatic factors and infestation levels was also suggested by Keunecke (2009), purporting a considerable influence of temperature and soil moisture with regard to germination of microsclerotia, colonization and symptom expression. Close observation of plant growth and repeated sampling throughout the entire vegetation period are therefore necessary to define the optimal time point for sampling of plant material for qPCR analysis.

For identification of resistant OSR genotypes a rapid greenhouse trial provides a valuable tool for evaluation of resistance prior to field tests. The four tested cultivars showed a good differentiation in symptom development under greenhouse conditions with markedly lower AUDPC values of cv. 'Oase' compared to the other cultivars. Similarly, in the field trial fungal DNA concentration in the stem tissue was also low in this cultivar. Overall, there is a clear relationship between the AUDPC values and the measured fungal DNA concentration in stem tissue. Symptom development expressed in yellowing and necrotization of leaves is correlated with fungal colonization measured in DNA concentrations. It is encouraging that this relation exists between controlled and field conditions. Within the scope of this study this relation is shown for cultivars that differ strongly in their susceptibility to V*. longisporum*. In separate investigations AUDPC values and qPCR data obtained from 39 different genotypes including our four cultivars Spearman rank correlations were lower, but significant (r_s = 0.378, Table 3.8). Additionally, the conventional stubble screening method shows a significant correlation with the newly applied qPCR method (r_s = 0.476). This demonstrates that the qPCR method can be an alternative to visual scoring based on microsclerotia abundance post harvest. Such a significant correlation between qPCR based detection of *Verticillium*

and conventional screening methods was also shown by Atallah *et al.* (2007). They reported that the qPCR-based method was more sensitive in the detection of *V. dahliae* in potato and Spearman correlation revealed a highly significant relation between qPCR quantification and plating assays. A similar result was also found by Larsen *et al*. (2007), who identified a positive correlation for *V. albo-atrum* DNA concentration detected by qPCR in alfalfa plants and disease severity index ratings based on visual scoring. Our data for the qPCR based screening assay for field plants show a strong relation to greenhouse data provided that the tested genotypes differ strongly in their levels of resistance to *V. longisporum*. In conclusion, the combination of greenhouse screenings and field trials provides a tool for classification of resistant genotypes for integration in breeding of resistant elite cultivars.

4. Histological investigations of resistance factors involved in the interaction of *B. napus* with *V. longisporum*

4.1 Introduction

The expansion of cultivation area for winter oilseed rape due to increased demand for oilseed rape oil is accompanied by higher crop rotation rates, which can cause phytosanitary problems. One of the major threats for *B. napus* that can compromise yields is the premature ripening caused by infection with the soil-borne vascular fungus *Verticillium longisporum* (Dunker *et al.*, 2008). Since at present efficient fungicides for intervention remain elusive, crop protection requires breeding for resistant cultivars. To optimize breeding efforts it is important to identify and characterize putative mechanisms of resistance and to utilize this knowledge in breeding programs.

The identification of plant disease responses that contribute to resistance requires detailed studies into the interaction of the host with the pathogen. In interactions of plants with *Verticillium* spp., resistance is considered to be achieved by exclusion of the pathogen from the host or by restriction of the pathogen within the vascular system. Immunity to infection by mechanisms such as hypersensitivity as commonly observed in biotrophic interactions is unlikely (Pegg and Brady, 2002). Various physical barriers (anatomical changes) and biochemical mechanisms exist by which the host inhibits the spread of the pathogen into the vascular system. The physical restriction of the pathogen can occur by reinforcement of cell walls, e.g. formation of papillae, vessel coating by deposition of callose, lignin or suberin and formation of tyloses, gels and gums (Aist, 1976; Wallis and Truter, 1978; Bishop and Cooper, 1984; Nicholson and Hammerschmidt, 1992; Beckman, 2000). Among the biochemical responses - i.e. the synthesis of antimicrobial compounds following fungal infection - phenolic compounds, phytoalexins and PR-proteins play a role. Both systems, the physical plant defense structures and the biochemical agents, operate together to minimize fungal distribution. The effectiveness of these defense systems is dependent on the interaction of host, pathogen and environment as well as the extent of the infection (Elgersma *et al.*, 1972).

The formation of physical barriers against vascular pathogens can be categorized into defense structures that either impede lateral or longitudinal spread of the pathogen. The very first constitutive barriers (preformed resistance factor) in the vascular system of plants are perforation plates that are located on the vessel end walls and serve as end-on-end connections of vessel elements (Evert, 2006). These vessel end walls are trapping sites that separate single vessel elements and thus help to screen out spores. For successful systemic spread in the vascular tissue spores that are trapped at such end plates thus have to

germinate quickly, penetrate through the barrier and proliferate again. Although these trapping sites cannot inhibit the spread of the pathogen completely, delay of fungal colonization creates a time window for initiation of defense mechanisms (Beckman, 1987, 2000).

Beckman *et al*. (1987, 2000) introduced a time-space model to explain the sequence of the different host defense responses that occur in a vascular element and the adjacent xylem parenchyma cells. A first modification of the plant cell wall for pathogen defense and an early response to infection is the deposition of callose (polymer of linear β-1,3 D-glucans) for reinforcement of the host cell wall. Callose deposition is often associated with the synthesis of papillae (cell wall appositions), which are deposited at the interior of the cell walls (Bell, 1981). Apart from the main constituent callose, papillae also consist of pectic substances, cellulose, lignin and suberin (Aist, 1976). While papillae formation plays an important role in preventing fungal penetration (Bishop and Cooper, 1983a) its role in resistance is debated since callose deposition is a non-specific defense reaction (Beckman, 1987) and can also result from mechanical damage (Aist, 1976).

Formation of callose deposition was reported in tomato infected with *F. oxysporum* f. sp. *lycopersici* (Beckman *et al.*, 1982) 6 to 12 h post inoculation. Daayf *et al*. (1997) investigated the plant response against *V. dahliae* in cotton roots of resistant and susceptible plants and found callose to constitute one of the early structures formed to reinforce structural barriers in papillae of phloem intercellular and plasmodesmatal areas. Resistant plants appear to more rapidly instigate formation of such reinforced barriers compared to susceptible plants. In tobacco roots infected by *Phytophthora parasitica* var. *nicotianae* callose was deposited on cell walls, sieve-tube members, plasmodesmata, intercellular spaces and papillae. It was suggested that the ß-1,3-glucans deposited on plant cell walls derived from the fungus itself, by action of the plant ß-1,3-glucanases and act as an inducer of different host responses (Benhamou, 1992).

One alternative to prevent fungal penetration into the cell is to encapsulate the fungal hyphae with a deposit consisting of callose, which can develop to a lignituber by infusion of phenolic substances (Agrios, 2007).

Another common defense structure of plants to prevent the lateral fungal spread in vessels is the vessel wall coating and/or plugging of the pit areas. According to Newcombe and Robb (1988) vascular coating on xylem vessel walls is one of the early responses in plant defense and occurs within 24 h after inoculation. Vessel lining materials consist of polysaccharides, phenolics, lignin and suberin (Beckman, 1987). Transmission electron microscopy (TEM) identified the presence of vessel coating material in *V. albo-atrum* infected tomato three days after stem inoculation. The coating material also was found to obstruct intertracheary and

xylem parenchyma pit areas (Bishop and Cooper, 1983b). Robb *et al*. (1989) confirmed the observation that vascular coatings are formed more rapidly in resistant compared to susceptible plants for the same pathosystem.

Similar vessel coatings were found in tomato after infection with *V. dahliae*. Here, occlusion of pit membranes was reported to be more effective in resistant cultivars compared to the susceptible cultivar in preventing fungal penetration into adjacent vessel elements (Gold and Robb, 1995). Likewise, defense mechanisms such as vascular coating on xylem vessel walls were found in resistant alfalfa plants infected with *V. albo-atrum*. Resistant plants thus appear to more efficiently restrict fungal growth through pits and subsequent penetration into adjacent vessels (Newcombe and Robb, 1988). Histochemical investigations of the same pathosystem revealed that the coating material consisted of either suberin or a closely related lipid-containing substance as a result of lipid conversion into coating material (Newcombe and Robb, 1989).

According to Newcombe and Robb (1988) the longitudinal restriction of fungal cells by formation of tyloses, gels and gums are late responses in vascular infections and occur within 24 to 72h. Tyloses are protrusions formed by parenchyma cells and extend through the pits into the adjacent vessel lumina. Cells developing tyloses are referred to as contact cells (Braun, 1967). Tyloses contain the nucleus and parts of the cytoplasm of the parenchyma cell. The tylose wall, also called protective layer, originates from the contact cell and is rich in pectin (Evert, 2006). In general, tylose formation occurs more frequently in resistant hosts (Tjamos and Smith, 1975; Pegg and Brady, 2002). Tylose formation caused by vascular pathogens was observed in interactions of *Verticillium* with various plant species, e.g. chrysanthemum infected with *V. dahliae* (Robb *et al.*1979a, Robb *et al*.1979b), sunflower infected with *V. dahliae* (Robb *et al*.1979a), and tomato infected with *V. albo-atrum* (Dixon and Pegg, 1969; Bishop and Cooper, 1984). Whereas for the interaction of *V. dahliae* with cotton roots, tyloses were never observed (Daayf, 1997), tylose formation was indeed found to play a role in resistance in *Fusarium*-plant-interactions, e.g. in tomato with *F. oxysporum* (Beckman et al., 1972) or in the interaction of staghorn sumac with *Fusarium oxysporum* f. sp. *callistephi* (Ouellette, 2006). Infection of *Platanus x acerifolia* with *Ceratocystis fimbriata* f. sp *platani* (Clérivet, 2000) also involves tylose formation. Apart from fungal infections, the formation of tylose structures is also common in vascular diseases of bacterial origin (Buddenhagen and Kelman, 1964; Grimault, 1994).

Another mechanism by which plants respond to vascular pathogen invasion is the formation of gels and gums that may prevent fungal spread by embedding and immobilization of spores (Beckman, 1987). The origin of the gels is still unclear. In *V. dahliae* interactions with nine plant species, VanderMolen *et al*. assume that gels consist of pectic compounds,

hemicellulose and additional carbohydrates originating from perforation plates, end walls and pit membranes by the distention of primary cell walls and middle lamellae (VanderMolen *et al.*, 1977). In turn, Moreau *et al*. (1978) suggested that newly synthesized carbohydrates and other materials are secreted by paravascular parenchyma cells into the vessel lumen through the pit membranes. Similarly, it was proposed that formation of gels is initiated when pits are too small for tylosis formation. More precisely, tylose formation does not occur when the nucleus of the tylose producing cell cannot pass the pit cavity (Talboys, 1958). In this case cell wall material is synthesized and released by paravascular parenchyma cells into the vessel lumen.

The occurrence of gums and gels during vascular infections was observed in different plant species, including tomato and pea (Bishop and Cooper, 1984), *Platanus x acerifolia* (Clérivet *et al.*, 2000), carnation (Ouelette *et al.*, 1999), banana (Beckman and Zaroogian, 1967; VanderMolen *et al.*, 1987) and alfalfa (Pennypacker and Leath, 1993).

In addition to the formation and fortification of physical barriers, the accumulation of phenolics and phenolic polymers such as lignin is a frequent hallmark of vascular diseases. Phenolic infusion into cell wall structures and gels can be induced by infectious stimuli and lead to accumulation of phenolic compounds at the site of infection (Beckman, 2000). Because of its complex structure, lignin is difficult to degrade and thus inhibits mechanical penetration by fungal pathogens. Furthermore, it was suggested that lignification of cell walls could hinder the exchange of water and nutrients between host and fungus and restrict the diffusion of fungal enzymes and toxins to the host cell (Ride, 1978; Vance et al, 1980).

Lignin biosynthesis is complex. However, the synthesized set of monolignols share the common precursor phenylalanine, which in a first step of lignin biosynthesis is enzymatically transformed to cinnamic acid by phenylalanine ammonia-lyase (PAL) and then further processed to the most important monolignols coumaryl alcohol, coniferyl alcohol and sinapyl alcohol. There are several studies about PAL activity in fungal-plant-interactions. Studies of Lee *et al.* (1992) showed that PAL expression was enhanced in resistant tomato plants infected with *V. albo-atrum*, whereas PAL expression was suppressed by the fungus in susceptible plants. Similar results were found in tomato cell cultures inoculated with *V. albo-atrum*. Here, PAL activity was also upregulated after infection (Bernards and Ellis, 1991).

Apart from the summarized morphological changes, the plant produces numerous specific stress compounds that exert direct antimicrobial activity. One such class of chemical response agents involves phytoalexins, inducible secondary metabolites that possess direct antimicrobial activity (Vidhyasekaran, 2008). Examples for phytoalexins are the terpenoids gossypol in cotton (Bell et al, 1978), rishitin in tomato (Tjamos and Smith, 1974; Tjamos and Smith, 1975) or brassinin in cruciferous plants (Pedras *et al.*, 2002). The only known

inorganic phytoalexin is elemental sulfur (Cooper *et al.*, 1996, Cooper and Williams, 2004; Williams and Cooper, 2003). Resistant lines of tomato were found to accumulate elemental S in vascular tissue following infection with *V. dahliae* (Williams *et al*., 2002). In addition to secondary metabolites and inorganic compounds, pathogenesis-related proteins (PR)-Proteins such as β-1,3-glucanases and various chitinases (Benhamou, 1995b) and peroxidases (Smit and Dubery, 1997) are also involved in resistance to pathogenic invaders.
To overcome these host responses, fungal pathogens developed several defense mechanisms that will be shortly summarized. Fungal cells produce a diverse set of enzymes to disrupt the host cell walls or to defend themselves against chemical compounds produced by the plant. During early plant defense papillae or lignitubers composed of callose can be degraded by fungal β-1,3-glucanases (Cooper *et al.*, 1988). Primary plant cell walls consisting of (hemi-) cellulose, pectins and proteins (structural proteins, e.g. hydroxyproline-rich proteins) can be degraded by cellulolytic enzymes (e.g. endo- β-1,4-glucanase and exo-glucanases), xylanases, pectic enzymes (e.g. pectin lyases, exo- and endopolygalacturonases) or proteases. Finally, fungal pathogens produce toxins such as e.g. wilting toxins in *V. dahliae* (Palmer et al., 2005).

Some of the described physical and chemical plant defense structures, e.g. fortification of cell walls, vascular plugging by gels or gums and the accumulation of soluble and cell wall-associated phenolic compounds were also found in the *V. longisporum*/*B. napus*-interaction and the hypocotyl tissue was identified to be of particular importance (Eynck *et al*., 2009). These various defense responses were reported to occur upon infection in both resistant and susceptible plants, but to vary in levels of intensity. Since defense structures were found to be more prominent in resistant genotypes, a first conclusion was that resistance is expressed by quantitative rather than qualitative signatures. Furthermore, analysis of phenol metabolism indicated that the investigated phenolics contribute to resistance by both high levels of constitutive synthesis already prior to infection and a subsequent time-dependent increase upon infection.
Although these studies suggest a mostly quantitative resistance response of the *V. longisporum*/*B. napus*-interaction, a detailed analysis of the various defense structures and their interaction with fungal elements is necessary in order to fully characterize the resistance potential of winter oilseed rape cultivars. Building on these recent findings, the present study therefore seeks to detail our understanding of resistance mechanisms such as occlusions and cell wall fortifications in the hypocotyl by mapping plant response elements of resistant (SEM) and susceptible (‘Falcon’) genotypes on the ultrastructural level using transmission

electron microscopy. We validated the presence of fungus by quantitative real-time PCR analysis of tissue in close proximity to the site of sample preparation for TEM sections.

4.2 Material and Methods

4.2.1 Plant material

Seeds of a susceptible winter oilseed rape cultivar (cv.) ('Falcon', Norddeutsche Pflanzenzucht, NPZ, Hans-Georg Lembke KG, Hohenlieth, Germany) and of a resistant genotype (SEM 05-500256, Lantmännen SW Seed, Svalöv, Sweden) were surface sterilized for 2 min in 70% EtOH and washed twice with sterile tap water. The seedlings were grown in sterile silica/quartz sand for 11 days followed by cultivation in a sterile sand-soil mixture until three leaf stage in a climate chamber subjected to day/night conditions of 14 h/10h at 23°C/20°C. Plants were then vernalised for about 13 weeks at 4°C in a climate chamber with day/night conditions of 16 h/8 h followed by one week of recovering in a climate chamber with conditions as described above.

4.2.2 Fungal isolate

The *Verticillium longisporum* isolate VL 43 isolated from *B. napus* (Zeise and Tiedemann, 2001, 2002a and 2002b) was used in this study. For the production of stock cultures conidial suspensions in Czapek-Dox medium were supplemented with 25% glycerol and stored at -80°C. Inoculum for the root dip inoculation was produced by cultivation of 500 ml of the stock solution in 150 ml PDB at 23°C on a rotary shaker at 100 rpm. After 7 to 10 days of cultivation the fungal culture was filtered and spore concentration was adjusted to 10^6 conidia/ml with a Thoma haemocytometer.

4.2.3 Inoculation procedure

The inoculation of the plants was performed by the root dip inoculation method (Eynck *et al.*, 2007). The vernalised plants (see 4.2.1) were removed from the pots and roots were cleaned by washing under tap water. For obtaining an equal penetration of *V. longisporum* into the plantlet roots and introduction into the vascular system of the roots, about one-third of the terminal roots were cut with scissors and placed in a beaker containing a conidial suspension (10^6 conidia/ml) of *V. longisporum* isolate VL 43 for 30 min. Control plantlets were dipped in tap water for the same time. Then plants were repotted into pots with 1:1 sand-soil substrate and cultivated in the climate chamber under conditions as described above.

4.2.4 Evaluation of the disease progress

The disease progress was recorded weekly with a 1 to 9 assessment key (Table 4.1) in a time period from 14 days post inoculation (dpi) to 35 dpi. After scoring and measuring, the plants were processed for TEM preparation and DNA extraction meaning that each week different plants were scored.

Using the disease scores, area under the disease progress curve (AUDPC) values were calculated according to the formula of Campbell and Madden (1990, modified from Shaner and Finney, 1977). The calculation includes the mean severity values of four time points and was calculated according following equation:

$$\text{AUDPC} = \sum_{i=1}^{n} (y_i + y_{i+1}/2) * (t_{i+1} - t_i)$$

In which n = number of observations, $_i$ = time point of observation, y_i = disease severity value at i*th* observation, and t_i = time (days) at the i*th* observation.

Next, net AUDPC ($AUDPC_{net}$) values were calculating which express the difference between the AUDPC value of the inoculated plant and the respective control plant (Eynck, 2008). These `net AUDPC values` consider alterations of the plant that occur in natural senescence such as yellowing of the leaves.

Table 4.1 Assessment key for the evaluation of the disease severity of *B. napus* plants infected by *V. longisporum*.

Score	Symptom development
1	No symptoms
2	Up to 10% of the leaves show yellowing/black veins or are dead.
3	11 - 20% of the leaves show yellowing/black veins or are dead.
4	21 - 40% of the leaves show yellowing/black veins or are dead.
5	41 - 60% of the leaves show yellowing/black veins or are dead.
6	61 - 80% of the leaves show yellowing/black veins or are dead.
7	81 - 100% of the leaves show yellowing/black veins or are dead.
8	Only apex is still alive.
9	The plant is dead.

Additionally, the height of the plants was recorded weekly because stunting of the plants is a typical symptom for *V. longisporum* infection. The height was measured from the origin of the cotyledons to the tip of the shoots.

4.2.5 Specimen preparation for TEM

For ultrastructural studies using TEM, five inoculated plants (and three control plants) were harvested each at 14, 21, 28 and 35 dpi. Samples originated from the lower hypocotyl (Figure 4.1). For preparation of the tissue samples a modified protocol was used according to A. Olbrich (2005). Five to ten small blocks of 1 mm in size from the hypocotyl part were cut with a razor blade in cooled PIPES buffer (0,1 M Piperazine-1,4-bis(2-ethane)sulfonic acid, pH 7.0) and immediately transferred to the first chilled fixative (2.5% glutaraldehyde and 2.0% formaldehyde buffered with 0.1 M PIPES pH 7.0). The aldehydes in this primary fixative mediate the cross linking of proteins (Flegler *et al*., 1995). Infiltration with the fixative was enhanced by exposing the samples to a pressure of 200 mbar in a desiccator for 1 to 2 h. Infiltration was followed by four times 15 min wash steps with cooled PIPES buffer. After removing the PIPES buffer the specimen were post-fixed in cooled 2% osmium tetroxide for 1 to 2 h. This fixative stabilizes the membranes and acts as contrast agent. Again samples were washed two times for 15 min with PIPES. Dehydration was performed in a graded ethanol series (25%, 50%, 75%, 100%) followed by a graded acetone series (25%, 50%, 75%, 100%), during which samples were incubated at room temperature for more than 4 h at each step. Finally samples were incubated three times in 100% acetone p.a. with a 3 nm molecular sieve (MERCK KGaA, Darmstadt, Germany) before embedding in Spurr`s resin, which is an appropriate embedding substance for plant cells with lignified cell walls (Spurr, 1969). For embedding the SPURR Embedding Kit (SERVA Electrophoresis GmbH, Heidelberg, Germany) was used in which the toxic ERL 4206 epoxy component is replaced by the less toxic compound ERL-4221 D. The Spurr resin (10 g ERL-4221D (3,4-Epoxycyclohexyl-methyl-3,4-epoxycyclohexylcarboxylate, 6.0 g D.E.R. 736 (Diglycidylether of polypropylene glycol), 26.0 g NSA (Nonenyl succinic acid anhydride) and 0.4 g Dimethylaminoethanol) was prepared according to the manual instructions for the standard recipe. Specimen were incubated in a graded Spurr series (15%, 30%, 45%, 60%, 75%, 90%, 100%) diluted with acetone p.a. with a 3 nm molecular sieve for 8 h each step on a rotating wheel (Agar Scientific Limited, Stansted, United Kingdom). The specimen were placed in silicone rubber embedding forms and covered with 100% Spurr resin. The resin was polymerized for 24 h at 60°C.

For preparation of sections for microscopy the resin blocks were trimmed free-hand with a razor blade, cut with a glass knife and either semithin sections (0.99 nm) for light microscopic

investigation or ultrathin sections (ca. 70 nm-90 nm) were produced with a diamond knife (Diatome AG, Bienne, Switzerland) using an ultramicrotome (Ultracut E, Reichert-Jung, Austria). The produced sections floating on the water surface of the knife-attached boat were picked up with grids. Additionally sections were mounted on glass slides and investigated in a Zeiss microscope for the presence of fungal structures by staining in 0.1% toluidine blue in borax. Object holders for the sections were 100 mesh hexagonal copper grids (Plano GmbH, Wetzlar, Germany) coated with a plastic foil (0.5% (w/v) polyvinylformaldehyde (Formvar) in water-free chloroform). The plastic foil serves for better attachment of the sections to the grids. All sections were first stained with 3% (w/v) uranyl acetate in 70% (v/v) methanol for 5 min followed by a washing step with methanol and staining in 0.3% (w/v) lead citrate (1ml H_2O bidest., 187.5 µl 1.3 M sodium citrate, 125 µl 1 M lead nitrate, 250 µl 1 M NaOH p.a.). Transmission electron microscopy was performed in collaboration with Michael Hoppert (Department for General Microbiology, University of Göttingen) on a Zeiss EM 902 microscope and in collaboration with Andrea Olbrich (Department of Forest Botany and Tree Physiology, University of Göttingen) on a FEI Tecnai G^2 Spirit microscope using an accelerating voltage of 80 kV.

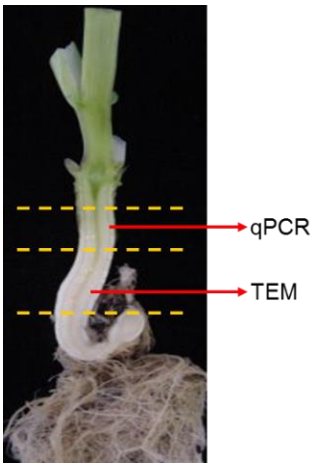

Figure 4.1 Specimen preparation for electron microscopy and qPCR analysis. Longitudinal section of a *B. napus* plant at 17 dpi. The upper hypocotyl part was prepared for DNA isolation and subsequent qPCR, small blocks of the lower hypocotyl part were fixed in glutaraldehyde/formaldehyde and osmium tetroxide for TEM (35 dpi).

4.2.6 DNA extraction and quantification of *V. longisporum* in infected plants

Quantitative real-time PCR (qPCR) was performed for detection of the fungus in the hypocotyl tissue close to the site of investigation for the TEM analysis. For DNA extraction a total of five inoculated plants (and three control plants) were harvested at 14, 21, 28 and 35 dpi. A tissue part of the upper hypocotyl (Figure 4.1) was first lyophilized/freeze-dried for 72 h (Freeze Dryer, Martin Christ Freeze Dryers, Osterode am Harz, Germany) and then crushed with a mixer mill (Retsch MM 200, Retsch GmbH, Haan, Germany). Total genomic DNA was isolated from about 20 mg of the fine tissue with the DNeasy Plant Mini Kit (Qiagen GmbH,

Hilden, Germany). The quality of the DNA was verified in an ethidium bromide stained agarose gel (1% Agarose in TAE buffer) after UV-visualization and documented by a gel documentation system (Quantity One, Version 4.5.0 Bio-Rad Laboratories, Hercules, USA). The qPCR reaction was performed in a CFX 384 Real-Time PCR detection system including a C1000 thermal cycler base with a CFX 384 optical reaction module. The primer pair OLG 70 (5`-CAG CGA AAC GCG ATA TGT AG-3`) and OLG 71 (5`-GGC TTG TAG GGG GTT TAG A-3`) was used to amplify a 261 bp fragment of the ITS region. The reaction mixture of 10 µl volume consisted of ≈ 2.5 ng purified genomic DNA and 0.3 µM of each primer in Thermo Scientific PCR Master Mix (Absolute Blue QPCR SYBR Green Fluorescein Mix: 10 nM Fluorescein, 3 mM $MgCl_2$). For each DNA-sample three replicates were used and the mean of the Ct-values was calculated. In order to quantify the samples with unknown fungal DNA content a standard curve in a 10-fold dilution-series from 1 ng to 0.001 pg was run on the same plate. For the standard curve genomic DNA of the *V. longisporum* isolate VL 43 was isolated with the DNeasy Plant Mini Kit (Qiagen GmbH, Hilden, Germany) and DNA concentrations of 5 µl aliquots were adjusted by densitometry of ethidium bromide (0.00003% (v/v)) stained agarose gels (1% (w/v) in TAE) using Lambda Phage DNA as the standard. Documentation and analysis was performed with the software Multi-Analyst (Version 1.1, Bio-Rad Laboratories, Hercules, USA). Previous studies confirmed that genomic plant DNA does not inhibit PCR amplification (see chapter 3).

DNA amplification was performed according to the following protocol: an initial activation step of 15 min at 95°C was followed by 40 cycles with 10 s at 95°C, 15 s at 60°C and 15 s at 72°C. Fluorescence emission was measured after each elongation step and completed with a final elongation step of 2 min at 72.0°C. Melting curve analysis was performed by an initial denaturation step at 95.0°C for 10 s, followed by a 55.0°C step for 10 s and subsequent measurements within a range of 55°C to 95°C in which measurements were made at 0.5°C temperature increments every 5 s.

4.2.7 Statistical analysis

Statistical analysis was performed with the Software STATISTICA for Windows Version 9.1 (Statsoft 2010, Tulsa, USA). The mean data of five replicates (three replicates for controls) was analyzed with analysis of variance (ANOVA). For determination of the least significant difference (LSD) between the mean values a Fisher LSD test was used at $P = 0.05$

4.3 Results

4.3.1 Disease development in resistant and susceptible genotypes

Approximately 14 days after inoculation of the plants the first vernalized plantlets developed a shoot, and at 21 dpi nearly all plants displayed shoots. First symptoms such as yellowing of the cotyledon leaves, formation of black veins and partial necrotisation of the oldest leaves did not develop until 14 dpi in either genotype. In cultivar ‘Falcon’ all screened plants showed either yellowing or abscission of the oldest leaves at 14 dpi, which is expressed in a mean disease score of 3.2 (Table 4.2). In contrast, for the genotype SEM 05-500256 (SEM) only 40% of the screened plants showed first *Verticillium* symptoms such as yellowing of the oldest leaves at the same time point (mean disease score 1.8, Table 4.2). At 21 dpi abscission of the oldest leaves also initiated in SEM. Differences in mean disease scores between control and inoculated plants were significant at all scoring time points for ‘Falcon’, while mean disease score for SEM was only significantly increased compared to control plants at 21 dpi.

Finally, disease progression occurred more rapidly in ‘Falcon’ as expressed in a net AUDPC value of 44.33 compared to an AUDPC value of 27.30 for the genotype SEM.

An additional symptom on *B. napus* caused by infection with *V. longisporum* under controlled greenhouse conditions is reduced growth, manifested as stunting of the plants. Significant stunting of the inoculated ‘Falcon’ plants was observed at all of the investigated time points except for 21 dpi. Plant height of inoculated SEM plants was first significantly reduced with respect to the water-inoculated plants at 28 dpi and the following time point 35 dpi. At this time point growth of the SEM plants was reduced by 46% whereas the plants of the genotype ‘Falcon’ showed a mean stunting of 64% (Table 4.3).

Figure 4.2 Phenotypes of *B. napus* cultivar ‘Falcon’ (left) and genotype SEM 05-500256 (right) at 28 dpi inoculated with *V. longisporum* (right) in comparison to control plants (left). Arrows indicate the stunting of the plants.

Table 4.2 Mean disease scores (1-9; standard deviations in brackets) of *B. napus* plants (genotype 'Falcon' and SEM 05-500256) inoculated with *V. longisporum* (+ VL) in comparison to control plants (mock) at 14, 21, 28 and 35 dpi. Values with the same letter within the same row do not differ significantly at a level of $p \leq 0.05$ (LSD).

	Falcon				SEM			
dpi	mock		+ VL		mock		+ VL	
14	1.67 (± 1.15)	b	3.20 (± 0.45)	a	1.00 (± 0.00)	b	1.80 (± 1.10)	b
21	2.00 (± 1.00)	b	4.20 (± 0.45)	a	2.00 (± 1.00)	b	3.80 (± 0.45)	a
28	4.00 (± 0.00)	b	5.20 (± 0.84)	a	3.33 (± 0.58)	b	4.00 (± 0.00)	b
35	4.33 (± 0.58)	b	5.60 (± 0.55)	a	4.33 (± 0.58)	b	4.80 (± 0.45)	b

Table 4.3 Average plant height (in cm) and standard deviations (brackets) of *V. longisporum* inoculated (+ VL) (n = 5) and control (n = 3) plants of *B. napus* genotypes 'Falcon' and SEM 05-500256. Values with the same letter within the same row do not differ significantly at a level of $p \leq 0.05$ (LSD).

	Falcon				SEM			
dpi	mock		+ VL		mock		+ VL	
14	12.43 (± 1.83)	a	08.50 (± 1.32)	b	09.00 (± 00.95)	b	08.92 (± 01.26)	b
21	16.27 (± 4.65)	a	15.12 (± 5.28)	a	23.23 (± 09.07)	a	16.10 (± 07.58)	a
28	42.93 (± 2.89)	a	16.12 (± 2.99)	c	44.30 (± 05.31)	a	27.92 (± 05.69)	b
35	62.30 (± 0.75)	a	22.54 (± 5.44)	b	63.63 (± 10.43)	a	34.60 (± 12.60)	b

4.3.2 Colonization of the hypocotyl by *V. longisporum* is accelerated in susceptible plants

The measurement of the fungal DNA content in the upper hypocotyl part by qPCR revealed a considerable fungal DNA concentration of 89 ng DNA/g dry weight (DW) in 'Falcon' plants at 14 dpi (Figure 4.3). At the same time point fungal DNA concentration in SEM plants was 15 times lower. In general, at all of the investigated time points fungal DNA concentration was increased in the susceptible genotype with a range of 37 ng to 104 ng DNA/g DW compared to the resistant genotype with fungal DNA values ranging from 2 ng to 12 ng DNA/g DW. This difference was significant at two of the four investigated time points (14 and 28 dpi). Contrary to expectation fungal DNA concentration in both genotypes did not increase throughout the investigated time course but rather followed a fluctuating signature.

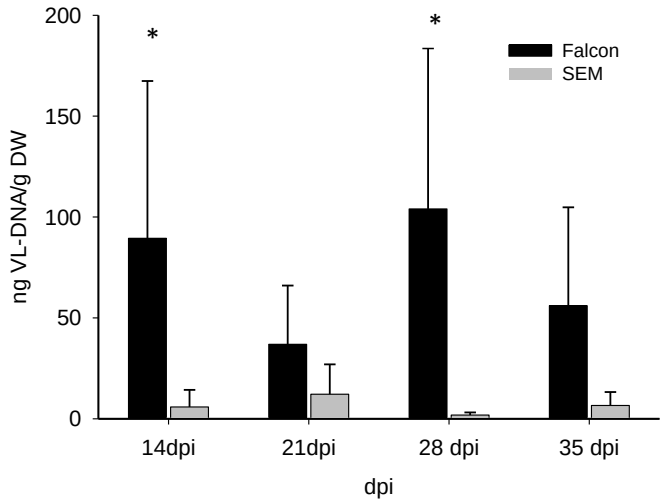

Figure 4.3 Mean fungal DNA concentrations and standard deviations in the upper hypocotyl part of B. napus genotypes 'Falcon' (black bars) and SEM (grey bars) detected by qPCR in the time course 14 dpi to 35 dpi. Asterisks indicate significant differences at a level of $P \leq 0.05$ (LSD).

4.3.3 *V. longisporum* infection induces ultrastructural changes in *B. napus* xylem-tissue

Colonization of vessel elements 35 days after inoculation

Transmission electron microscopy (TEM) was applied to investigate ultrastructural differences in cellular organization of hypocotyl xylem tissue between resistant and susceptible genotypes. First, toluidine blue-stained transverse sections of the hypocotyl at 35 dpi were studied by light microscopy to locate cellular alterations, vascular occlusions and fungal structures. No occlusions were detected in control sections of plants that had not been inoculated with *V. longisporum*. In contrast, occlusions were clearly visible in inoculated hypocotyls of both genotypes (Figure 4.4).

Interestingly, hyphal structures in the susceptible cv. 'Falcon' (see inset in Figure 4.4a), but not cv. SEM (Figure 4.4b) were present. In these plants, the fungus was exclusively located in individual vessel elements and was never found to colonize the entire vascular system. Strong colonization was only observed in highly infected plants of cv. 'Falcon' derived from greenhouse screening experiments (see chapter 2) at 38 dpi (Figure 4.5). Following the initial characterization by light microscopy sections were analyzed in detail using TEM. In micrographs of infected 'Falcon' hypocotyl, massive spread of the fungus was observed across the whole xylem tissue (Figure 4.5). Nearly all vessel elements and neighboring xylem parenchyma cells were colonized with fungal hyphae. These were found in close contact with the secondary walls of the vessel elements.

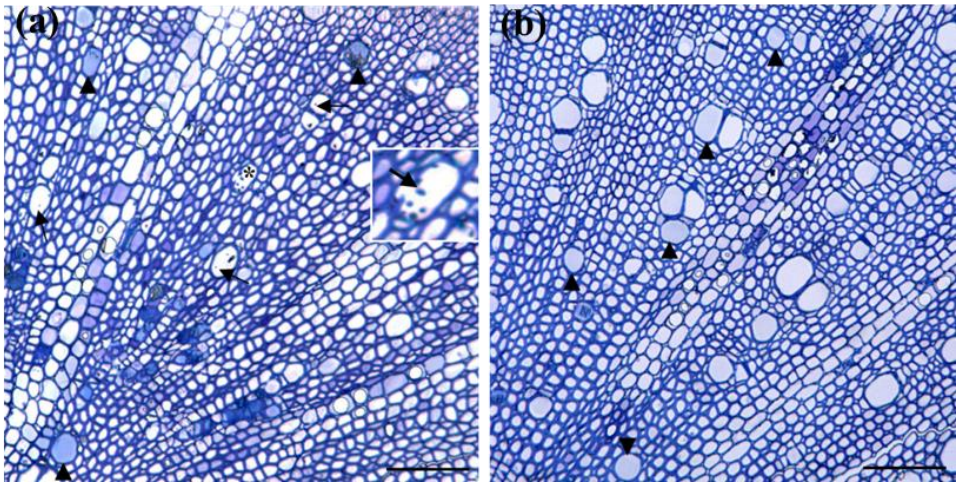

Figure 4.4 Light microscopy image of *V. longisporum* inoculated *B. napus* plants of the susceptible cultivar 'Falcon' (a) and the resistant genotype SEM 05-500256 (b). Transverse hypocotyl sections of the vascular tissue were fixed in glutaraldehyde/formaldehyde and osmium tetroxide at 35 dpi and stained with 0.1% toluidine blue. (a) In cv. 'Falcon' single vessels are colonized by *V. longisporum* (arrows) whereas other vessels are free of fungus. The inset is a magnification of a vessel colonized by fungal cells (asterisk). Vessel occlusions appear in blue (arrow heads); occlusion-free tracheary elements are white. (b) Some vessels are occluded (arrow heads) although from the investigated sections the presence of fungal structures is not obvious for those. Bar = 100 µm.

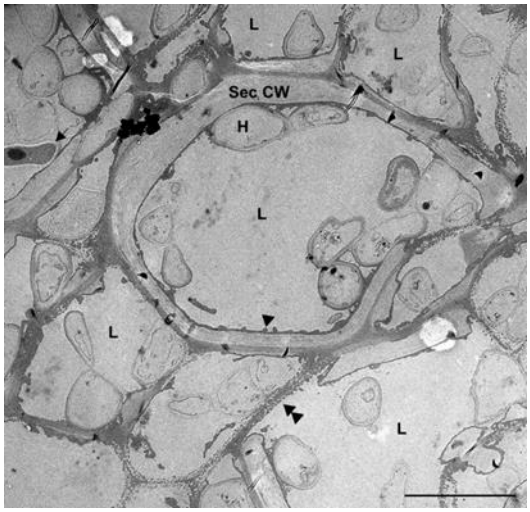

Figure 4.5 Transmission electron micrograph obtained from a *B. napus* plant of the susceptible cultivar 'Falcon' infected by *V. longisporum*. Transverse hypocotyl sections of the vascular tissue were fixed in glutaraldehyde/formaldehyde and osmium tetroxide at 38 dpi. Hyphae (H) are located in close contact to the secondary cell walls (Sec CW) of the vessels. Hyphae are already degraded; the arrow indicates a vital hyphal cell. Disease is far progressed: vessel elements and adjacent parenchyma cells are colonized with fungus and pit membranes are degraded (double arrow head). Note the electron dense substance covering the infected vessel (arrowhead). L = vessel lumen. Bar = 5 µm.

At 35 dpi, the fungus was found to attach to the secondary wall along the long axes of the vessel element in individual vessels of the susceptible cultivar 'Falcon' (Figure 4.6a). Interestingly, the pathogen is surrounded by a vascular substance that seems to derive not from the fungus itself, but from adjacent xylem parenchyma cells and that forms the vessel occlusions (Figure 4.6a, b). The vascular substance is either equally distributed in the vessel

element around the fungus (Figure 4.6a) or is restricted to the surrounding area of the fungal cells (Figure 4.6b).

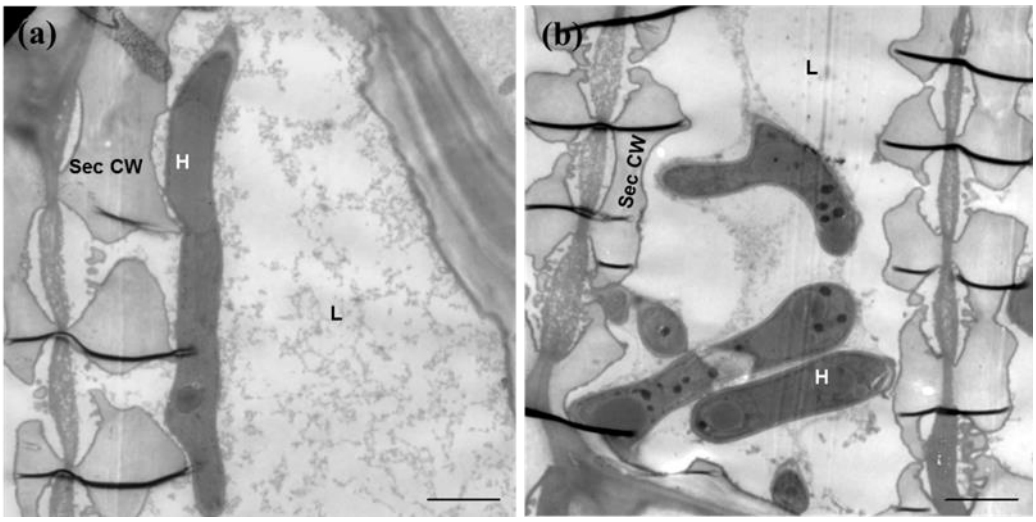

Figure 4.6 Transmission electron micrographs of *B. napus* plants of the susceptible cultivar 'Falcon' infected by *V. longisporum*. Hypocotyl sections (longitudinal) of the vascular tissue were fixed in glutaraldehyde/formaldehyde and osmium tetroxide at 35 dpi. (a) and (b) pit membranes are swollen and degraded, (a) Hyphae (H) attached to the secondary cell walls (Sec CW) are surrounded by a vessel occlusion substance, (b) Hyphae encapsulated by a vascular substance enter pit for spread into an adjacent vessel. L = vessel lumen. Bar = 2 µm.

The direct interaction of the fungal cell with the plant vessel surface was investigated at higher magnification. Distinct sites of fungal hyphae in close contact to secondary walls of vessel elements revealed that different adhesion structures mediate the attachment of the fungus to the secondary cell walls (Figure 4.7a, b). Either hyphal tips with an outer fibrillar layer attached to the host surface via tight contacts (Figure 4.7a) or, alternatively, a hyphal tip mediates the contact to the secondary cell wall through a layer that surrounds the cell wall (Figure 4.7b). Furthermore fungal cells were found with fibrillar layers completely covering the outer cell wall (Figure 4.7c, d). While the layer around the hyphae in Figure 4.7c appears fibrillar, the sheath lining the hyphae in Figure 4.7d has a more granular texture and nearly doubles the diameter of the hyphae.

In addition to the vertical spread of *V. longisporum* into the upper plant parts via the transpiration stream, colonization of the vascular tissue apparently also occurred by fungal growth through bordered pit-pairs, however, to much smaller extent. In Figures 4.8a-c hyphae seem to move towards the pit membrane, but successful penetration of the pit was only observed in a single specimen where the hyphae were located centrally in the pit membrane (Figure 4.8d). Such pit membranes near fungal cells were abnormally denatured and swollen (Figure 4.8a-d).

Furthermore, fungal hyphae were never found to penetrate xylem parenchyma cells. However, these cells were found in a partially disrupted condition (Figure 4.10b).

With respect to fungal propagation, the applied method did not permit a proper assessment to evaluate whether conidia were formed by budding or produced on conidiophores.

Although fungal cells were never detected in any of the screened sections of the resistant genotype SEM, low concentrations of fungal DNA detected by qPCR indicate the presence of fungus also in these samples. Therefore, ultrastructural changes observed in these sections can likely be attributed to infection with *V. longisporum* independent of the explicit presence of fungal structures.

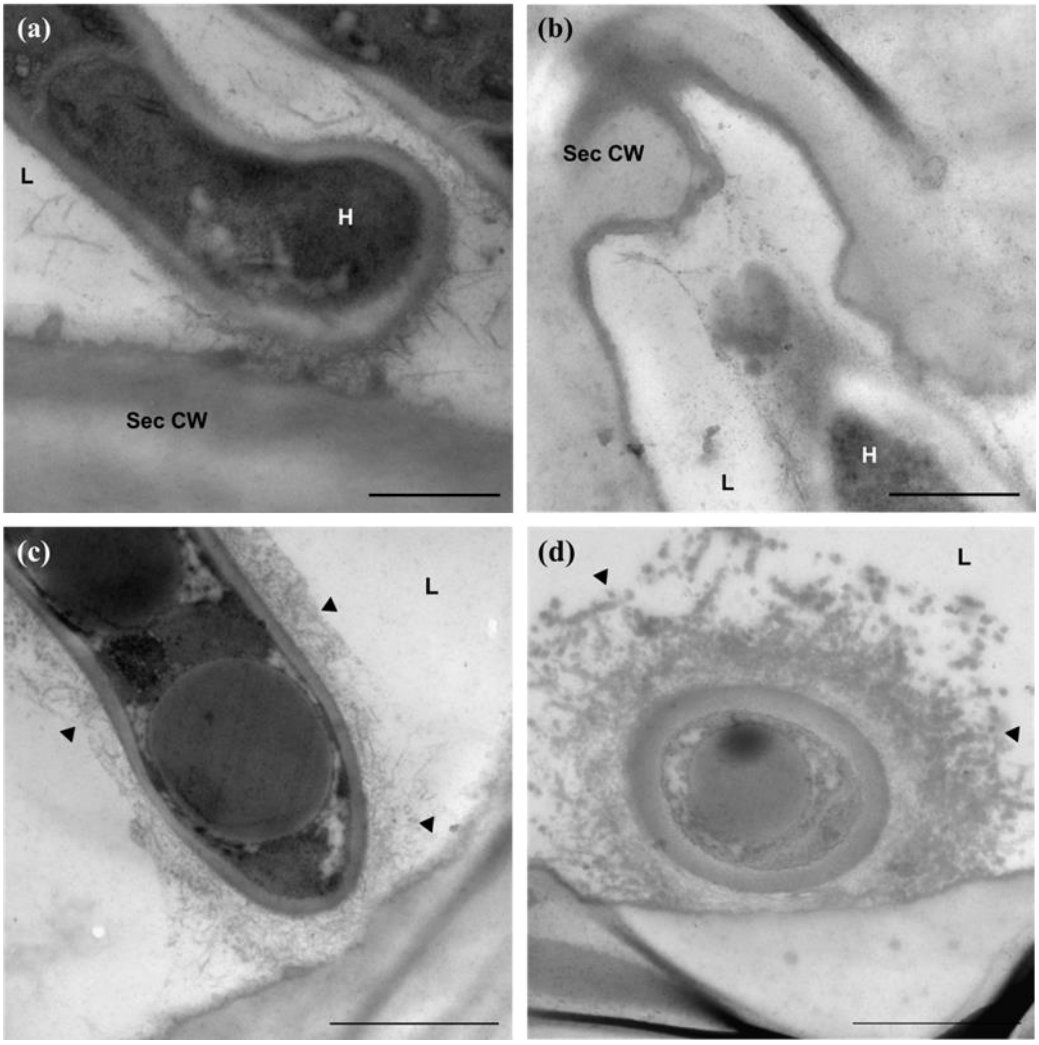

Figure 4.7 Close-up of fungal attachment to the inside of plant vessel walls. Transmission electron micrographs of *B. napus* plants of the susceptible cultivar 'Falcon' infected by *V. longisporum*. Longitudinal hypocotyl sections of the vascular tissue were fixed in glutaraldehyde/formaldehyde and osmium tetroxide at 35 dpi. (a)-(d) Fungal attachment to the secondary host cell wall. Various forms of coatings were found on hyphal cells. (a) Close attachment of a fungal cell to the cell wall, (b) hyphal cell in a rim-like bay of the secondary cell wall (Sec CW), which seems to be partially degraded. (c) The fungal cell wall is three-layered and the outermost layer is covered with a substance of fibrillar texture or granular appearance (arrowhead). (d) A thick layer surrounding the fungal cell (arrowhead). The fungal sheath appear to be granular-like. L = vessel lumen, H = fungal hypha. Bar in (a) und (b) = 500 nm, in (c) and (d) = 1 µm.

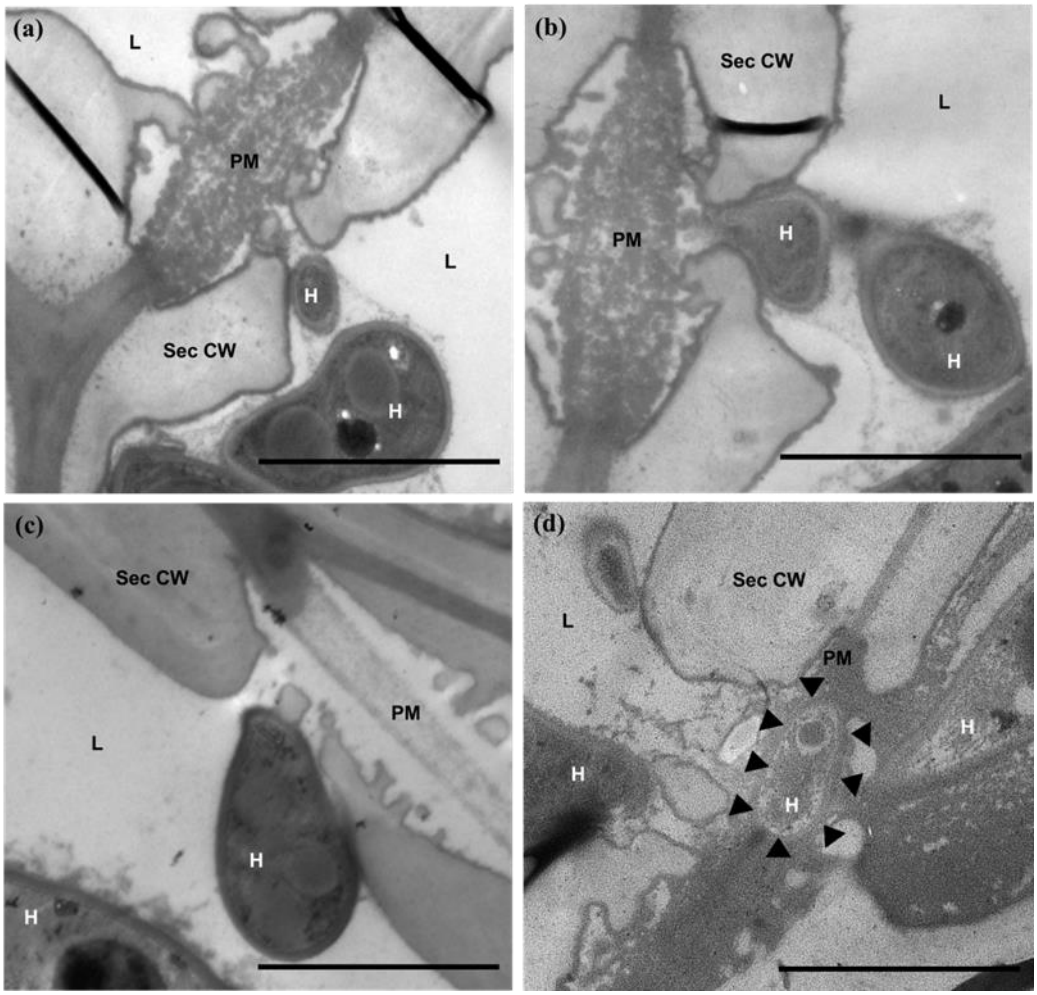

Figure 4.8 Transmission electron micrographs of *B. napus* plants of the susceptible cultivar 'Falcon' infected by *V. longisporum*. Hypocotyl sections ((a) and (b) longitudinal, (c) and (d) transverse) of the vascular tissue were fixed in glutaraldehyde/formaldehyde and osmium tetroxide at 35 dpi. (a)-(d) Spread by entering the adjacent vessel element, (d) Hyphal structure located in a pit membrane (PM, arrow heads), Prim CW = primary cell wall, Sec CW = secondary cell wall, L = vessel lumen, H = fungal hyphae. Bar = 2 µm.

Ultrastructural alterations of infected xylem vessel elements of the hypocotyl

Next we investigated ultrastructural changes of infected cells and the adjacent cellular environment. Ultrastructural alterations were clearly visible for hypocotyl sections of both 'Falcon' and SEM.

Three distinct changes were observed between infected and non-infected plants of either genotype. Firstly, infected vessels displayed a degradation of intertracheary pit membranes of bordered pit pairs (Figure 4.9a, c). The membranes seemed to be swollen and loose in texture if compared to pit membranes of control plants, where half bordered pit-pair membranes appear compact and smooth (Figure 4.9b, d). For SEM (Figure 4.9c) the degradation of the pit membrane seems to be further advanced compared to the membranes of 'Falcon' (Figure 4.9a), but this was only the case for a single specimen.

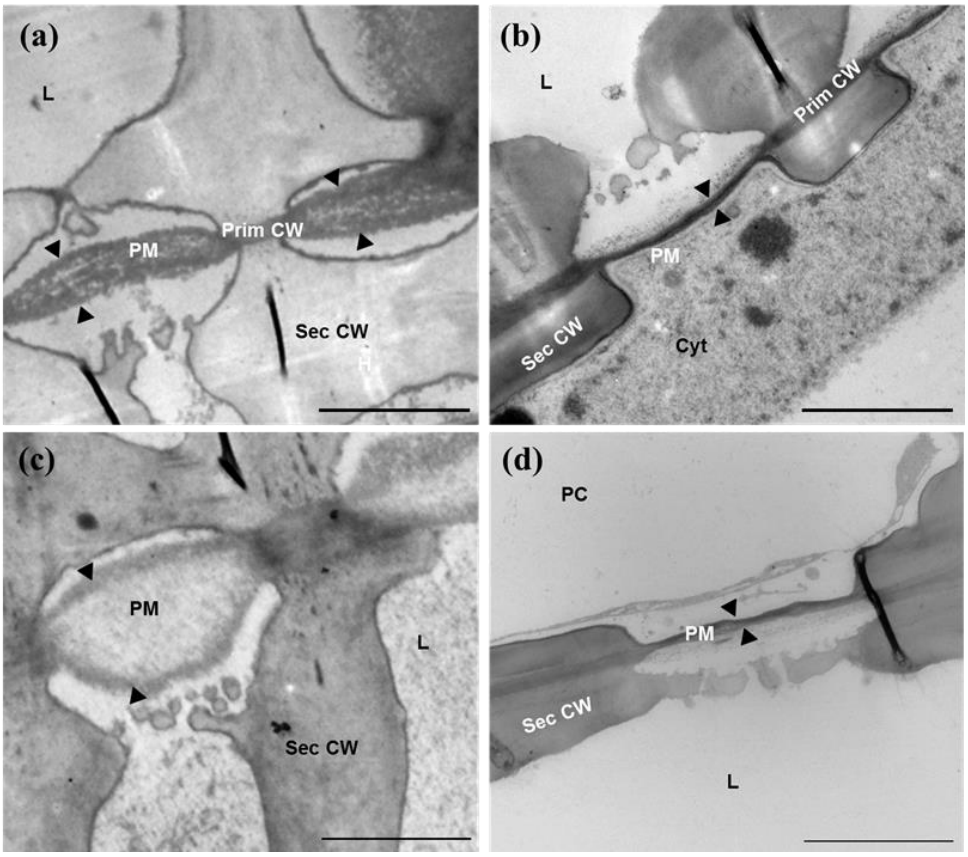

Figure 4.9 Transmission electron micrographs of *V. longisporum*-infected *B. napus* plants of the susceptible cultivar 'Falcon' (a), the resistant genotype SEM 05-500256 (c) and respective control plants (b, d). Hypocotyl sections ((a)-(c) longitudinal, (d) transverse) of the vascular tissue were fixed in glutaraldehyde/formaldehyde and osmium tetroxide at 35 dpi. (a, c) The pit membranes (PM) of bordered pit pairs in vessel members (intertracheary pits) are degraded (arrow heads) in infected cv. 'Falcon' (a) and SEM (c). The pit membrane of half-bordered pit-pairs between a vessel element and a neighboring parenchyma cell (arrow heads) is intact in control plants of 'Falcon' (b) and SEM 05-500256 (d). Prim CW = primary cell wall, Sec CW = secondary cell wall, L = vessel lumen, Cyt = cytoplasm, PC = xylem parenchyma cell. Bar = 2 µm.

In the resistant genotype additional alterations were observed at the pit area after infection with *V. longisporum* (Figure 4.10a, b). Newly synthesized cell wall material is deposited on the vessel-facing side of infected cells, obviously to block the connection between the vessel element and the adjacent parenchyma cell. This manifestation of vessel obstruction was found only in the resistant genotype.

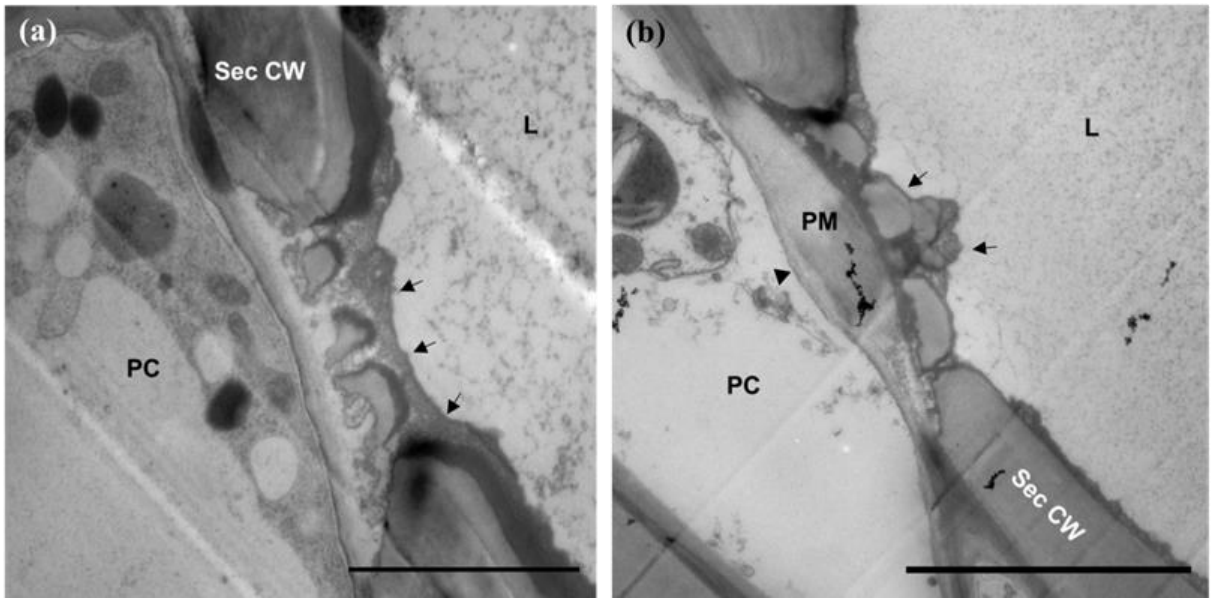

Figure 4.10 Transmission electron micrographs of *V. longisporum*-inoculated *B. napus* plants of the resistant genotype SEM 05-500256. Hypocotyl sections (transverse) of the vascular tissue were fixed in glutaraldehyde/formaldehyde and osmium tetroxide at 35 dpi. Reinforcement of the pit membrane (arrows in a and b) seems to block the connection between the vessel and the parenchyma cell (PC). (a) PC seems to be intact in (a) in contrast to cell lysis in (b). Sec CW = secondary cell wall, L = vessel lumen, PM = pit membrane. Bar = 2 µm.

Secondly, in nearly all sections continuous vessel wall coating was observed in infected plant samples of both susceptible and resistant genotypes (Figure 4.11a, c). The material covering the secondary cell wall thickenings is electron opaque and seems to consist of several layers. In particular, the pits seem to be strengthened (Figure 4.11a). In healthy plants such a layer of electron dense material stacked on secondary cell walls was never observed (Figure 4.11 b, d).

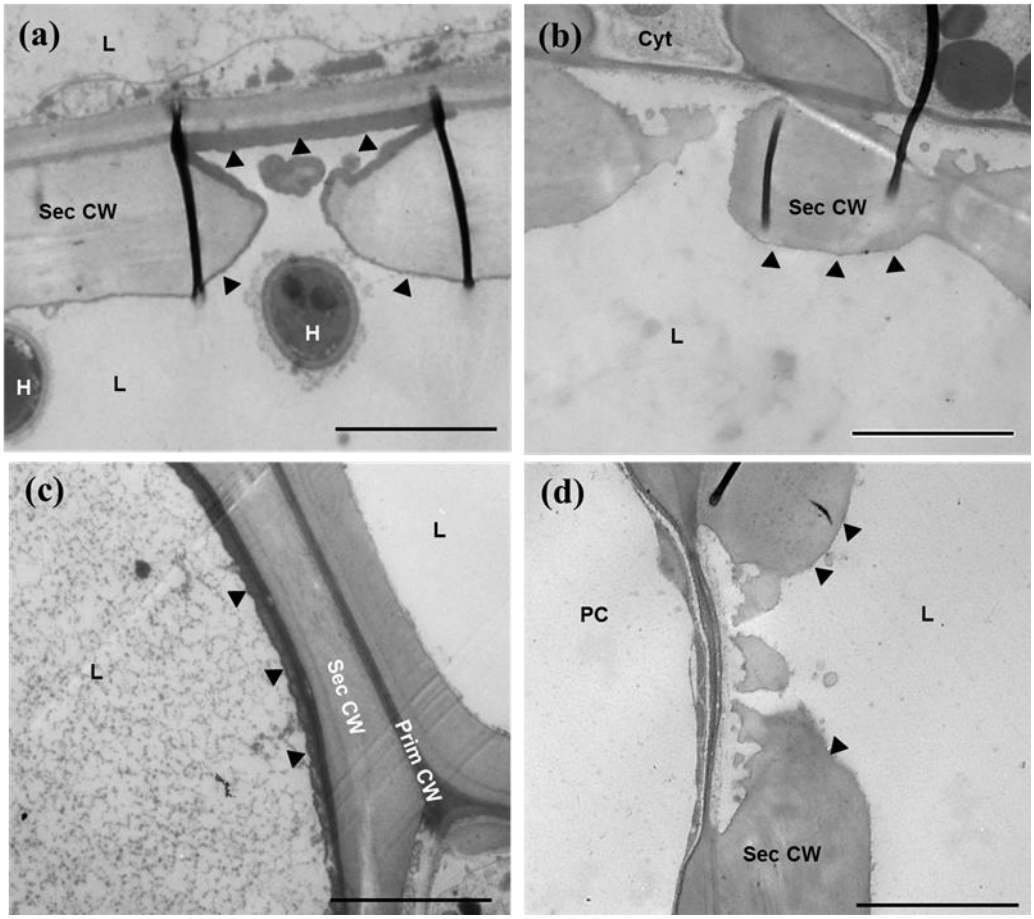

Figure 4.11 Transmission electron micrographs of *V. longisporum*-infected *B. napus* plants of the susceptible cultivar 'Falcon' (a) and the resistant genotype SEM 05-500256 (c) and respective control (b, d) plants. Hypocotyl sections ((a) and (b) longitudinal (c) and (d) transverse)) of the vascular tissue were fixed in glutaraldehyde/formaldehyde and osmium tetroxide at 35 dpi. (a, c) Secondary cell walls near fungal hyphae (a) or in occluded vessels (c) are covered by several layers of electron dense material (arrow heads). Note that secondary cell walls of mock inoculate plants are free of covering layers (b, d, arrow heads). Prim CW = primary cell wall, Sec CW = secondary cell wall, L = vessel lumen, Cyt = cytoplasm, PC = xylem parenchyma cell, H = fungal hyphae, Bar = 2 µm.

Thirdly, the plant is producing vessel occlusions of both granular and fibrillar structure apparently in order to prevent the upward spread of the fungus inside the vessels and to restrict the proliferation of the fungus (Figure 4.12a-d) in both the resistant and susceptible genotype. In some cases vessel occlusions occurred in direct contact to a vessel free of obstructions (Figure 4.11c). Our method was not suited to identify the substance the vessel plugs consist of.

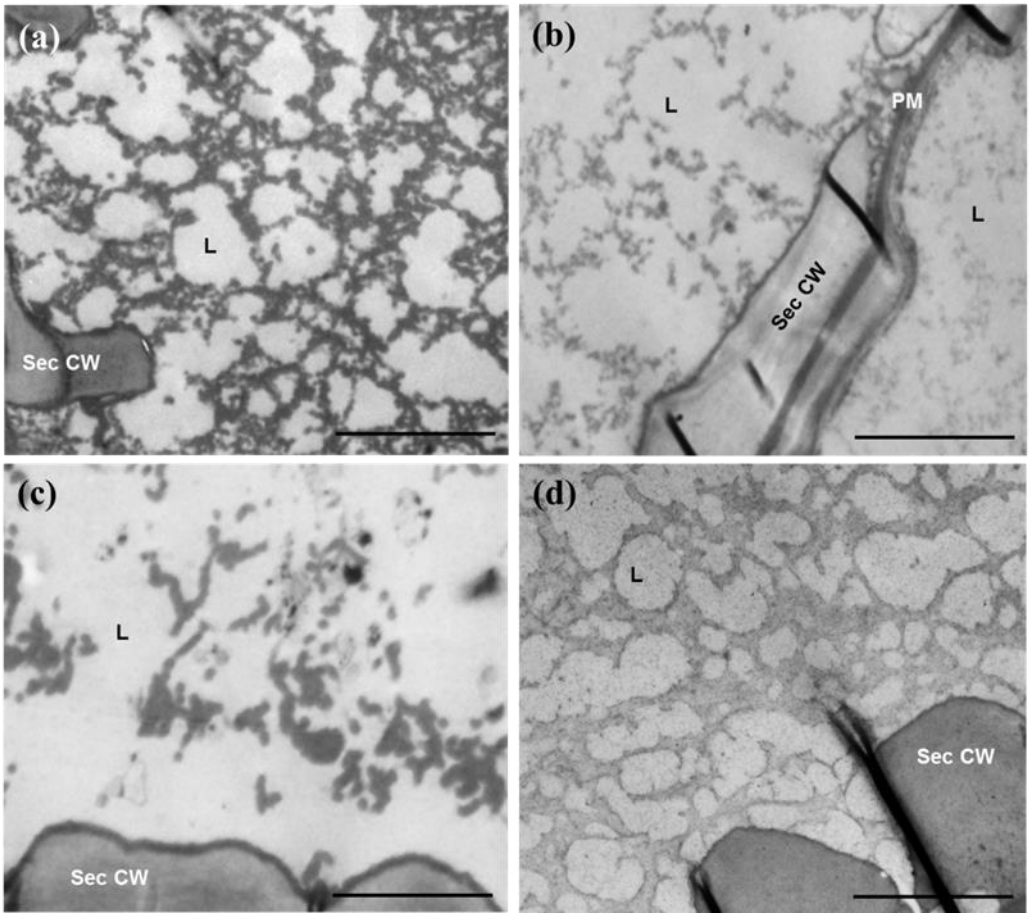

Figure 4.12 Transmission electron micrographs of *B. napus* plants of the susceptible cultivar 'Falcon' (a, b) and the resistant genotype SEM 05-500256 (c,d) infected by *V. longisporum*. Longitudinal hypocotyl sections of the vascular tissue were fixed in glutaraldehyde/formaldehyde and osmium tetroxide at 35 dpi. (a, c) Formation of fibrillar (a, d) or granular (b, c) vessel occlusions occur after infection with *V. longisporum* in 'Falcon' (a, b) and SEM (c, d). Sec CW = secondary cell wall, L = vessel lumen, PM = pit membrane. Bar = 2 µm.

4.4 Discussion

Plants have developed a diverse set of strategies to protect themselves from pathogenic invaders. Colonization of the plant vascular system may result in resistance responses that impede vascular invasion by the formation of physical barriers as well as inducing synthesis and secretion of antimicrobial agents to prevent systemic distribution of the pathogen. We here investigated whether ultrastructural changes in the vascular system may contribute to defense mechanisms in the *V. longisporum-B. napus*-interaction.

A previous study compared the resistance mechanisms to infection of oilseed rape with *V. longisporum* of the same resistant and susceptible genotypes also used in this study and suggested that differences in susceptibility of the tested genotypes arise from differences in abundance of resistance structures in the hypocotyl part of the plant. Using light microscopy it was found that a larger number of vascular occlusions were present in the hypocotyl of the resistant genotype SEM 05-500256 and that lignification of vessel elements was increased compared to the susceptible cultivar ‘Falcon’. Furthermore, biochemical investigations of the phenol content in infected hypocotyl tissues of the resistant genotype indicated an increase in constitutive and induced levels of soluble and cell wall-associated phenolic substances. Additionally, upon infection the increase in lignin content was more prominent in the resistant genotype compared to the susceptible cultivar (Eynck *et al.*, 2009). As an extension of these studies we used TEM together with qPCR to characterize resistance structures in hypocotyl sections of the resistant genotype SEM and the susceptible cultivar ‘Falcon’ at the ultrastructural level and to follow the growth and colonization of the fungus in close proximity to these sections over time.

Characterization of the dynamics of fungal spread in infected plants requires reliable quantification of fungus over time. For the time course of 14 dpi to 35 dpi qPCR analysis demonstrates accelerated colonization of the hypocotyl tissue of cv. ‘Falcon’ compared to the resistant genotype SEM 05-500256, where the fungal DNA concentrations remained low. These low levels of fungal DNA in the hypocotyl tissue of SEM plants confirm the resistance of SEM, since with the employed inoculation procedure (cutting roots before root dipping) it is unavoidable that conidia reach the xylem system. However, in the study by Eynck *et al*. (2009) with uncut roots low amounts of fungal DNA were detectable in the hypocotyl, revealing that host resistance does not result from penetration resistance. Rather, defense structures appear to be activated in the hypocotyl part or upper root parts to prevent the longitudinal spread of the fungus (Eynck *et al.*, 2009). Eynck *et al*. (2009) demonstrated the inhibition of fungal colonization of the upper stem parts in SEM plants. Here, qPCR results from a time course of 16 dpi to 79 dpi revealed that in SEM plants fungal DNA concentration in the hypocotyl was always below 25 g DNA/g fresh weight (FW) and in the upper stem

parts fungal DNA was not detected until 79 dpi while never exceeding 5 ng DNA/g FW. Moreover, it was found that in the cv. 'Falcon' colonization progressed until 79 dpi with highest concentrations of fungal DNA values of 203 ng DNA/g FW in the upper stem parts.

In contrast, qPCR data in this study show that fungal DNA content in the upper hypocotyl part fluctuates rather than increasing over time. One explanation for those fluctuating DNA concentrations could be the short time frame during which colonization is apparently not sufficiently strong to observe significantly increased levels of fungal DNA. Investigations of Eynck *et al.* (2009) were performed over a longer time period (16 dpi to 79 dpi), suggesting that this extended sampling is necessary to clearly observe a time-dependent increase in fungal DNA levels. Moreover, the sampling rate and sample number for qPCR analysis was probably too low to compensate for differences in individual plants of the same treatment. Hyphal lysis could be an alternative explanation for those fluctuating DNA concentrations (Dixon and Pegg, 1969).

Concerning the colonization pattern in the susceptible cv. 'Falcon', light microscopy studies performed on TEM sections confirmed the finding that fungal colonization is initially restricted to individual vessels and not present in xylem parenchyma cells (Eynck *et al*., 2007). Additionally, in this study, TEM investigations on hypocotyl tissue of susceptible greenhouse plants show that the fungus leaves vessel elements and colonizes the adjacent parenchyma cells, however at this state of the disease surrounding tissue is already necrotized and host plants are dead (Figure 4.5). At 35 dpi, the fungus is well established in 'Falcon' plants: Hyphal structures are found in close contact to secondary vessel walls and attachment appears to be mediated by special fungal adhesion structures or by plant cell wall material that has been degenerated by fungal enzymes. The observations demonstrate the existence of different types of extracellular layers covering the hyphal cells, possibly due to differences in hyphal age or in developmental stages of the fungus, i.e. spore or germination stadium. The chemical composition of such fungal adhesives or sheath is diverse; carbohydrates, proteins and glycoproteins were found to be components of fungal adhesions (Jones, 1994). Apart from the role of the sheath/extracellular layers in adhesion it was proposed that plant-derived covering material around hyphae of *V. dahliae* serves as an encapsulating agent that prevents the transfer of xylem sap nutrients of *Impatiens balsamina* plants to the fungal cell (Niederleitner *et al.*, 1991). Our TEM data support a similar observation: In the cross section of a hyphal cell in Figure 4.7d the structure of the coating material around the fungus appears to be distinctly different from those surrounding hyphal cells in Figures 4.7a-c. It seems that in this particular case encapsulation is associated with a partial loss of hyphal cytoplasm. However, hyphal encapsulation is unlikely to prominently contribute to resistance

since upon infection coating of hyphae is frequently found also in susceptible plants (Pegg and Brady, 2002), which is supported by our data.

In our study we never observed spores that were trapped in vessel end plates although this is likely to occur during infection. Whether these vessel-separating structures are involved in resistance has to be resolved.

In Falcon plants, colonization of the vascular system in longitudinal direction was hampered by production of gels consisting of different texture. Colonization into neighboring vessel elements was impeded by extensive vessel wall coating. This was also true for intertracheary pit (pits between vessel elements) regions. However, in spite of these efforts, hyphae were often found close to intertracheary pits and growth was directed towards the pit membrane, indicating imminent penetration. To some extent, we observed hyphae that had already entered into pit membranes. Such crossing of vessel separating pit membranes has previously been observed in highly susceptible tomatoes inoculated with *V.albo-atrum* (Bishop and Cooper, 1983b). However, we did not observe penetration of secondary vessel walls such as described for tomato (Bishop and Cooper, 1983b) or *B.napus* inoculated with *V. dahliae* (Niederleitner *et al*., 1991).

Although we could not identify fungal structures in any of the investigated specimen of resistant SEM plants, our qPCR data indicate the presence of the fungus also in these sections. An increase in the number of investigated specimen would increase the probability to discover fungal cells, probably in interaction with resistance structures. These data could provide further possibilities to characterize in detail how resistance is expressed in SEM.

Our TEM investigations also demonstrate that infection with *V. longisporum* results in several ultrastructural changes of the vascular elements. Intriguingly, this was true for both susceptible and resistant plants.

First, degradation of intertracheary pit membranes was found in both infected resistant and susceptible plants. Compared to control plants membranes of infected plants were swollen. Yet, we were not able to identify intertracheary pit membranes in control plants by TEM and therefore our data do not permit an appropriate comparison of pit membranes of control and infected plants. Degradation of pit membranes, which consist of the primary cell wall and the pectin-rich middle lamella, is likely caused by fungal exoenzymes such as cellulases or pectinases. The existence of pectic enzymes produced by *Verticillium* species is well established (Talboys and Busch, 1970; Wiese *et al.*, 1970). In susceptible tomatoes infected with *V. albo-atrum* the disintegration of middle lamella was found in conjunction with a high activity of endo-pectin-lyase (Cooper and Wood, 1980). A similar modification of the pit membrane was found in pea infected with *Fusarium* o*xysporum* f. sp. *lycopersici*, where membranes of the susceptible cultivar appeared to be swollen and fibrillar in texture (Bishop

and Cooper, 1983b). Similar to our pathosystem a previous study on *B. napus* and *V. dahliae* also described swelling and degeneration of intertracheary pit membranes. Furthermore it is reported that hyphae become well established in the vascular system in advanced disease states (Niederleitner *et al.*, 1991). In fact it is now assumed that in this study *B. napus* was infected by *V. longisporum* rather than *V. dahliae* since recent studies demonstrated that *B. napus* is not a suitable host for *V. dahliae* (Eynck *et al.*, 2007). In our study degradation of pit membranes seems to be equally present in both resistant and susceptible genotypes. Obviously, the resistant genotype does not inhibit membrane degradation. In contrast to findings by Bishop and Cooper (1983b) where fungal cells were present in vessel elements with degraded pit membranes, in a subset of our observations pit membrane degradation was independent of fungal hyphae in close proximity. This suggests that fungal enzymes are released at different sites in the vessel element and may diffuse upwards with the vascular stream (Cooper and Wood, 1974).

Second, we discovered abundant vessel coating in most of the infected vessels of resistant and susceptible plants vessel. Another investigation of *V. albo-atrum*-infected tomatoes described two different types of vascular coating consisting of either lignin or suberin in resistant and susceptible plants. The formation of these vessel coatings was delayed in susceptible plants (Robb *et al*., 1987). Although we did not further characterize the chemical nature of the coating material, we noted a morphological difference between secondary vessel wall lining material (Figures 4.11a, c) compared to material covering pit membranes between vessel elements and neighbouring xylem parenchyma cells in individual specimen of the SEM plants (Figures 4.10a, b). Whether these barrier-like structures are involved in resistance has to be resolved. Bishop and Cooper (1983b) found electron-dense material covering and occluding pit cavities between vessels as well as between vessels and parenchyma cells in susceptible interactions of tomato/*F. oxysporum* f. sp. *lycopersici* or *V. albo-atrum* and pea/ *F. oxysporum* f. sp *pisi*, which suggests that at least for this specific pathosystem pit membrane coatings are part of a general response to pathogenic invaders rather than a hallmark of resistance. In contrast, a study by Daayf *et al*. (1997) suggests to include cell wall strengthening as a factor of resistance mechanisms. In roots of resistant cotton plants infected by *V. dahliae* a layer coating the secondary cell wall of a vessel was identified as β-1,4-glucans (cellulose) using gold-conjugated exoglucanase. This cell wall reinforcement with cellulose together with terpenoid and phenolic production were detected earlier in resistant cotton lines compared to susceptible lines. It was therefore proposed that resistant and susceptible cotton lines can sense the site of infection, but defense mechanisms are activated earlier in resistant plants.

Third, our data indicate that vascular occlusions occur frequently in specimen of both resistant and susceptible genotypes. Eynck *et al.* (2009) demonstrated a positive relationship between the presence of occlusions and the level of resistance. We could not confirm these findings since our ultrastructural studies do not support a systemic investigation. However, we were able to distinguish two different types of vascular occlusions: Plugs observed in vessel elements appear to occur in either granular form or fibrillar type. Additional methods are required to identify and further characterize the composition of these plugging substances. Interestingly, the interaction of the fungus with vascular gels/gums was only observed in susceptible plants (Figure 4.6a, b). In resistant SEM plants the gels were never found, since the fungus was not present. It is possible that resistant plants provide a faster and more efficient response to invading pathogens suggesting that resistance structures are activated already in the upper root part and impede propagation of the fungus into the hypocotyl.

Several other reports exist that describe mucilage production in a variety of hosts due to invasion of vascular pathogens based on ultrastructural investigations (Bishop and Cooper, 1984; Ouelette *et al*., 1999; Clérivet *et al.*, 2000). For example, production of fibrillar and granular gel types were also observed in tap roots of pea infected with *Fusarium oxysporum* (Bishop and Cooper, 1984). It was proposed that the pathogen was restricted to the roots due to vessel plugs in the tap roots and the specific type of gel formation was suggested to be modified by different conditions in the vessels, such as Ca^{2+} or quinones. There is ample evidence that vessel occlusions originate from the host and not from the fungal pathogen (Beckman, 1964).

Furthermore, in our study, vascular occlusions by tylose formation were never observed in both resistant and susceptible genotypes.

The histological investigations of resistance structures in the interaction of *B. napus* with *V. longisporum* revealed several typical features that are commonly involved in vascular invasion of fungal pathogens and similar to those in other vascular diseases. As one of these features the plugging of vessels may compromise water transport to the upper plant parts and thus can cause drought stress in the plant. However, the *B. napus*/*V. longisporum* pathosystem does not involve wilting symptoms. One explanation would be that the fungus and hence the obstructions are restricted to single vessels and thereby strictly localized, so that systemic water transport can still be maintained at adequate levels. In addition, contrary to *V. dahliae* and *V. albo-atrum* (Pegg and Brady, 2002) no wilt inducing toxins of *V. longisporum* have been discovered so far.

Our data do not reveal significant ultrastructural differences between hypocotyl tissue of resistant and susceptible plants. Since our qPCR data demonstrate that fungal DNA content

is significantly reduced in the resistant genotype this suggests that resistant plants impede fungal colonization more efficiently and at an earlier stage. Resistant plants apparently respond more rapidly to pathogenic invasion, which manifests in a time dependent expression of resistance mechanisms. Similar to related pathosystems we suggest that susceptible genotypes fail to rapidly localize the pathogen and launch an adequate physical and chemical response at this site (Daayf *et al.*, 1997; Harrison and Beckman, 1982).

Immunocytochemical methods will allow to further characterize resistance structures observed in our TEM analysis and to identify the components that contribute to these resistance structures in SEM plants. Since resistance apparently involves a marked time-dependency in formation of these defense structures, a detailed description of these mechanisms will require a time course of similar investigations.

5. Assessment of *V. longisporum* resistance under drought stress conditions[1]

5.1 Introduction

Premature ripening caused by *Verticillium longisporum* is a prominent disease in oilseed rape (OSR) in Northern Europe and can cause yield losses when conditions are favorable (Dunker *et al.*, 2008). At present, fungicides for the control of *Verticillium* diseases are not available. Alternative options that can minimize the extent of *V. longisporum* infestation in the field include extension of the rapeseed crop rotation (Hornig, 1987; Daebeler *et al.*, 1988; Zeise and Seidel, 1990; Steinbach *et al.*, 2005; Ahlers, 1987), a later sowing time point (Keunecke, 2009) as well as the avoidance of cruciferous weeds and non-cruciferous crops (Zeise and Tiedemann, 2002a; Zeise and Steinbach, 2004). Moreover, the cultivation of resistant cultivars holds great potential (Ahlers, 1987; Hornig, 1987; Happstadius *et al.*, 2003, Rygulla *et al*., 2007). Recently, promising genotypes of *Brassica* species with improved resistance performance against *V. longisporum* have been identified (Rygulla *et al.*, 2007a; Rygulla *et al.*, 2007b, 2008).

The basis for efforts in resistance breeding is the understanding of the mechanisms of plant resistance. In *Verticillium* diseases, resistance responses such as chemical and morphological restriction are predominantly activated in the vascular tissue. Recent studies have shown that resistance of *B. napus* to *V. longisporum* is achieved by elevated constitutive and induced phenol levels, accumulation of lignin and increased numbers of vascular occlusions in hypocotyl vascular tissues. In particular, formation of vascular occlusions seems be crucial for inhibition of the pathogen spread in upper plant parts. What appears to be an effective resistance mechanism, however, can also negatively affect the efficiency of systemic water and nutrient transport in the plant. Under such conditions, limited supply of water may lead to severe changes in plant metabolism, which becomes manifest in reduction of agronomically important traits such as yield and oil quality (Shao *et al.*, 2009). The interference of upward water translocation by vascular pathogens can be due to the physical presence of the fungus itself in the xylem, secretion of fungal metabolites such as polysaccharides or by plant-derived substances such as gums, gels or tyloses (Agrios, 2005).

[1]This experiment was conducted by M.Sc. Daniel Lopisso within the framework of a research internship at the Department of Crop Sciences, Section of General Plant Pathology and Crop Protection

The water stream cannot pass these vessel obstructions and water supply to the upper plant parts is impeded. Under these conditions, stomata are closed to prevent wilting, which at the same time impedes gas exchange and thus results in reduced transpiration and CO_2 uptake (McElrone, 2004; Shao *et al.*, 2009) or alternatively, reduction in photosynthesis rate is redcued as a cause of direct effects on biochemical pathways (Bowden *et al.*, 1990).

In plant interactions with *Verticillium* spp., vessel clogging is thought to cause wilting symptoms. This is, however, not the case for *V. longisporum* on OSR. One of manifold reasons for this distinct characteristic could be absent secretion of wilt toxins by *V. longisporum* in contrast to its related species *V. dahliae* and *V. albo-atrum*. Since colonization of xylem vessels was found to be restricted to individual vessels, it has also been speculated that the plant possibly compensates for individual occluded vessels by production of new xylem elements (Eynck *et al.*, 2009).

The response of plants to drought stress is expressed by manifold physiological, biochemical and molecular alterations. Typical physiological modifications caused by drought stress are loss of turgor, reduced leaf water potential, stomatal closure with associated decrease in gas exchange and reduced photosynthesis, which ultimately leads to reduction in plant biomass production (Shao *et al*., 2009). Molecular responses to water deficit include increased synthesis of abscisic acid that is transported acropetally to upper plant parts, where it elicits drought response (Hartung *et al*., 2002). In addition, drought stress triggers a variety of biochemical responses such as decrease in photochemical efficiency, increase in antioxidative enzymes and accumulation of metabolites such as glutathione and proline (Shao *et al.*, 2009).

The purpose of the present study was to assess the effect of resistance structures induced in OSR plants upon infection with *V. longisporum* on the plant water potential and drought stress resistance. Our analysis of plant responses to drought stress focused on several selected parameters that include gas exchange measurements, proline analysis and fresh and dry weight determination. One interesting aspect is the question whether resistant genotypes subjected to both drought stress and *V. longisporum* infection have a disadvantage in drought resistance compared to equally treated susceptible plants (with lower number of vessel plugs). In a complex study we analyzed the physiological status of the resistant plant inoculated with *V. longisporum* and simultaneously exposed to drought stress. The performance of photosynthesis was investigated by gas exchange measurements. Furthermore, we compared the performance of resistant and susceptible plants by assessment of several agronomically important parameters such as phenological growth stages, number of side branches per plant and yield parameters such as, number of pods per plant, as well as shoot fresh and dry weight. To assess the ability of the plants to

respond to induced drought stress, we also monitored the accumulation of the osmoprotectant proline in leaf tissue.

5.2 Material and Methods

5.2.1 Experimental set-up

Various parameters monitoring potential effects of the *V. longisporum* infection on the water supply of the OSR plant were tested in a 2x2x2 factorial experiment arranged in a completely randomized design. Factors included were pathogen *V. longisporum* (inoculated and non-inoculated control plants), water supply (drought stressed = 30% field capacity; and well-watered = 60% field capacity) as well as genotype (‘Falcon’, susceptible and SEM, resistant). A total of 8 treatment combinations with 10 replications resulted in 80 experimental units.

5.2.2 Plant material

Seeds of the susceptible winter OSR cultivar (cv.) (‘Falcon’, Norddeutsche Pflanzenzucht, NPZ, Hans-Georg Lembke KG, Hohenlieth, Germany) and of the resistant genotype (SEM 05-500256, Lantmännen SW Seed, Svalöv, Sweden) were surface sterilized for 2 min in 70% EtOH and washed twice with sterile tap water. Three to four seeds per pot were planted in a multi-pot plate filled with sterile silica sand/soil mixture (1:1) and grown until three leaf stage in the greenhouse at 20°C with 16 h day and 8 h night conditions. Subsequently seedlings were separated, resulting in two seedlings per pot. Seedlings were vernalized for 13 weeks in a 4°C climate chamber with day/night conditions of 16 h/8, followed by a three day recovering phase in the climate chamber subjected to day/night conditions of 14 h/10 h at 23°C/20°C. Finally, plantlets were inoculated as described in the following paragraph.

Throughout the duration of the experiment plants were fertilized four and seven weeks after inoculation with Hakaphos (15% N, 11% P_2O_5, 15% K_2O; Compo, Münster, Germany). To control thrips infestation, biocontrol methods such as application of predatory mites and green lacewings (Katz Biotech AG, Germany) were applied at 7, 14, 35 and 42 dpi.

5.2.3 Fungal isolate and root dip inoculation

Verticillium longisporum isolate VL 43 was used for root dip inoculation of partly cut roots. The inoculation method is described in detail in chapter 4 (4.2.3). After inoculation, seedlings were transplanted to pots filled with sand-potting soil (Fruhstorfer Erde, Type P: upland moor peat, volcano clay, bark humus, pH 6.0; Hawita-Gruppe, Vechta, Germany) mixture (1:3) and grown in the greenhouse with temperature conditions of 20°C and 16 h/8 h day/night.

5.2.4 Drought stress conditions

Drought stress conditions were established gravimetrically according to Laermann (1972) and Gödecke (2007). In a first step, initial water content (iwc) in the sand-potting soil substrate was determined by calculating the weight difference of the sand-soil substrate before and after drying in an oven for 24 h at 105°C. Apart from determination of the soil water content, the capacity of the soil to hold water was calculated. For this purpose, a 2 cm layer of coarse gravel (Ø 0.2 -0.5 cm) was filled into plastic tubes (20 cm, Ø 5 cm) closed on one side with a plastic net (mesh size: ~ 2 mm) and immersed in tap water for 15 min. Plastic tubes were placed on a grid for a 15 min drying period after which weight was determined (W_1). Subsequently, 200 g of the oven-dried substrate was filled into the plastic tubes, which were then placed in water for 2 h to saturate the substrate. Plastic tubes were then placed again on grids to drain the water for 2 h, followed by 10 min drainage on absorbent paper. Subsequently the weight was determined (W_2) and finally the field capacity (FC) was calculated according to the following formula:

$$FC \text{ (water in g / 100 g soil)} = [(W_2 - 200g - W_1) / 2]$$

The adequate water content (AWC) that is considered to be sufficient for plant requirements is assumed to be 60% of the calculated FC (cFC, Gödecke, 2007). Taking into account the water content already included in the substrate (IWC), the AWC can then be calculated according to:

$$AWC = (60\% \text{ of cFC}) - (\text{IWC per } 100g \text{ of substrate})$$

In the beginning of the experiment, all plants were supplied with sufficient amount of water by adjusting and maintaing the soil moisture to 60% of FC. This was performed by weighing the pots (13 x 13 x 13 cm), calculating the amount of water to obtain the available FC of 60% and adding the amount of water required to attain 60% of FC. The drought stress treatment was started three weeks after inoculation with *V. longisporum* (21 dpi) when disease was fully established. The days following drought stress treatments were denoted as days post water treatment (dpwt). To induce drought stress the soil moisture was reduced by 50%

(Naderikharaji *et al.,* 2008) resulting in 30% of FC. Drought stress conditions were maintained for 7 weeks by weighing the pots every 2 to 3 days and supplying only the required amount of water according to each treatment. In order to consider the increasing plant biomass in the course of the experiment, additional plants were potted and increment in plant biomass was determined. For this purpose, two plants from each treatment were harvested every week, and average plant weight was determined after substrate of the roots was washed off with running tap water.

5.2.5 Disease assessment

Disease severity was recorded on a weekly basis from 14 to 49 dpi with a 1-9 assessment key (Table 5.1) and area under the disease progress curve (AUDPC) values was calculated as described previously (chapter 4, paragraph 4.2.4). Next, net AUDPC ($AUDPC_{net}$) values were calculated. Here, the calculated AUDPC values for the control treatments (FHN, SHN) and low water treatments (FLN, SLN) were subtracted from the corresponding AUDPC values of the inoculated treatments. These `net AUDPC values` consider alterations in the plant that occur due to drought stress and natural senescence phenomena such as yellowing of the leaves.

Table 5.1 Assessment key for the evaluation of the disease severity of *B. napus* plants infected by *V. longisporum*.

Score	Symptom development
1	No symptoms
2	Up to 10% of the leaves show yellowing/black veins or are dead
3	11 - 20% of the leaves show yellowing/black veins or are dead
4	21 - 40% of the leaves show yellowing/black veins or are dead
5	41 - 60% of the leaves show yellowing/black veins or are dead
6	61 - 80% of the leaves show yellowing/black veins or are dead
7	81 - 100% of the leaves show yellowing/black veins or are dead
8	Only apex is still alive
9	The plant is dead

Besides disease scoring, the plant height was recorded on a weekly basis, because stunting of the plants is a typical symptom for *V. longisporum* infection. Measurement of plant height was performed from the origin of the cotyledons to the tip of the shoots.

5.2.6 Physiological measurements

The physiological status of the plant was investigated by gas exchange measurements, including net photosynthesis rate, stomatal conductance and transpiration rate. The measurements were conducted with the portable Photosynthesis system (HCM-1000 WALZ, Effeltrich, Germany) once per week for a period of five weeks. The first measurement started at 28 dpi, i.e. seven days after initiation of drought stress. Data with the WALZ device were sampled between 9:30 am and 3:30 pm. For the measurement of the leaf gas exchange, the 2nd or 3rd fully expanded leaf was placed in the leaf chamber. The difference between the gas compositions (CO_2 and H_2O) of the in-streaming air and the out-streaming air chamber was detected by an infrared gas analyser (IRGA, type BINOS-100/4PS). With the collected gas exchange data, the photosynthesis rate, stomatal conductance and transpiration rate were calculated. The measured leaf area of 5 cm^2 was subjected to the following leaf chamber conditions: Gas flow rate was 804 ml min^{-1}, the photosynthetic active radiation (PAR) was adjusted to 800 µmol m^{-2} s^{-1}, temperature was 20°C and relative humidity was within 57 to 80%.

5.2.7 Determination of proline content

In order to monitor proline accumulation in leaves, we measured the proline content at 14, 28 and 35 days after the initiation of drought stress (accordingly 35, 49 and 56 days after inoculation) in the 2nd and 3rd fully expanded leaves according to a modified protocol of Bates *et al.* (1973). Harvested leaves were shock frozen in liquid nitrogen until further use. The plant material was crashed to fine powder with a mortar and pestle and 0.5 g of the leaf powder was immediately mixed with 10 ml 3% aqueous 5-sulfosalicylic acid (w/v) (Roth, Karlsruhe, Germany) in 50 ml reaction tubes. Following centrifugation at 5200 rpm for 20 min at room temperature, 500 µl of the supernatant was mixed with 500 µl acid Ninhydrin (2.5 g ninhydrin (Roth, Karlsruhe, Germany) in 100 ml of a mixture containing glacial acetic acid, 85% orthophosphoric acid and distilled water in a ratio of 6:3:1) and 500 µl of glacial acetic acid in a 2 ml reaction tube and subsequently boiled at 100°C for 1 h. After boiling, the mixture was placed on ice for 5 - 10 min and then 800 µl were transferred to a new reaction tube and proline extraction was achieved by adding an equal amount of toluene and vigorous mixing for 15 min. For the spectrophotometric measurement, 200 µl of the toluene phase were transferred to a 96 well plate (Sarstedt, Newton, USA) and absorbance was measured in triplicate at 520 nm (µQuant, Bio-Tek Instruments, Bad Friedrichshall). Pure toluene served as a blank. For quantification of proline a standard curve was produced with L-proline (Fluka, Biochemika, Buchs, Schweiz) with concentrations of 100.0, 80.0, 60.0, 40.0, 20.0,

10.0, 5.0, and 0.5 µg/ml and the final concentration of proline in the leaves was calculated according following formula (Bates, 1973):

[(µg proline/ml × ml toluene) / 115.5 µg/µmole] / [(0.5 g) /5] = µmoles proline / g fresh weight

5.2.8 Assessment of agronomic parameters

The effect of water stress associated with a *V. longisporum* infection was expected to be reflected in yield parameters. Therefore, the following agronomically important parameters were investigated: Number of side branches per plant was recorded during the period from 14 to 49 dpi and the phenological growth stage during the time course from 21 to 49 dpi according to Weber and Bleiholder (1990) and Lancashire *et al*., (1991) (Appendix Table A 3). At 64 dpi, plant stem diameter was measured at the cotyledon origin with an electronic caliper. At the final sampling time point (65 dpi) when plants were in GS 80-85, number of pods per plant was determined. In addition to this, shoot fresh and dry weight was determined from the plant part above the hypocotyl. For fresh weight determination, the shoot biomass was weighed immediately after harvesting and subsequently dried for 60 h at 80°C to determine the dry weight.

5.2.9 DNA extraction and quantitative PCR analysis

Quantitative real-time PCR (qPCR) was performed for detection of the fungus in the lower stem part (hypocotyl tissue). A 5 cm stretch of the lower stem part of all 80 experimental units was harvested at 65 dpi. The plant material was then immediately placed on ice and stored at -20°C until further preparation. The stem tissues were lyophilized for 72 h (Freeze Dryer Alpha 1-4, Martin Christ Freeze Dryers, Osterode am Harz, Germany) and milled in a mixer mill (Retsch MM 200, Retsch GmbH, Haan, Germany). To reduce the sample number per treatment, plant tissue samples from two plants each were pooled resulting in 5 samples per treatment. Then total genomic DNA was isolated as described above (see chapter 4, paragraph 4.2.6). Preparation of qPCR reaction mixture with primer pair OLG 70/ OLG71 and analysis in a CFX 384 Real-Time PCR detection system including a C1000 thermal cycler base with a CFX 384 optical reaction module was performed as previously described (see chapter 4, paragraph 4.2.6).

5.2.10 Statistics

STATISTICA for Windows Version 9.1 (Statsoft, Inc. 2010) was used for statistical analysis. The mean of 10 (disease and agronomic data), 5 (qPCR analysis), 3 (physiological data) and 2 (proline measurement) samples was analyzed with analysis of variance (ANOVA) and least significant difference (LSD) between the mean values was determined by a Fisher LSD test at $P = 0.05$.

5.3 Results

5.3.1 Disease development in resistant and susceptible genotypes exposed to drought stress

Approximately 21 dpi first *Verticillium* symptoms such as yellowing or even abscission of the oldest leaves were observed in inoculated 'Falcon' and SEM plants, but to a higher extent in 'Falcon' plants. At this time, all screened 'Falcon' plants expressed symptoms, while in resistant SEM plants only approximately 40% of the plants showed first symptoms. This time point also marks the initiation point of the drought stress treatment, which implies that the observed differences between SLI and SHI are not due to drought stress. At 28 dpi, when individual water treatments are established, no significant differences in disease scores were observed between the drought stressed and sufficiently watered inoculated 'Falcon' plants (Table 5.2). A slight difference between the drought stressed (SLI) and normally watered (SHI) inoculated SEM plants was detected at 28 dpi, but similar or higher disease scores for the treatment SLI were already present at 21 dpi, when water stress had just been initiated. In this case, higher disease values cannot be explained by the drought stress factor. Mean disease scores for the drought stressed control treatments FLN and SLN doubled from 28 dpi to 35 dpi (7 dpwt to 14 dpwt), meaning that drought stress induce similar symptoms as infection due to *Verticillium.*

Although disease symptoms were clearly present in both inoculated genotypes, disease progression in 'Falcon' plants over a screening period of 35 days occurred more rapidly as expressed in a higher AUDPC value of 92.05 compared to 25.2 for inoculated SEM plants (Figure 5.2). This remarkably high AUDPC value for inoculated 'Falcon' plants does not differ significantly when the factor drought stress is also included. In contrast, the net AUDPC value increased markedly when inoculated SEM plants were simultaneously exposed to drought stress (SLI) (Figure 5.2). However, these plants did already exhibit more disease symptoms before drought stress was applied (Table 2) as discussed above.

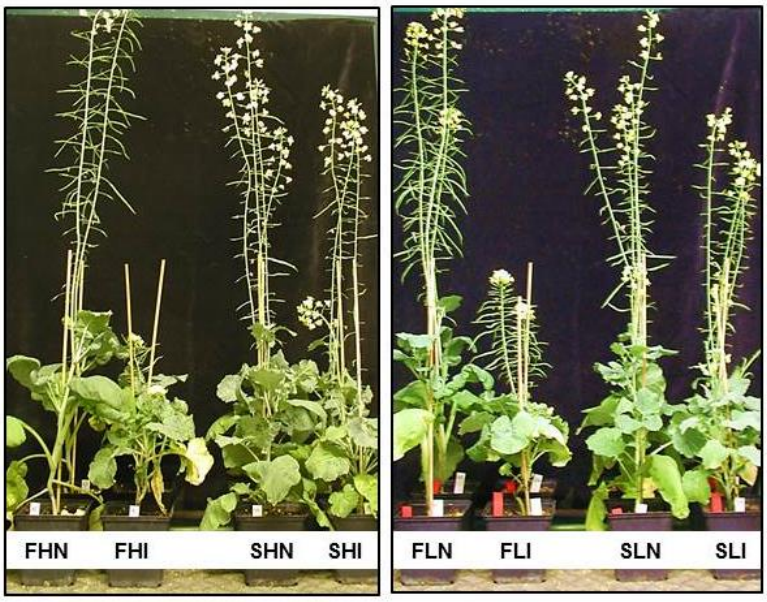

Figure 5.1 Phenotypes of *B. napus* cultivar 'Falcon' (F) and genotype SEM (S) at 42 dpi inoculated with *V. longisporum* (I) in comparison to control plants (N = non-inoculated) subjected to drought stress (L = low water level) or normal sufficient watered plants (H = high water level).

Table 5.2 Mean disease scores and standard deviations (brackets) of *V. longisporum* inoculated *B. napus* plants of the genotype 'Falcon' (F) and SEM (S) subjected to 60% (H = high water level) or 30% (L = low water level) of field capacity in comparison to control plants (N = non-inoculated) at 14, 21, 28, 35, 42 and 49 dpi and 7, 14, 21 and 28 dpwt respectively. Disease score is based on 1-9 assessment key in paragraph 4.2.4. Means followed by the same letter do not differ significantly at a level of $p \leq 0.05$ (LSD).

	dpi (dpwt)					
treatment	**14**	**21 (0)**	**28 (7)**	**35 (14)**	**42 (21)**	**49 (28)**
FHN	1.4 (± 0.84) ab	1.2 (± 0.63) ab	1.7 (± 0.67) bcd	2.6 (± 0.70) efg	4.8(± 0.79) mno	5.3 (± 0.48)opq
FHI	1.0 (± 0.00) a	3.9 (± 0.57) jkl	5.9 (± 0.32) qrs	6.4 (± 0.52) stu	6.9(± 0.33) u	6.8 (± 0.42) tu
FLN	1.2 (± 0.63) ab	1.4 (± 0.84) ab	1.3 (± 0.67) ab	2.8 (± 0.79) fgh	4.6 (± 0.70) mn	5.1 (± 0.57)nop
FLI	1.2 (± 0.63) ab	3.7 (± 0.82) ijk	5.6 (± 0.70) pqr	6.3 (± 0.44) stu	6.8 (± 0.42) tu	6.8 (± 0.42) tu
SHN	1.0 (± 0.00) a	1.0 (± 0.00) a	2.2 (± 1.03) def	3.3 (± 1.16) hij	4.4 (± 0.73) lmn	5.4 (± 0.70)opq
SHI	1.0 (± 0.00) a	1.3 (± 0.67) ab	3.1 (± 0.88) ghi	4.3 (± 1.06) klm	5.6 (± 0.70) pqr	6.4 (± 0.84) stu
SLN	1.4 (± 0.84) ab	1.1 (± 0.32) ab	1.5 (± 0.71) abc	2.9 (± 1.29) gh	4.8 (± 1.40)mno	6.1 (± 0.99) rs
SLI	1.2 (± 0.63) ab	2.1 (± 0.88)cde	4.2 (± 0.63) klm	5.3 (± 1.16)opq	6.2 (± 0.63) rst	6.9 (± 0.32) u

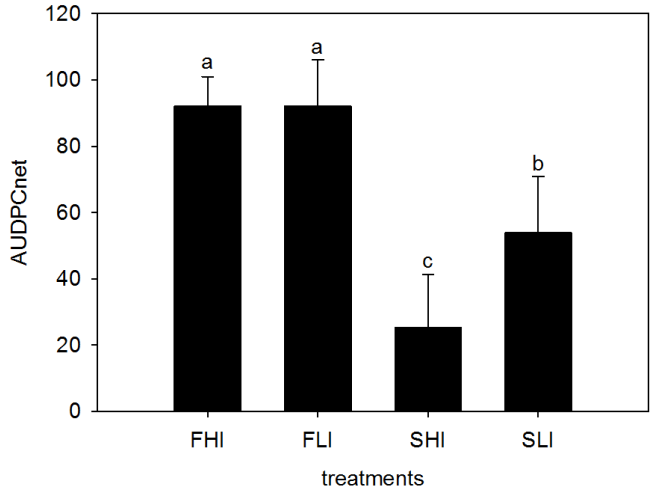

Figure 5.2 Net AUDPC values of inoculated (I) oilseed rape plants with a 1-9 assessment key from 14 to 49 dpi and standard deviations of 'Falcon' (F) or SEM (S) plants subjected to 60% (H = high water level) or 30% (L = low water level) of field capacity. Values with the same do not differ significantly at a level of $p \leq 0.05$ (Fisher`s LSD test).

Since *V. longisporum* infection under controlled conditions causes stunting in plants, this parameter was additionally monitored from 14 to 49 dpi by measuring plant height. The plant height of inoculated plants of the susceptible cv. 'Falcon' was significantly reduced at all investigated time points compared to the corresponding control plants (Figure 5.1 and 5.3). While reduction in plant height was on average approximately 20% at 14 dpi, a clearly reduced plant height of roughly 70% on average was observed 49 days after inoculation. Drought stress did not significantly influence the plant height of cv. 'Falcon': statistical analysis revealed no significant differences between inoculated plants under drought stressed and inoculated normally watered control plants at all investigated time points. Remarkably, there was no significant reduction in plant height in inoculated plants of the resistant genotype SEM at any of the investigated time points except 49 dpi where we observed that drought stress seems to affect plant height. At this time point, plant height of SLI treatments was significantly reduced compared to both SLN and SHI treatments. Obviously, drought stress more strongly affects SEM plants; however this was statistically significant only at one time point throughout the period of data collection.

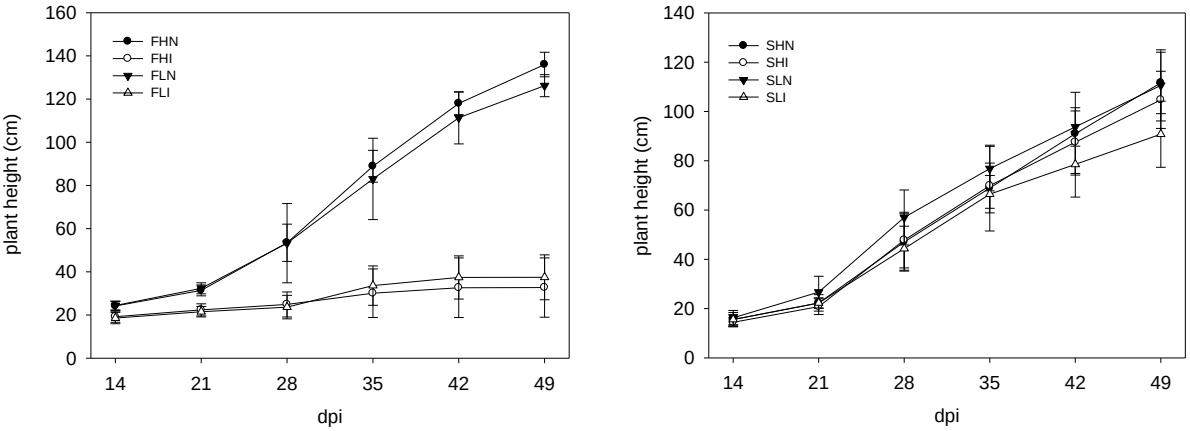

Figure 5.3 Development of the plant height from 14 to 49 dpi of *V. longisporum* inoculated (I) 'Falcon' plants (left side) or SEM plants (right side) and respective control plants (N = non-inoculated) subjected to 60% (H = high water level) or 30% (L = low water level) of field capacity.

5.3.2 Infection by *V. longisporum* in combination with drought stress has no significant effect on photosynthesis rate, transpiration rate and stomatal conductance

A good measure for studying the combined effect of a vascular infection and drought stress is the measurement of the physiological state of the plant. For that purpose the net photosynthesis rate, transpiration rate and stomatal conductance was measured weekly from 28 to 56 dpi (7 to 35 dpwt). Measurements of these parameters requires time-consuming calibration of the leaf chamber and hence we reduced the number of investigated plants from 10 to 3. The data obtained for the photosynthesis rate were not statistically firm because of high variation between different time point measurements (Figure 5.4). However, data from the first measuring time point (28 to 42 dpi; beginning of flowering) revealed that inoculated, less watered plants of both genotypes exhibited a trend towards lower values compared to non-inoculated, well-watered control plants, indicating that both reduced water supply and the infection with *V. longisporum* cause stress in the plant. At the following measurement points from 49 to 56 dpi differences between the treatments were not significant. At 49 dpi, net photosynthesis rate of the different treatments of cv. SEM were even similar. At 56 dpi, the treatment SLN showed a trend to lower net PS-rates.

Transpiration rate and stomatal conductivity data showed a high variability within the three replications, resulting in high standard deviations. However, from 28 to 42 dpi, non-inoculated, well-watered treatments of 'Falcon' and SEM displayed a trend to increased conductance values, meaning that stomatal closure is reduced. This promotes gas exchange in these treatments and thus increases net PS-rates as already mentioned above.

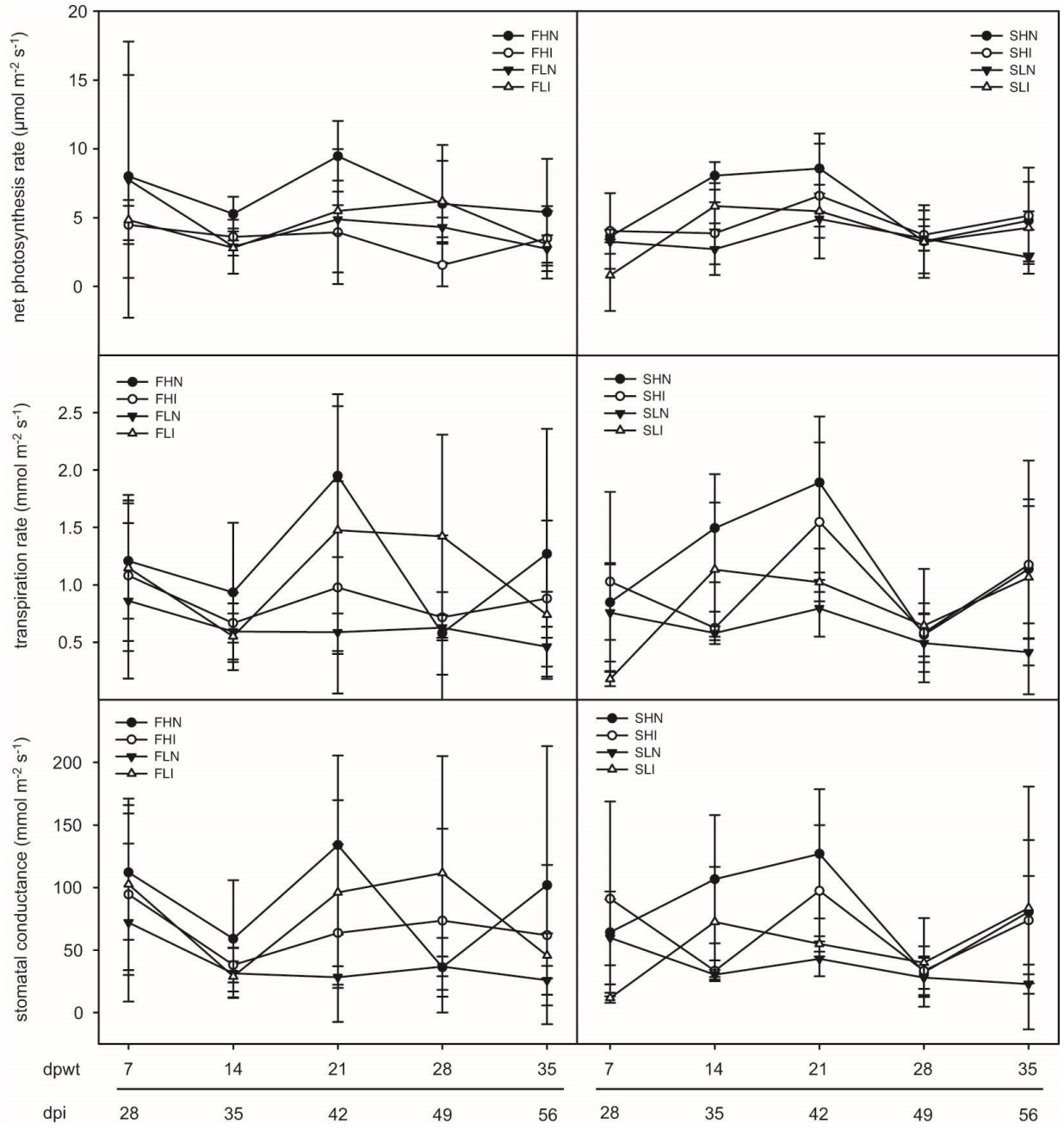

Figure 5.4 Photosynthesis rate, transpiration rate and stomatal conductance measured on the 2nd or 3rd fully expanded leaf weekly from 28 to 56 dpi. Plants were either inoculated with *V. longisporum* (I) or control (N = non-inoculated) and subjected either to 60% (H = high water level) or 30% (L = low water level) of field capacity. Dpi = days post inoculation, dpwt = days post water treatment.

5.3.3 Drought stress induces proline accumulation at moderate levels

A frequent indication for a drought-induced stress in plants is the accumulation of free L-proline (Delauney and Verma, 1993). We therefore measured proline content in order to quantify the intensity of the drought stress protection. The high accuracy of our proline standard curve (Figure 5.5) permits precise quantification of proline concentrations. Since proline measurements could only be performed in duplicate, statistically significant differences among treatments are difficult to detect. However, at 14 dpwt, when drought stress was established, we observed differences in proline concentration between different genotypes. In the SHN, SLN and SLI treatments twice as much proline was found compared to 'Falcon' plants (Table 5.3). Since proline content in control treatment SHN was at a similar level compared to low watered treatments of SEM genotypes, a higher constitutive level of proline can be assumed in these plants. This observation was supported by data obtained at 21 dpwt and the last time point 35 dpwt. In contrast, the low watered treatment FLN showed a markedly increased accumulation of free proline at 28 dpwt, although these data remain inconclusive due to high standard deviation. Higher constitutive levels of proline could possibly promote drought resistance in SEM and this has to be confirmed by repeating the experiment with an increased number of replicates.

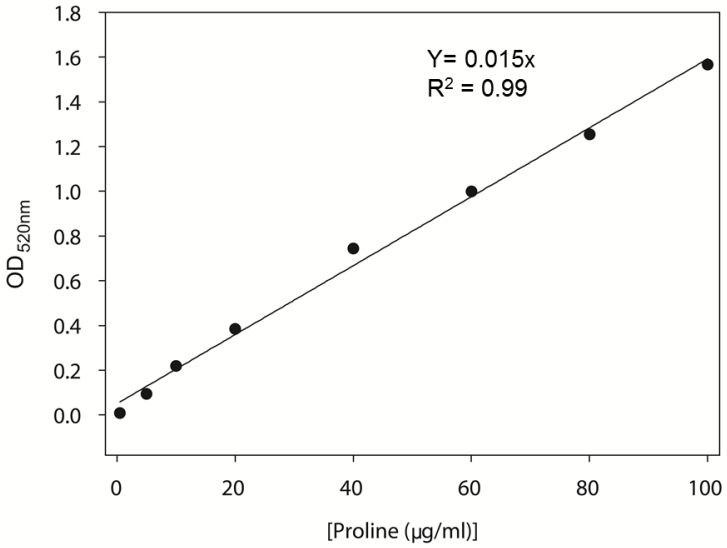

Figure 5.5 Standard curve for proline quantification. Known L-proline concentrations were prepared according to description in paragraph 5.2.7 and absorption at 520 nm was quantified spectrophotometrically.

Table 5.3 Mean proline content (n = 2) and standard deviations (brackets) of *V. longisporum* inoculated *B. napus* plants of the genotype 'Falcon' (F) and SEM (S) subjected to 60% (H = high water level) or 30% (L = low water level) of field capacity in comparison to control plants (N = non-inoculated) at 35, 49 and 56 dpi and 14, 28 and 56 dpwt respectively. Values with the same letter in each column do not differ significantly at a level of $p \leq 0.05$ (Fisher`s LSD test).

	dpi (dpwt)		
treatments	35 (14)	49 (28)	56 (35)
FHN	0.70 (± 0.19) a	0.41 (±0.08) a	0.46 (± 0.02) a
FLN	0.71 (± 0.29) a	1.56 (±1.77) a	0.54 (±0.12) a
FHI	0.86 (±0.11) a	0.47 (±0.13) a	0.53 (±0.08) a
FLI	0.75 (± 0.18) a	0.60 (±0.06) a	0.55 (±0.11) a
SHN	1.59 (± 1.32) a	0.34 (±0.06) a	0.52 (±0.05) a
SLN	1.56 (± 0.75) a	0.88 (±0.37) a	0.88 (±0.31) b
SHI	0.59 (± 0.13) a	1.79 (no s.d.) a	0.66 (±0.12) ab
SLI	1.41 (± 1.16) a	0.87 (±0.21) a	0.58 (±0.07) ab

5.3.4 Agronomical parameters

5.3.4.1 Analysis of phenological growth stages reveals growth delay of inoculated susceptible cultivar

Fungal infection or drought stress affects plant development and therefore phenological growth stage analysis was performed from 21 to 49 dpi. In cv. 'Falcon', the onset of flowering seems to be delayed in inoculated treatments both under conditions of normal water supply and drought stress (Table 5.4). There was no statistically significant difference between the inoculated drought treatment and normally watered treatment at 35 dpi and thus the observed alteration in growth pattern cannot be ascribed to drought conditions. The retardation in plant development was only observed for the beginning of the flowering growth stages. Towards the end of the flowering stage, differences between inoculated and control plants were not significant anymore. In contrast to 'Falcon', no delay in flowering and growth retardation was observed in SEM plants. Infection obviously caused changes in growth development only in the susceptible cultivar 'Falcon'.

Table 5.4 Average phenological growth stages and standard deviations (brackets) of 10 *B. napus* plants of the cultivar 'Falcon' (F) and genotype SEM (S) inoculated with *V. longisporum* and/or subjected to drought stress. Plant development was scored with assessment key according to Weber and Bleiholder (1990); Lancashire *et al*. (1991). Values with the same letter do not differ significantly at a level of p ≤ 0.05 (Fisher`s LSD test).

	dpi				
treatments	21	28	35	42	49
FHN	47 (± 0.33) a	63 (± 2.16) efghij	67 (± 0.84) klmn	67 (± 0.00) klmn	68 (± 00.63) klmn
FLN	50 (± 0.63) abcd	61 (± 6.84) e	66 (± 2.02) jklm	67 (± 0.32) klmn	69 (± 03.06) n
FHI	48 (± 4.62) a	62 (± 4.13) efgh	62 (± 7.62) efgh	61 (± 6.98) efg	66 (± 10.83) jklmn
FLI	49 (± 3.54) ab	62 (± 3.53) ef	62 (± 6.93) efghi	65 (± 5.13) ghijkl	68 (± 06.96) mn
SHN	49 (± 3.68) abc	63 (± 4.50) efghij	65 (± 4.94)fghijklm	67 (± 0.63) klmn	68 (± 00.53) klmn
SLN	54 (± 5.12) d	66 (± 1.97) ijklmn	67 (± 0.00) klmn	67 (± 0.00) klmn	68 (± 00.32) klmn
SHI	52 (± 3.37) bcd	65 (± 2.39) fghijkm	67 (± 0.63) klmn	67 (± 0.63) klmn	68 (± 00.52) ln
SLI	53 (± 4.40) cd	65 (± 1.26) hijklm	67 (± 0.00) klmn	67 (± 0.00) klmn	68 (± 00.42) klmn

5.3.4.2 Side branching is enhanced in Falcon plants upon infection and dry weight is significantly reduced

For evaluation of agronomic performance of the different treatments, the production of side branches was investigated. A remarkable production of side branches was observed in inoculated 'Falcon' plants at 49 dpi (Figure 5.6). *V. longisporum* infected plants possessed about 3 to five 4 more side branches compared to non-inoculated plants. This strong side branching production was only observed in 'Falcon' plants. Of note, low-watered non-inoculated plants of both genotypes had one side branch less at this time point, indicating a moderate effect of drought stress on side branching development.

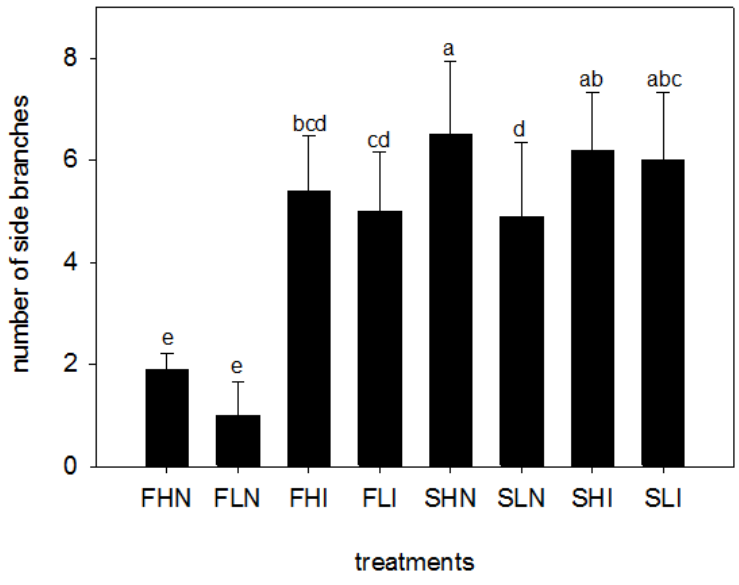

Figure 5.6 Average number of side branches and standard deviations of 10 *B. napus* plants at 49 dpi. 'Falcon' (F) or SEM (S) plants are either *V. longisporum* inoculated (I) or control plants (N = non-inoculated) subjected to 60% (H = high water level) or 30% (L = low water level) of field capacity. Values with the same letter do not differ significantly at a level of p ≤ 0.05 (Fisher`s LSD test).

5.3.4.3 Stem diameter development is genotype specific

A further trait that was determined to evaluate the influence of *Verticillium longisporum* infection and drought stress was the stem diameter at the cotyledon origin. Precise measurements were conducted with an electronic calliper at 65 dpi shortly before plants were harvested for biomass determination. In general, stem diameter was genotype specific since control plants of SEM (SHN) developed a bigger stem with an average value of 7.6 mm while control 'Falcon' plants displayed a stem diameter of 6.5 mm (Figure 5.7). There were no statistically significant differences between the different treatments, demonstrating that stem diameter is neither affected by drought nor by infection for either genotype.

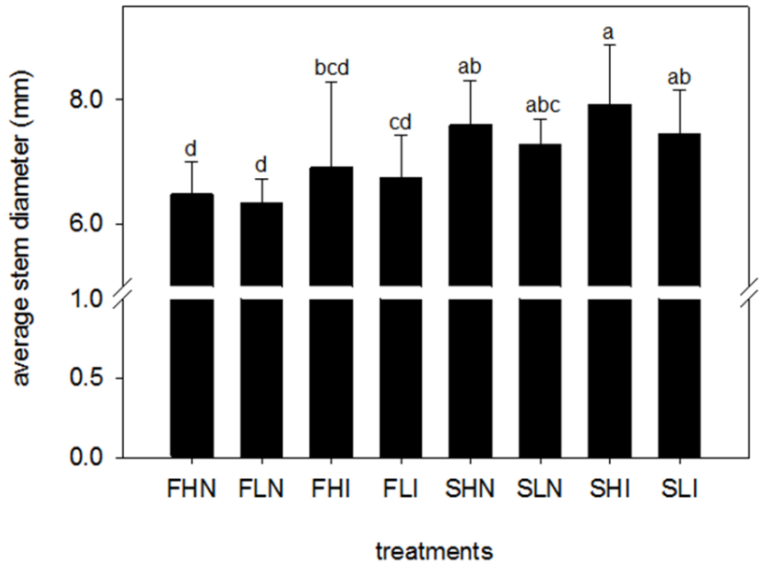

Figure 5.7 Average stem diameter and standard deviations of 10 *B. napus* plants at 64 dpi. Plants were inoculated with *V. longisporum* (I) or control (N = non-inoculated) and subjected to either 60% (H = high water level) or 30% (L = low water level) of field capacity. Values with the same do not differ significantly at a level of $p \leq 0.05$ (Fisher`s LSD test).

5.3.4.4 Vascular infection and drought stress affect pod development

The trait "number of pods per plant" was monitored at 65 dpi when harvest stage was almost achieved. A remarkable reduction of pod number was observed in the inoculated 'Falcon' plants (Figure 5.8). The treatment FHI exhibited about 64% reduced pod number compared to the control treatment and FLI produced about 46% less pods per plant. However, there was no statistically significant difference between inoculated drought stressed and normally watered plants, implying that drought stress did not markedly affect pod production. In fact the drought stressed treatment produced more pods per plant. Control SEM plants produced on average 25% less pods per plant compared to the control plants of 'Falcon'. Surprisingly, the low watered plants (SLN) produced significantly more pods compared to the plants with sufficient water supply. Both inoculated treatments of SEM drought stressed did not produce significantly less pods compared to the treatment SHN.

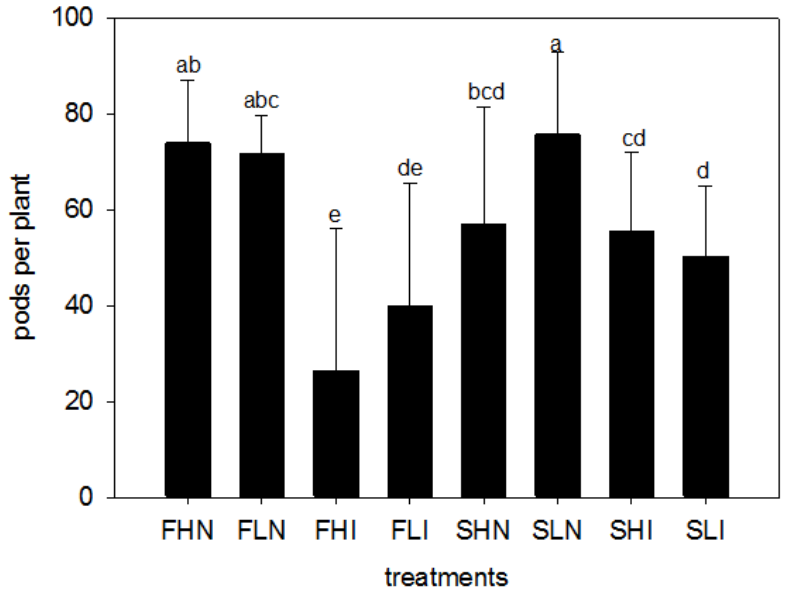

Figure 5.8 Average pod per plant and standard deviations of 10 *B. napus* plants at 65 dpi. Plants were inoculated with *V. longisporum* (I) or control (N = non-inoculated) and subjected either to 60% (H = high water level) or 30% (L = low water level) of field capacity. Values with the same letter do not differ significantly at a level of $p \leq 0.05$ (Fisher`s LSD test).

5.3.4.5 Fresh and dry biomass weight is reduced in the inoculated susceptible cultivar

Changes in fresh and dry biomass weight of shoots were observed at 65 dpi. While the infection with *V. longisporum* in SEM plants did not lead to a significant reduction in fresh and dry weight, the influence of drought stress was evident in fresh and dry weight values (Figure 5.9). In plants of cv. 'Falcon' drought stress had only a slight effect on fresh weight, while infection with *V. longisporum* had a significantly higher impact on fresh weight with biomass reductions of up to 54% compared to the control treatment (FHN).

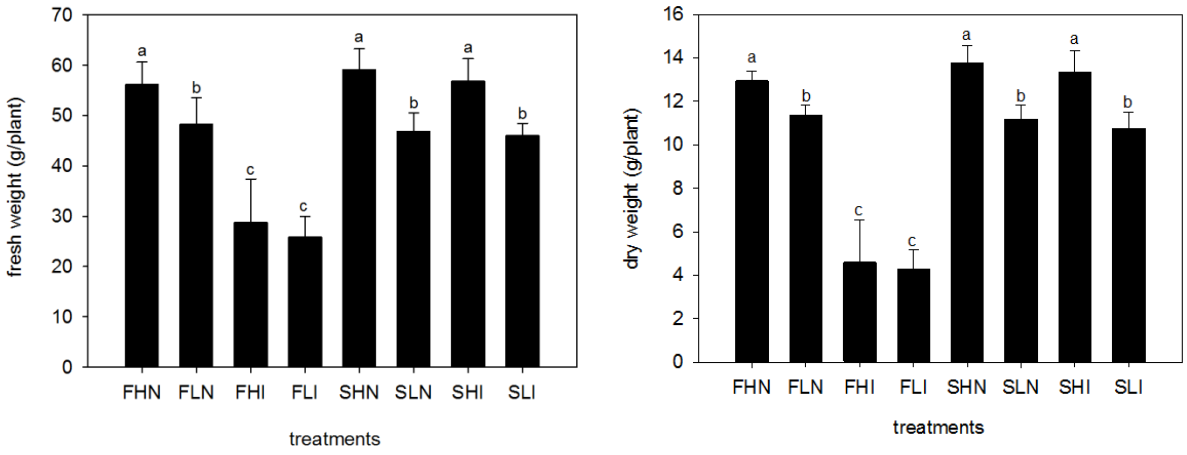

Figure 5.9 Average fresh biomass weight (left) and dry biomass weight (right) in grams per plant and standard deviations of 10 *B. napus* plants at 65 dpi. Dry weight data of the plants were obtained by drying the plants for 60 h at 80°C. Plants were either inoculated with *V. longisporum* (I) or control (N = non-inoculated) and subjected either to 60% (H = high water level) or 30% (L = low water level) of field capacity. Values with the same letter do not differ significantly at a level of $p \leq 0.05$ (Fisher`s LSD test).

5.3.5 Colonization of the stem base by *V. longisporum*

QPCR analysis was performed to study the spread of *V. longisporum* in OSR cultivars of the different treatments. For that purpose, the hypocotyl was harvested at 65 dpi for DNA extraction and subsequent qPCR analysis. Remarkably, 400 times more fungal DNA was detected in inoculated plants of cv. 'Falcon' compared to inoculated SEM plants (Figure 5.10). While our data show that drought stress does not clearly affect disease and agronomical parameters of cv. 'Falcon', fungal DNA concentration in drought stressed plants was significantly lower (209 ng/g dry weight) compared to plants only subjected to inoculation with a mean value of 374 ng/g dry weight. Remarkably, in inoculated SEM plants fungal DNA concentration in the hypocotyl part was clearly lower (about 500 times) compared to data obtained from 'Falcon' plants. Interestingly, SLI treatments showed a trend towards lower values compared to SHI treatments, indicating that resistance to *V. longisporum* infection was maintained despite drought stress conditions. In non-inoculated plants low amounts of *Verticillium* DNA were inevitably detected, but values were treated as background data since DNA concentrations were below 0.1 ng DNA/g dw.

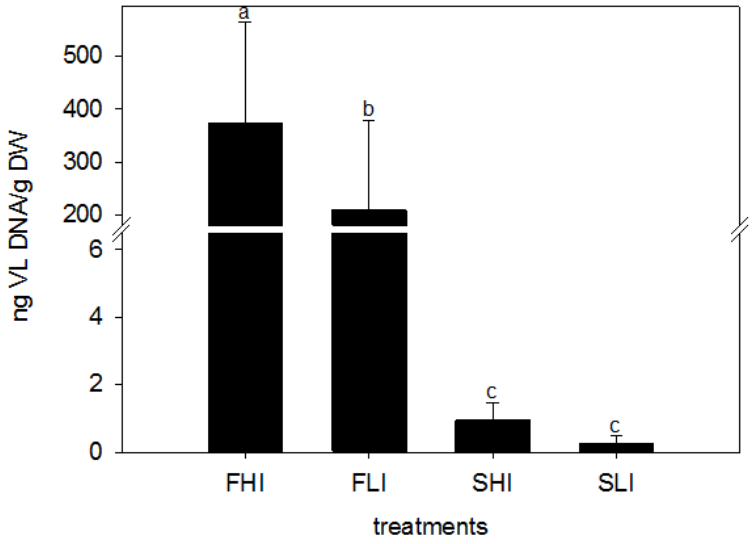

Figure 5.10 Fungal DNA content at 65 dpi in lower stem parts (hypocotyl) of 'Falcon' (F) or SEM (S) plants subjected to 60% (H = high water level) or 30% (L = low water level) of field capacity. Values with the same letter do not differ significantly at a level of $p \leq 0.05$ (Fisher`s LSD test).

5.4 Discussion

While genotype-specific resistance to *V. longisporum* has been demonstrated for SEM under controlled greenhouse conditions, ultimate stability of plant resistance has to be tested in field conditions where plants are challenged by high disease pressure and large fluctuations in water supply. A *V. longisporum* infection in *B. napus* plants causes enhanced vessel clogging of vascular elements in resistant genotypes and thus impediment of water translocation. In the present study the resistant genotype SEM was simultaneously exposed to fungal infection and drought stress to address the question whether resistant genotypes are inferior in terms of drought resistance compared to susceptible genotypes with less intensive vessel clogging.

Our data demonstrate that the disease pressure of *Verticillium* infection in combination with the exposure to drought stress does not affect the resistance level of SEM plants. We monitored disease severity to quantify the effect of drought stress on resistance levels of SEM plants. From the calculated AUDPC values it became apparent that disease progress was markedly accelerated in the susceptible 'Falcon' plants compared to SEM. Here, AUDPC values in 'Falcon' plants were more than doubled compared to SEM. Drought stress did not further increase the AUDPC value, suggesting that soil moisture (30% FC) was presumably still sufficient to meet plants requirements so that serious effects caused by drought stress would not be measurable unless soil moisture is further reduced. In subsequent studies an additional treatment with drought stress adjustments of FC < 30% may address this question. Furthermore, a putative drought stress effect could also be masked by strong *Verticillium* symptoms. The decelerated disease progress in SEM plants is expressed in an AUDPC value that is significantly lower than values found for the susceptible cv. 'Falcon'. A moderate, but significant increase of this AUDPC value was observed in the treatments with additional drought stress conditions (SLI). An effect of drought stress in this case, however, can most likely be excluded since SLI plants exhibited higher score values compared to plants of the SHI treatment already before drought stress was initiated at 21 dpi (Table 2).

One prominent symptom of a *Verticillium* infection under controlled conditions is the reduced growth of plants. Studies by Floerl *et al*. (2008) showed that *V. longisporum*-induced stunting of *B. napus* is not due to inhibition of photosynthesis, water shortage or nutrient limitations. Riediger (2008) reported a potential role of NO signalling in stunting. More recent studies of *V. longisporum* inoculated rapid cycling rape plants revealed a relation between shoot length and the concentration of the plant hormones salicylic acid and salicylic acid glucoside (Ratzinger *et al.*, 2009). In our drought stress experiments we observed marked stunting for the inoculated FHI and FLI treatments, however, also in this case drought stress did not

further enhance this symptom. Surprisingly plant height of SEM plants was nearly unaffected by both infection and exposure to drought stress. Plant height of SHI and SLI treatments nearly match those of control treatments. We only observed a moderate but significant difference between SHI and SLI at 49 dpi, where SLI plants were more stunted.

Another typical symptom of *Verticillium* infection is the yellowing of leaves, which results in a decreased chlorophyll content and in turn reduced photosynthesis (PS) (Agrios, 2005). In addition, a reduction in photosynthesis rate is also caused by the physical presence of fungus, which may occlude vessels similar to plant-own resistance structures and thereby inhibit water translocation to the leaves (Agrios, 2005). For these reasons, one would likely expect a reduction in net PS-rate in either drought or pathogen stressed plants. Data obtained from the gas exchange measurements, however, revealed a lower PS rate in plants subjected to biotic or abiotic stress only at the first three measurements (7 to 21 dpwt). For the various treatments of both 'Falcon' and SEM we observe a comparable decrease in PS rates, suggesting that drought stress does not dramatically aggravate the physiological status of the plant. Reduction of PS rates in VL-inoculated OSR was also not observed in a previous investigation (Floerl *et al.*, 2008).

The first three measurements, where differences between control and other treatments were visible fell into the flowering period. The period of flowering until the end of seed set is considered a critical phase in plant growth, since it drastically affects yield components (Champolivier and Merrien, 1996). Shortly after the beginning of flowering, the leaf area index decreases because of shading by flowers, which in turn leads to reduction in photosynthesis and thus decreased yield (Diepenbrock, 2000; Masoud Sinaki *et al*., 2007). The trend towards reduced PS rates in control plants from 28 to 35 dpi could be explained by this shading effect. However, the experiment should be repeated with an increased number of replicates to explicitly confirm this finding. Other studies have demonstrated that the plant is susceptible to drought stress during flowering stage (Diepenbrock, 2000; Bouchereau *et al*., 1996).

Stomata closure was observed in both drought stressed and infected plants, leading to decreased stomatal conductance and transpiration rate. A reduction of these parameter values was observed for 7 to 21 dpwt, but not for the other measurement points. Investigations of Floerl *et al*. (2008) found no effect of VL43 infection on rapeseed transpiration, from which they conclude that fungal infection does not cause drought stress by inducing the formation of occlusive resistance structures.

A delay in the onset of flowering was observed for FLI treatments and even more pronounced for FHI, but not for SHI and SLI. Contrasting observations were found for *A. thaliana* plants susceptible to *V. dahliae,* where flowering was accelerated (Veronese *et al.*,

2003). In our studies we did not observe differences in growth development at the end of flowering.

However, when analyzing numbers of pods per plant a possible influence of late flowering of FHI plants becomes apparent, since FHI treatment showed the lowest number of pods per plant. Diepenbrock (2000) pointed out that pod and seed number are determined during the flowering period and dependent on continuous assimilate supply. Closer inspection of our data illustrates a significant decrease in pod number for inoculated 'Falcon' plants, but no additional effect in inoculated plants when drought stress was applied, implying that in this case *V. longisporum* infection dominates the observed effect. Similarly, no effect of drought stress on pod number was observed for SEM treatments. Also here, further reduction of soil moisture may clarify the observations.

Disease and drought stress can also influence the development of side branches. A dramatic effect of infection is apparent from our data for inoculated 'Falcon' plants. For this particular treatment, we found three to four more side branches compared to control plants. A similar phenomenon has been described previously for *V. longisporum* inoculated *B. napus* plants; here infection also caused an increased production of leaves (Zeise, 1992). In addition, a more recent study also reported on enhanced axillary branching in *V. longisporum* infected Arabidopsis thaliana plants (Häffner *et al.*, 2010). This abnormal branching pattern is possibly due to modifications in hormone balances. While infection lead to increased leave production, we found that drought stress caused development of a slightly lower number of side branches. A reduced number of branches per plant in *B. napus* plants subject to drought stress conditions has also been shown previously (Richards and Thurling, 1978).

We do not observe alterations in stem diameter caused by either drought stress or infection. In contrast, Sangtarash *et al.*, (2009) did observe a decrease of stem diameter of rapeseed seedlings subjected to drought stress. Similarly, in soybean plants drought stress was shown to be related to a decrease of stem diameter, suggesting that this parameter is indeed determined by water supply (Ohashi *et al*., 2006).

Analysis of the yield components also included recording of fresh and dry biomass weight at harvest. Interestingly, while an infection did not lead to a reduced biomass in SEM plants, decrease in soil moisture by induced drought stress reduced plant weight significantly. However, plant resistance seems to be unaffected by water shortage, since in the case of combined treatments biomass of infected plants is not further reduced by additional drought stress.

In addition to physiological and yield parameters, fungal colonization in the different treatments was investigated by qPCR at the time point of harvest. Although we did not monitor progress of fungal colonization by time series and only locally determined fungal

DNA content in the hypocotyl tissue, we find a remarkable 500 times decrease of fungal DNA concentrations in inoculated SEM plants compared to equally treated 'Falcon' plants, demonstrating a clear relationship between symptom expression and fungal DNA content. Surprisingly, fungal DNA concentrations differ between treatments FHI and FLI. Drought stress conditions in FLI treatments obviously affect fungal spread, since fungal DNA concentrations here are significantly reduced compared to the FHI treatment. Addressing the hypothesis that drought stressed potato cultivars are more resistant to *V. dahliae*, Arbogast *et al*. (1997) investigated the relationship between soil moisture levels and disease severity of *Verticillium* wilt and identified a positive relationship between mild soil moisture stress and the level of resistance.

A reliable indicator for drought stress in plants is the accumulation of the amino acid L-proline (Delauney and Verma, 1993). Due to its amphiphilic character this organic osmolyte serves as an osmoprotectant by retaining water within the cells (Janská *et al.*, 2010). An additional function of proline is the scavenging of free radicals (Smirnoff and Cumbes, 1989) and proline can act as molecular chaperone protecting the structure of proteins (Verbruggen and Hermans, 2008). Proline accumulation levels vary dependent on the plant species and in certain plants proline accumulation can be up to 100 times greater compared to control plants (Verbruggen and Hermans, 2008).

In the pathosystem investigated in the present report, proline accumulation was more prominent in SEM plants. Since drought stress did not considerably increase proline content in SEM plants, the observed increase can be ascribed to higher constitutive levels. Whether these higher proline levels indeed play a role in drought resistance of SEM has to be evaluated in a repeated experiment involving additional replicates and measuring time points.

Another aspect associated with a *V. longisporum* infection was investigated by Floerl *et al.* (2008). This group assessed whether vessel occlusions also leads to impediment of nutrient transport. Analysis of the respective levels of macro-nutrients (N, P and S) and elements potassium, calcium, magnesium, iron and manganese revealed that *B. napus* infection with *V. longisporum* isolate VL43 did not result in nutrient limitations.

Our analysis of the performance of a *V. longisporum* resistant genotype simultaneously exposed to drought stress demonstrates that resistance of SEM is not influenced by drought stress at a level of 30% FC, i.e. increased formation of vessel occlusions does not significantly affect water transport. Resistance was expressed in low AUDPC values as well as moderate stunting of plants and low fungal DNA concentrations 65 dpi. Analysis of agronomical parameters such as numbers of pods and biomass weight indicated resistance by stable values for infected SEM plants. An effect on yield performance by water shortage

was only found in biomass weight. The persistence of resistance of the genotype SEM should be proven by additional experiments with increased levels of drought stress.

6. General Discussion

Intensification of winter OSR production and the associated increase in frequency of OSR in crop rotation cycles promotes diseases such as premature ripening caused by *V. longisporum*. The current lack of efficient fungicides makes studies aiming at a detailed understanding of the *B. napus*/*V. longisporum* interaction an important element in breeding efforts for resistant cultivars. Within this context, the present work seeks to provide novel insights into the fundamental aspects of this pathosystem and to develop techniques that aid the improvement of winter OSR resistance to *V. longisporum*. The development of a novel detection method for *V. longisporum* in OSR was motivated by the life cycle of this soil-borne vascular fungus, which is characterized by a long latency period in the field. Adequate methods for an early and reliable detection of the fungus inside the plant tissue are not currently available. Among the conventional detection methods used to select for resistance is the visual scoring of microsclerotia in rapeseed stubbles. One disadvantage of this method is the discussed interdependence between the ripening pattern of the plant and microsclerotia formation (chapter 3). In addition, in rapeseed cultivation areas with high infestation levels, such as at sites in Fehmarn or Svalöv, a classification into resistance classes based on the post-harvest stubble screening procedure is hampered by the difficulties to accurately differentiate disease severities owing to high overall infection levels. Analysis of the degree of colonization by *V. longisporum* earlier during plant development would facilitate monitoring of fungal spread while the fungus still is in the biotrophic phase of its life cycle, and would also provide a means to (indirectly) quantify the plants' genotype-specific ability to activate and maintain defense mechanisms. Among the diagnostic methods for detection of fungal pathogens, enzyme-linked immunosorbent assays (ELISA) are one alternative to phenotypical assessment of disease symptoms (Eibel *et al*., 2005). In the context of *V. longisporum* disease in the field, studies by Dunker (2006) showed that detection of fungus by ELISA was not possible until the beginning of ripening at GS 83, when first *Verticillium* symptoms become visible. Similarly, unequivocal detection of *V. longisporum* in roots and stems of OSR was not possible until GS 89 in a different ELISA-based approach (Eynck, 2008). This demonstrates that these serological methods are obviously not suited for detection of the fungus before symptom expression in the field.

A more sensitive and accurate approach can be found in PCR-based methods (Lievens *et al.*, 2006). First efforts to identify *V. dahliae* and *V. albo-atrum* by PCR with primers targeting the ITS (internal transcribed spacer) region were made in the beginning of the 1990s by Nazar *et al*. (1991). Shortly after, a similar assay for detection of *V. tricorpus* was developed by Moukhamedov (1994). In 1993 Hu *et al*. reported the development of a PCR method

suited to detect and quantify *Verticillium* DNA in alfalfa and sunflower plants, that is based on previously designed ITS primers (Nazar *et al.*, 1991). Heinz *et al*. (1998) determined fungal biomass with the same primers in *V. albo-atrum* infected tomatoes. A PCR-based method with the same primers was also used to quantify *V. dahliae* in potato plants (Dan *et al.*, 2001). Due to the high sensitivity inherent to all PCR-based methods, the accurate quantification of fungal infection levels by PCR-based methods pose high demands on the specificity of the applied primer system. Frequently, genetic variation between closely related species can be very low and thereby severely complicate the design of appropriate primers. In molecular diagnostics, primer systems designed to discriminate between closely related species therefore often target sequences that are located between conserved regions such as the ITS or the IGS (intergenic spacer) regions. These genomic regions are rapidly evolving and consequently characterized by high sequence variation, which often allows to minimize cross-hybridization of primers to non-target DNA even among closely related species. Moreover, ribosomal DNA regions, and hence ITS regions, are present in multiple copies in the fungal genome, which promotes sensitivity of primers designed from this region (Robb *et al.*, 1994; Ma and Michailides, 2006). In addition to the ITS region several other genetic loci frequently serve as alternative target regions in the development of primers for diagnostic purposes or phylogenetic analysis of fungal plant pathogens, e.g. the mitochondrial small sub-unit rRNA genes (differentiation of *V. dahlia*e from other *Verticillium* species, Li *et al*., 1994 or for phylogenetic analysis of closely related *Verticillium* species, Fahleson *et al*., 2004), the β-tubulin-genes (discrimination of *V. dahliae* from *V. albo-atrum* and *V. tricorpus*, Atallah *et al.*, 2007; phylogenetic analysis of *Verticillium* isolates, Qing-Ming *et al*., 2006), as well as actin genes and elongation factor 1α (Inderbitzin *et al*., 2011).

Early studies aiming at the quantification of infestation levels by determination of fungal DNA concentrations were based on a competitive PCR method that employed an internal standard PCR for quantification of the fungal pathogen (Hu *et al.*, 1993, Robb *et al*., 1994; Heinz *et al*., 1998 and Dan *et al*., 2001). Today, real-time based PCR methods are more common for detection and quantitative assessment of fungal plant pathogens. For example, a qPCR method was successfully applied for the detection of *V. dahliae* in field-grown potato and was suggested to replace the conventional plating assay (Atallah *et al*., 2007). A qPCR method for quantification of *V. albo-atrum* in alfalfa demonstrated that disease severity correlated with fungal DNA levels (Larsen *et al*., 2006). Also colonization of olive genotypes by *V. dahliae* was monitored by qPCR (Mercado-Blanco *et al.*, 2006; Markakis *et al*., 2009).

Several parameters are pivotal for the successful application of qPCR as a diagnostic tool in plant pathology. Primer sensitivity is one important requirement for adequate quantification of fungal DNA in plant tissue. The comparison of the sensitivity of ITS primers with that of

tubulin primers in our study revealed superior performance of the ITS-based system and demonstrated that the application of tubulin based primers is clearly not suited to detect *V. longisporum* during early stages of disease. Similar to our observations, Debode *et al.* (2009) compared ITS- with β-tubulin based primer systems in PCR-based diagnostics and concluded that the ITS approach was more suitable for detection of *C. acutatum* in strawberry leaves for reasons of sensitivity. Another study comparing the performance of an ITS and α-tubulin targeting approach using conventional PCR also confirmed the lower sensitivity of the tubulin-based system (Consolo *et al.*, 2009). However, Atallah *et al*. (2007) pointed out disadvantages of ITS primer-based PCR by noting that the number of rDNA copies is linked to the age of the organism and thus fluctuates, which together with non-orthologous copies of the ITS fragment within species is considered to hamper reproducibility of the quantification. These concerns prompted them to propose the use of primer systems targeting single copy regions. However, the observed correlation of PCR-based quantification of fungal biomass with our ITS system and disease scores obtained from stubbles screening suggests that this complication does not necessarily limit the applicability of our highly sensitive ITS-based primer system for pathogen quantification in the field. In fact, the high sensitivity of qPCR with ITS primers permitted us to detect *V. longisporum* in stem parts of winter OSR already at GS 65, clearly before symptom expression such as one-sided brownish discoloration of stems. Unfortunately, detailed information about the disease development between GS 65 and the beginning of ripening is not available at present, since the next time point of our analysis was GS 80 when ripening had just initiated. Several additional measurements within this critical time span would allow for a more conclusive description of the precise dynamics of fungal colonization in the plant. Nevertheless, our data from field experiments demonstrate a clear relationship between the susceptibility of the cultivars and the levels of fungal DNA in rapeseed stems and therefore support the application of this method for screening resistant cultivars in the field.

Apart from primer sensitivity, the specificity of primers employed in qPCR protocols is of paramount importance, especially for diagnostic purposes in field experiments. A qPCR method based on ITS primers (OLG70/71) has recently also been applied to the quantification of *V. longisporum* in xylem sap of *B. napus* plants (Floerl *et al*., 2008) and *A. thaliana* (Häffner *et al*., 2010; Floerl *et. al*., 2010). Although these methods were successful in quantification of the pathogen under controlled conditions, the application of this method to naturally infested samples from field experiments required a rigorous assessment of primer specificity. While this is a general requirement for PCR-based diagnostics, it is of particular importance for *V. longisporum* diseases in view of the persisting controversy of the evolutionary origin of this species and its discrimination from *V. dahliae*. The complex

phylogeny of *Verticillium* species emphasizes the associated difficulties in the development of a specific PCR-based diagnostic for these fungal pathogens. This is reflected in our comparison of the specificity of ITS and tubulin primers, demonstrating that our ITS primers could not discriminate between *V. dahliae* and *V. longisporum* isolates and that also *V. albo-atrum* and *V. tenerum* are detected by these primers. We showed that it is possible to alleviate these complications by (a) using the rapeseed stem as the sampling site since *V. dahliae* does not colonize the stem (Eynck *et al*., 2007), and (b) restricting the number of PCR cycles to 34 cycles to avoid amplification of non-target species such as *Alternaria* spp. While the tubulin primers exclusively amplified *V. longisporum* species and thereby provide a means to successfully discriminate isolates from *V.dahliae*, this system failed to detect several long-spored isolates (Vl 82, Vl 60 and Vl Eschwege) for which morphological analysis revealed elongated conidia (>7 µm) and microsclerotia characteristic for the species *V. longisporum* (Zeise and Tiedemann, 2001). Our specificity test may emphasize the associated difficulties in the development of specific PCR-based diagnostics for these fungal pathogens. Indeed, a recent study by Inderbitzin *et al*. (2011) revealed a considerable complexity of the evolutionary origin of the hybrid *V. longisporum*. This study grouped *V. longisporum* isolates into three distinctly different classes, of which only the progenitor A1 was shared by all lineages. Among the isolates investigated by this study were three *V. longisporum* isolates (Vl 40, `Chalons en champs`and V.l. 84) and two *V. dahliae* isolates (Vd 85 and Vd 88) that were also selected for the specificity test in the present work. The three *V. longisporum* isolates were clustered into the *V. longisporum* lineage A1/D1 consisting of unknown taxa. *V. longisporum* has previously been divided into two different subgroups (lsp and lsp*) differing in their level of aggressiveness against OSR (Zeise and Tiedemann, 2002a). The A1/D1 group was found to consist of members previously classified into the lsp group with high aggressiveness on OSR. Interestingly, the isolate `Chalons en champs` was also determined as A1/D1, although pathogenicity tests in the greenhouse have shown that, similar to *V. dahliae,* rapeseed plants inoculated with this isolate did not exhibit disease symptoms (Heseker, 2009). If classification into lsp and lsp* correlates with virulence one would expect this isolate to group into the A1/D3 (lsp*) lineage derived from a *V. dahliae* parental line (D3) with decreased aggressiveness to OSR (Zeise and Tiedemann, 2002a). The two *V. dahliae* isolates were indeed confirmed as *V. dahliae* by this study.

A robust method to monitor *V. longisporum* in field-grown winter OSR is indispensable for screening for resistance. Our investigations have shown that the ITS-based qPCR approach can serve as a sensitive diagnostic tool of the fungus in the field, and supports the classification of tested accessions into different resistance levels.

To understand the underlying resistance mechanisms in the *B. napus* plant two *B. napus* genotypes ('Falcon' and SEM) differing in their resistance to *V. longisporum* were investigated by transmission electron microscopy (chapter 4). The genotype SEM 05-500256 was selected to serve as a model resistant genotype, since previous investigations have demonstrated the resistance of this genotype, which manifested in elevated phenol levels, enhanced formation of occlusions and low fungal colonization (Eynck *et al.*, 2009). Consequently the next step was to investigate whether the reported formation of physical barriers in the form of occlusions and lignin accumulation contribute to inhibition of fungal spread inside the plant. To this end, the degree of colonization near the site investigated by electron microscopy was first determined by measuring fungal DNA content by qPCR. Analysis of fungal DNA levels in the hypocotyl of inoculated SEM plants revealed significantly lower fungal DNA concentrations compared to 'Falcon'. The inoculation method used in our studies (i.e. cutting of roots followed by root dip inoculation with a spore suspension) did not permit to investigate whether resistance in SEM 05-500256 is caused by failure of root penetration. This question, however, was already addressed in previous studies using a different inoculation protocol (Eynck *et al*., 2009). Here it was demonstrated, that roots of SEM 05-500256 were indeed penetrated by *V. longisporum* since low amounts of fungal DNA were detected in hypocotyls. This is in agreement with the general definition plant resistance in interaction with vascular pathogens. In this context resistance is generally characterized by limited pathogen spread and expression of few symptoms, while in susceptible interactions the pathogen spread in the plant proceeds systemically, resulting in symptom expression (Robb, 2007). While our studies focused on resistance structures in hypocotyl sections, further studies should include the microscopic investigation of the upper root part, accompanied with qPCR analysis. Identification and investigation of spores trapped at vessel end plates or pit cavities in the root tissue may elucidate if spore germination and penetration of germ tubes into adjacent vessel elements is impeded.

In our TEM investigations of the *V. longisporum*/*B. napus* interaction we were not able to detect fungal structures in the hypocotyl of resistant plants. Indeed, qPCR analysis revealed very low amounts of fungal DNA near the investigation site for the resistant genotype, which together with the limited sampling area of TEM sections explains the failure of detecting fungal structures and again confirms the resistance of SEM 05-500256. Nevertheless, it would be of interest to more closely characterize the interaction of resistant genotypes with such fungal structures in order to identify potential differences in their response compared to susceptible plants. To this end, alternative inoculation methods may increase the chance to detect such interactions. For example, a more artificial inoculation protocol employing an injection needle for directly infuse the conidia into the vascular system (Keunecke, 2009)

would facilitate the localization of the fungus by microscopy. A targeted preparation of the tissue near the puncture possibly allows to detect fungal structures in interaction/in contact with plant resistance structures. Alternatively, Newcombe and Robb (1988) cut stems of alfalfa plants and infused a spore suspension of *V. albo-atrum* by enhanced transpiration. Samples were taken in a time course from 12 hours post inoculaton (hpi) to 168 hpi at a distance of 1.5 cm from the cutting site, tested to be optimal in preliminary experiments.

Despite the fact that detection of fungal hyphae in the resistant genotype was not possible by TEM analysis, we could demonstrate alterations in vascular hypocotyl tissue upon infection with *V. longisporum* occurring in both genotypes. Cellular modifications involved in *V. longisporum* infection were the degradation of pit membranes, thickening of secondary cell walls by electron dense material and the formation of vascular occlusions consisting of granular- or fibrillar structures. Further research may include a more detailed characterization of the chemical nature of these resistance structures involved in host defense of *B.napus*, which could be achieved by using immunological approaches combined with TEM. Applications using enzyme or antibody-linked colloidal-gold particles are frequently used in detection of plant resistance structures. For instance, callose (β-1,3-glucans) and β-1,4-glucans (Benhamou, 1992, 1995a; Benhamou and Garand, 2001), pectin (Kpémoua *et al*., 1996, Ouellette *et al*., 1999), or pectic polysaccharides (Rioux *et al*., 1998) were identified by immunocytochemical methods. The cellular modifications induced upon infection that were discovered in our study seem to be crucial in resistance and may be controlled and synthesized in a regulated way. This interplay between the different defense responses obviously functions more successful in the resistant genotype. Further investigations of the pathosystem may focus on investigation of a time course of the *V. longisporum*/*B. napus* interaction, which may identify critical stages triggering the onset of different resistance mechanisms and may help to understand this complex plant defense response in a time-dependent manner. The knowledge about the chemical composition of the involved plant resistance structures together with information about the genotype-specific production of these structures provided by such time course studies can contribute to a more complete understanding about the mechanism inducing resistance to *V.longisporum* in SEM 05-500256.

The finding that occlusions were more abundant in the resistant genotype SEM 05-500256 brings about the question whether such enhanced vessel plugging leads to interference with the water transport in the plant (chapter 5). In addition, water transport in the vessels may be hindered by vessel lining materials that are suggested to function as waterproofing (Bishop and Cooper, 1983b). We therefore investigated whether a resistant genotype subject to both drought stress and coincident *V. longisporum* infection is disadvantaged compared to

susceptible plants with a less pronounced accumulation of vessel occlusions. Based on our data a *V. longisporum* infection in combination with drought stress conditions does not affect the resistance of SEM plants. Disease parameters such as net AUDPC value and stunting showed that SEM 05-500256 plants were only marginally affected by infection and drought stress compared to the susceptible 'Falcon' plants. Pennypacker *et al*. (1991) demonstrated that disease scores of *V. albo-atrum* infected alfalfa plants were lower in drought-stressed treatments compared to well-watered conditions. Contrary, in our study disease ratings were slightly higher in infected and drought-stressed resistant plants. The gas exchange measurements did not provide evidence that additional drought stress affects the net photosynthesis rates, stomatal conductance or transpiration rates of infected resistant plants: In either inoculated, drought stressed or both factor plants PS rates, transpiration rates and stomatal conductance were equally reduced compared to control treatments from 28 to 42 dpi. Further studies can be augmented by other measurements to assess whether additional drought stress indeed has no effect on resistant plants. For example, another frequently used method to control the water status in the plant is the measurement of the leaf water potential. In addition, chlorophyll fluorescence measurements can serve as a means to monitor photosynthetic performance and can be used to assess the plants' physiological status.
Measurement of fungal DNA concentrations in hypocotyls of the different treatments by qPCR showed that drought-stressed plants both of 'Falcon' and SEM 05-500256 harbored less fungal DNA compared to fully watered plants. Drought stress leads to a reduced stomatal conductance, and as a result, reduced transpiration (Pennypacker *et al*., 1991), which slows water transport in the vessels and consequently translocation of conidia to upper plant parts (Cook and Papendick, 1972). In this respect drought stress appears to be favorable for hosts that are also subject to infections. Indeed, a similar conclusion was drawn by Pennypacker *et al*. (1991), who found the effect of *V. albo-atrum* infection on stem dry weight to be greater without additional drought stress than with drought stress. Our data do not confirm this hypothesis for the *V. longisporum/B. napus* pathosystem: dry biomass weight of the resistant genotype was significantly reduced only by drought stress, indicating that resistance to *V. longisporum* in SEM 05-500256 is not affected by drought stress.
Overall, histological and physiological studies of the performance of SEM 05-500256 with respect to resistance to the vascular pathogen *V. longisporum* demonstrated the outstanding resistance of this genotype even under conditions of drought stress. These findidings should be confirmed under field conditions.

Owing on the current lack of efficient fungicides against *V. longisporum*, breeding of resistant *B. napus* lines is paramount to control the disease. A suitable screening method forms the basis for selection of resistant lines.

Apart from a reproducible greenhouse screening approach, our studies have shown that qPCR provides a sensitive and accurate diagnostic tool for resistance screening in field experiments. Eventually, only a combination of high-throughput resistance screening of numerous different genotypes under controlled greenhouse conditions and validation of the stability of resistance under environmental conditions in the field can lead to the long-term improvement of resistance against *V. longisporum*.

Summary

Recent years have seen an intensification of oilseed rape (OSR) cultivation, which, together with shorter crop rotations has led to a rapid increase in infestation by the soil-borne vascular pathogen *V. longisporum*. The fungus forms survival structures, termed microsclerotia, that can accumulate in the soil and thereby lead to persistent contamination. An infection by *V. longisporum* can already occur in autumn, when root exudates stimulate microsclerotia to germinate, after which hyphae grow towards the roots and penetrate the root epidermis of the OSR plant. The intra- and intercellular spread of the fungus towards the vessel elements is followed by a latency period within the vascular system. While initially plants do not show prominent symptoms during this latency period, half-sided discoloration of stems emerges towards the end of plant development and premature senescence can cause significant yield losses. The fungus remains restricted to the vascular system until the plant enters the senescence phase. This transition initiates the colonization of adjacent parenchyma cells and the formation of microsclerotia, which can be recycled into the soil together with plant debris.

Since presently fungicides remain elusive, cultivation of resistant cultivars is an efficient measure to curb fungal spread and to counteract accumulation of microsclerotia in the soil. This thesis provides a vital contribution to the breeding efforts for novel resistant *B. napus* genotypes. For identification of resistant *B. napus* cultivars (including DH lines), phenotypisation was performed under controlled greenhouse conditions in Göttingen. In addition, the resistance of selected *B. napus* lines has been assessed during two consecutive years under natural environmental conditions at several field sites in Nothern Germany and one field site in Southern Sweden. Greenhouse screenings of *B. napus* accessions tested between 2004-2009 were analyzed with respect to the frequency distribution of calculated, normalized AUDPC values. It could be explicitly demonstrated that the resistance level in the most recent screening had significantly improved compared to the first screenings. Consistency in normalized AUDPC values of reference cultivars ‘Falcon’ and ‘Express’ confirmed the reproducibility of the screenings. The robustness of the method is reflected in the normalized AUDPC values of the reference accessions, which were consistently lower for the moderately resistant cultivar ‘Express’ compared to those of the susceptible cultivar ‘Falcon’. A comparison of greenhouse and field experiments reveals a moderate correlation between accessions tested under controlled or field conditions and illustrates the complexity of these studies. Greenhouse experiments are indispensable for a rapid and comprehensive screening of a large number of genotypes. However, the transition to field trials is ultimately necessary to evaluate resistance under environmental conditions that can cause additional abiotic stress. Parallel to the assessment of the infestation level

(disease incidence and severity) by stubble screening, an alternative approach for evaluation of resistance of OSR plants under field conditions was established. The development of a sensitive real-time PCR (qPCR) method for the detection of *V. longisporum* in rapeseed stems comprised the evaluation of two different primer pairs targeting either the internal transcribed spacer region (ITS) or beta-tubulin region, with respect to their sensitivity and specificity. The ITS primers showed high sensitivity for fungal genomic DNA, but were poor in their specificity towards *V. longisporum* isolates. Rather, apart from *V. longisporum* these primers also similarly detected *V. dahliae* isolates and two additional *Verticillium* species. In contrast, the tubulin primers also evaluated in this study showed high specificity towards *V. longisporum* and failed to detect only 12 out of 15 tested isolates. However, the sensitivity of these tubulin primers was strongly reduced by a factor of 2^{14} compared to the ITS primers.

Application of ITS-based qPCR permitted the detection of the pathogen before emergence of symptoms in the field. It could be demonstrated during the season 2008/2009 that early infections already occurred at BBCH 65 and within a few weeks resulted in massive colonization of susceptible cultivars. Moreover, it was possible to quantify fungal DNA concentrations in infected rapeseed stems of cultivars of varying susceptibility, and to demonstrate that these concentrations correlate with the traditional stubble screening in field trials and the phenotypic greenhouse screening with respect to the classification into resistance classes. These results support the application of the molecular method for disease diagnostics as an additional method to the traditional stubble screening.

Apart from the improvement of field-based detection methods for *V. longisporum*, detailed studies of the host-pathogen interaction were performed to characterize the formation of resistance mechanisms. For this purpose, the hypocotyl sections of two differently susceptible *B. napus* lines were investigated at the histological and molecular level after inoculation with *V. longisporum*. Previous studies have identified the hypocotyl, which marks the segment from the root crown to the cotyledon, as the key tissue for the formation of resistance structures (Eynck et al. (2009)). Building on these studies, genotype-specific resistance structures such as vessel occlusions and morphological changes of the vascular system were investigated by transmission electron microscopy (TEM) and, in parallel the spread of the pathogen was monitored by qPCR. Although qPCR results demonstrated a markedly accelerated colonization of the susceptible genotype compared to resistant genotype, both genotypes revealed similar ultrastructural changes of the vascular system upon infection by *V. longisporum*. These morphological changes included alterations of cell walls such as electron-dense depositions and degradation of primary cell walls in pit areas. It was further shown that infection leads to occlusion of vessel elements by gel-like structures.

Our studies suggest that, in order to elicit a targeted resistance response, the resistant genotype is able to recognize infection more rapidly and to activate defense mechanisms more efficiently.

The increased formation of vessel occlusions in the hypocotyl segment in the resistant genotype SEM 05-500256 upon infection by *V. longisporum* (Eynck *et al*., 2009) suggested that these resistance structures might affect the water transport system of the plant. To clarify this point, the resistant genotype was subjected to drought stress (30% field capacity) in addition to infection by *V. longisporum* and physiological parameters (gas exchange) as well as infestation levels (AUDPC, stunting) and agronomic parameters (phenological growth stages, number of branches and yield parameters) were evaluated and compared to the performance of the similarly treated, susceptible cultivar ‘Falcon’. Neither infestation parameters nor agronomic parameters revealed indications of compromised resistance of *V. longisporum*-infected SEM in combination with drought stress.

Zusammenfassung

Die Intensivierung des Rapsanbaus in den letzten Jahren hat zu einem verstärkten Aufkommen des bodenbürtigen Gefäßpathogens *V. longisporum* geführt. Die für den Pilz charakteristischen Mikrosklerotien können langjährig im Boden überdauern, akkumulieren und somit zur fortdauernden Bodenkontamination führen. Eine Infektion mit *V. longisporum* kann bereits im Herbst erfolgen, wenn durch Wurzelexsudate stimulierte Mikrosklerotien auskeimen und direkt die Wurzelepidermis der Rapspflanze penetrieren. Einer sowohl intra- als auch interzellulär gerichteten Ausbreitung bis zu den Gefäßelementen schließt sich eine langanhaltende Phase des Pilzes im Gefäßsystem an. In dieser latenten Phase zeigen sich keine auffälligen Symptome an der Pflanze, erst zum Ende der Pflanzenentwicklung zeigt sich halbseitige Stängelverbräunung und vorzeitige Abreife kann zu Ertragseinbußen führen. Der Pilz bleibt so lange auf die Gefäße beschränkt bis die Pflanze in die Seneszenzphase eintritt. Dann erfolgt eine Besiedelung der angrenzenden parenchymatischen Zellen und die Bildung von Mikrosklerotien. Mit Pflanzenresten können diese wieder in den Boden gelangen. Da derzeit keine adequaten Pflanzenschutzmittel zur Verfügung stehen, ist der Anbau resistenter Sorten eine wirkungsvolle Maßnahme die Verbreitung des Pilzes einzudämmen und der Anreicherung von Mikrosklerotien im Boden entgegenzuwirken. Im Rahmen dieser Arbeit wurde ein entscheidender Beitrag zur Züchtung neuer resistenter Genotypen geleistet. Phänotypisierungen zur Identifizierung resistenter *B. napus*-Linien (darunter auch DH-Linien) erfolgten unter kontrollierten Bedingungen im Gewächshaus in Göttingen. Darüber hinaus wurde die Resistenz ausgewählter *B. napus*-Linien in zwei aufeinander folgenden Jahren anhand von Feldversuchen in Göttingen, an verschiedenen Standorten in Norddeutschland und an einem Standort in Südschweden evaluiert. Eine Untersuchung der von 2004 bis 2009 im Gewächshaus getesteten *B. napus* Akzessionen wurde hinsichtlich der Häufigkeitsverteilungen der berechneten normierten AUDPC-Werte betrachtet. So konnte deutlich gezeigt werden, dass sich das Resistenzlevel in den aktuellsten Screenings deutlich verbessert hat im Vergleich zum Beginn der Screenings. Die Reproduzierbarkeit der Screenings wurde deutlich durch die Betrachtung der normierten AUDPC-Werte der Referenzsorten ‘Falcon’ und ‘Express’. So waren die normierten AUDPC-Werte der mittelgradig resistenten Referenzsorte ‘Express’ durchgängig niedriger im Vergleich zu der anfälligen Sorte ‘Falcon’, was für die Robustheit der Methodik spricht. Der Vergleich zwischen Gewächshaus- und Feldversuchen zeigte, dass eine geringe Korrelation zwischen den im Feld und Gewächshaus getesteten Akzessionen besteht und macht die Komplexität der Untersuchungen deutlich. Ein Screening von Genotypen kann jedoch nur schnell und in großem Umfang unter Gewächshaus-Bedingungen erfolgen. Die erweiterte

Testung im Feld ist dann jedoch nötig, um die Resistenz unter zusätzlichem abiotischem Stress zu evaluieren.

Neben der Bewertung des Befallsgrades (Befallshäufigkeit, Befallsstärke) mittels Stoppelbonitur wurde eine alternative Bewertungsmethode zur Evaluierung der Resistenz im Feld kultivierter Rapspflanzen gegenüber *V. longisporum* entwickelt. Die Entwicklung einer sensitiven real-time PCR (qPCR)-Methode zur Detektion von *V. longisporum* in Rapsstängeln beinhaltete die Bewertung zweier unterschiedlicher Primer, abzielend auf die internal transcribed spacer (ITS) Region bzw. auf die β-Tubulin-Region, die hinsichtlich ihrer Sensitivität und Spezifität analysiert wurden. Die hier getesteten ITS-Primer wiesen eine hohe Sensitivität gegenüber genomischer Pilz-DNA auf, jedoch wurde keine Spezifität gegenüber *V. longisporum* Isolaten festgestellt; vielmehr wurden *V. dahliae* Isolate und zwei weitere *Verticillium* Arten mit ITS-Primern detektiert. Das zweite getestete Primerpaar zeigte hingegen eine hohe Spezifität gegenüber *V. longsiporum* Isolaten, lediglich 3 von 15 getesteten *V. longisporum* Isolaten wurden nicht erfasst. Die Sensitivität dieser Primer war jedoch im Vergleich zu den ITS-Primern stark verringert (2^{14}x). Die ITS-basierte qPCR Analyse führte zur Detektion des Pathogens noch vor der Symptomausbildung im Feld. So konnte in der Saison 2008/09 am Standort Göttingen gezeigt werden, dass frühe Infektionen bereits zu BBCH 65 auftraten und innerhalb weniger Wochen eine massive Besiedelung anfälliger Sorten erfolgte. Zudem konnte die pilzliche DNA-Konzentration in infizierten Rapsstängeln verschieden anfälliger Sorten quantifiziert und eine Korrelation zwischen der herkömmlichen Stoppelbonitur und dem Screening im Gewächshaus hinsichtlich der Einordnung der Resistenzniveaus hergestellt werden. Dies unterstützt die Verwendung der molekularen Methode als Alternative zur Stoppelbonitur.

Neben der Verbesserung der Detektion von *V. longisporum* im Feld wurde die Pathogen-Wirt-Interaktion hinsichtlich der Ausbildung von Resistenzmechanismen charakterisiert. Dazu wurden zwei verschieden anfällige *B. napus*-Linien nach Inokulation mit *V. longisporum* sowohl auf histologischer als auch auf molekularbiologischer Ebene im Hypokotylbereich untersucht. Dieser Abschnitt, der den Bereich vom Wurzelhals bis zum Keimblattansatz markiert, konnte in vorangegangenen Untersuchungen als Schlüsselgewebe für die Ausbildung von Resistenzstrukturen identifiziert werden (Eynck *et al.*, 2009). Anknüpfend an diese Untersuchungen wurden mittels Transmissionselektronenmikroskopie (TEM) genotypabhängige Resistenzstrukturen wie Gefäßverschlüsse und morphologische Veränderungen des Gefäßbereiches untersucht und begleitende qPCR-Messungen dokumentierten die Pathogenausbreitung. Diese ließen erkennen, dass der anfällige Genotyp im Vergleich zum resistenten Genotyp schneller besiedelt wird. Jedoch zeigten beide mit *V. longisporum* inokulierten Genotypen ähnliche ultrastrukturelle Veränderungen im

vaskulären Bereich. So konnten Veränderungen an vaskulären Zellwänden wie elektronendichte Ablagerungen und Degradation primärer Zellwände im Bereich der Tüpfel beobachtet werden. Zudem konnte das Verschließen von Gefäßelementen mittels gelartiger Strukturen nachgewiesen werden. Unsere Untersuchungen lassen vermuten, dass der resistente Genotyp fähig ist Infektionen schneller zu erkennen und Resistenzmechanismen zielgerichteter und intensiver zu aktivieren.

Da eine *V. longisporum*-Infektion in dem untersuchten resistenten Genotyp SEM 05-500256 u. a. zu einer verstärkten Bildung von Gefäßbarrieren im Hypokotylbereich führt (Eynck *et al*., 2009), wurde eine Beeinträchtigung des pflanzlichen Wassertransportes vermutet. Zur Klärung dieser Frage wurde der resistente Genotyp zusätzlich zu einer Infektion mit *V. longisporum* Trockenstressbedingungen (30% Feldkapazität) ausgesetzt und physiologische Parameter (Gaswechselmessungen), Befallswerte (AUDPC, Stauchung) und agronomische Parameter (Phänologisches Entwicklungsstadium, Anzahl Seitentriebe, Ertragsparameter) erfasst und im Vergleich zu der anfälligen Sorte ‘Falcon’ evaluiert. Weder die Befallsparameter noch die agronomischen Parameter zeigten eine Beeinträchtigung der Resistenz von SEM bei *V. longisporum*-Infektion in Kombination mit Trockenstress an.

References

Agrios, G. N. (2005) Plant Pathology. Elsevier Academic Press, Burlington, USA, fifth edition.

Ahlers, D. (1987) Untersuchungen über den Erreger der krankhaften Abreife an Winterraps. *Gesunde Pflanzen* 39: 375-383.

Aist, J. R. (1976) Papillae and related wound plugs of plant cells. *Annual Review of Phytopathology*, 14: 145-163.

Arbogast, M., Powelson, M. L., Cappaert, M. R. and Watrud, L. S. (1997) Response of potato cultivars to plant available water and *Verticillium dahliae.* In: Tjamos, E. C., Rowe, R. C., Heale, J. B., Fravel, D. R. Advances in *Verticillium*: Research and disease management. *Proceedings of the Seventh International Verticillium Symposium*, APS Press, St. Paul, Minnesota, pp. 180-186.

Atallah, Z. K., Bae, J., Jansky, S. H, Rouse, D. I. and Stevenson, W. R. (2007) Multiplex real-time quantitative PCR to detect and quantify *Verticillium dahliae* colonization in potato lines that differ in response to *Verticillium* wilt. *Phytopathology* 97: 865-872.

Bahnweg, G., Schulze, S., Möller, E. M., Rosenbrock, H., Langebartels, C. and Sandermann, H. (1998) DNA isolation from recalcitrant materials such as tree roots, bark, and forest soil for the detection of fungal pathogens by Polymerase Chain Reaction. *Analytical Biochemistry* 262: 79-82.

Barbara, D. J. and Clewes, E. (2003) Plant pathogenic *Verticillium* species: how many of them are there? *Molecular Plant Patholog*: 297-305.

Bates, L. S., Waldren, R. P. and Teare, I. D. (1973) Rapid determination of free proline for water-stress studies. *Plant and Soil* 39: 205-207.

Beckman, C. H. (1972) The Localization of fusarial infections in the vascular tissue of single-dominant-gene resistant tomatoes. *Phytopathology* 62: 1256-1260.

Beckman, C.H. (1987) The nature of wilt diseases of plants. The American Phytopathological Society, St Paul, MN

Beckman, C. H. (2000) Phenolic-storing cells: keys to programmed cell death and periderm formation in wilt disease resistance and in general defence responses in plants? *Physiological and Molecular Plant Pathology* 57: 101-110.

Beckman, C. H., Mueller, W. C., Tessier, B. J. and Harrison, N. A. (1982) Recognition and callose deposition in response to vascular infection in fusarium wilt-resistant or susceptible tomato plants. *Physiological Plant Pathology* 20: 1-10.

Beckman, C.H., Talboys, P.W. (1981) Anatomy of resistance. In: Fungal wilt diseases of plants. Mace, M.E., Bell, A.A., Beckman, C.H. (eds.) Academic Press, New York, pp. 487-518.

Beckman, C.H., Zaroogian, G.E. (1967) Origin and composition of vascular gel in infected banana roots. *Phytopathology* 57: 11-13.

Bell, A. A. (1981) Biochemical mechanisms of disease resistance. *Annual Review of Plant Physiology* 32: 21-81.

Bell, A. A., Stipanovic R. D., O'Brien D. H. and. Fryxell P. A. (1978) Sesquiterpenoid aldehyde quinones and derivatives in pigment glands of *Gossypium. Phytochemistry* 17: 1297-1305.

Benhamou, N. (1992) Ultrastructural detection of ß-1,3-glucans in tobacco root tissues infected by *Phytophthora parasitica* var. *nicotianae* using a gold-complexed tobacco [beta]-1,3-glucanase. *Physiological and Molecular Plant Pathology* 41: 351-370.

Benhamou, N. (1995a) Ultrastructural and cytochemical aspects of the response of eggplant parenchyma cells in direct contact with Verticillium-infected xylem vessels. *Physiological and Molecular Plant Pathology* 46: 321-338.

Benhamou, N. (1995b) Immunocytochemistry of plant defense mechanisms induced upon microbial attack. *Microscopy Research and Technique* 31: 63-78.

Benhamou, N. and Garand, C. (2001) Cytological analysis of defense-related mechanisms induced in pea root tissues in response to colonization by nonpathogenic *Fusarium oxysporum* Fo47. *Phytopathology* 91: 730-740.

Bernards, M. A. and Ellis B. E. (1991) Phenylalanine ammonia-lyase from tomato cell cultures inoculated with *Verticillium albo-atrum*. *Plant Physiology* 97: 1494-1500.

Bishop, C. D. and Cooper, R. M. (1983a) An ultrastructural study of root invasion in three vascular wilt diseases. *Physiological Plant Pathology* 22: 15-27.

Bishop, C, and Cooper, R. M. (1983b) An ultrastructural study of vascular colonization in three vascular wilt diseases I. Colonization of susceptible cultivars. *Physiological Plant Pathology* 23: 323-343.

Bishop, C. and Cooper, R. M. (1984) Ultrastructure of vascular colonization by fungal wilt pathogens. II. Invasion of resistant cultivars. *Physiologial Plant Pathology* 24: 277-289.

Bowden, L. R., Rouse, D. I. and Sharkey, T. D. (1990) Mechanism of photosynthesis decrease by *Verticillium dahliae* in potato. *Plant Physiology* 94: 1048 -1055.

Bouchereau, A., Clossais-Besnard, N., Bensaoud, A., Leport, L. and Renard, M. (1996) Water stress effects on rapeseed quality. *European Journal of Agronomy* 5: 19-30.

Brandfass, C., and Karlovsky, P. (2008) Upscaled CTAB-based DNA extraction and real-time PCR assays for *Fusarium culmorum* and *F. graminearum* DNA in plant material with reduced sampling error. *International Journal of Molecular Sciences* 9: 2306-2321.

Braun, H. J. (1967) Entwicklung und Bau der Holzstrahlen unter dem Aspekt der Kontakt Isolations-Differenzierung gegenüber dem Hydrosystem. I. Das Prinzip der Kontakt-Isolations-Differenzierung. *Holzforschung* 21: 33–37.

Brouwer, M., Lievens, B., Van Hemelrijck, W., Van den Ackerveken, G., Cammue, B. P. A and Thomma, B. P. H. J. (2003) Quantification of disease progression of several microbial pathogens on *Arabidopsis thaliana* using real-time fluorescence PCR. *FEMS Microbiology Letters* 228: 241-248.

Buddenhagen, I. and Kelman A. (1964) Biological and physiological aspects of bacterial wilt caused by *Pseudomonas solanacearum*. *Annual Review of Phytopathology* 2: 203-230.

Campbell C. L. and Madden L. V. (1990) Introduction to Plant Disease Epidemiology. John Wiley and Sons, New York City, USA.

Cardullo, R. A., Agrawal, S., Flores, C., Zamecnik, P. C. and Wolf, D. E. (1988) Detection of nucleic acid hybridization by nonradiative fluorescence resonance energy transfer. *Proceedings of the National Academy of Sciences of the United States of America* 85: 8790-8794.

Champolivier, L. and Merrien, A. (1996) Effects of water stress applied at different growth stages to *Brassica napus* L. var. *oleifera* on yield, yield components and seed quality. *European Journal of Agronomy* 5: 153-160.

Clérivet, A., Déon V., Alami I., Lopez F., Geiger J. and Nicole M. (2000) Tyloses and gels associated with cellulose accumulation in vessels are responses of plane tree seedlings (*Platanus* × *acerifolia*) to the vascular fungus *Ceratocystis fimbriata* f. sp *platani*. *Trees - Structure and Function* 15: 25-31.

Clewes, E., Edwards, S. G. and Barbara, D. J. (2008) Direct molecular evidence supports long-spored microsclerotial isolates of *Verticillium* from crucifers being interspecific hybrids. *Plant Pathology* 57: 1047-1057.

Collins, A., Okoli, C. A. N., Morton, A., Parry, D, Edwards, S. G. and Barbara, D. J. (2003) Isolates of Verticillium dahliae pathogenic to crucifers are of at least three distinct molecular types. *Phytopathology* 93: 364-376.

Consolo V. F., Albani, C. M., Berón, C. M., Salerno, G. L. and Cordo, C. A. (2009) A conventional PCR technique to detect *Septoria tritici* in wheat seeds. *Australasian Plant Pathology* 38: 222–227.

Cook, R. J. and Papendick, R. I. (2011) Influence of water potential of soils and plants on root disease. *Annual Review of Phytopathology* 10: 349-374.

Cooper, R. M., Longman, D., Campbell, A., Henry, M. and Lees, P. E. (1988) Enzymic adaptation of cereal pathogens to the monocotyledonous primary wall. *Physiological and Molecular Plant Pathology* 32: 33-47.

Cooper, R. M., Resende M. L. V., Flood J., Rowan M. G., Beale M. H. and Potter U. (1996) Detection and cellular localization of elemental sulphur in disease-resistant genotypes of *Theobroma cacao*. *Nature* 379: 159-162.

Cooper, R. M. and Williams, J. S. (2004) Elemental sulphur as an induced antifungal substance in plant defence. *Journal of Experimental Botany* 55: 1947-1953.

Cooper, R. M. and Wood, R. K. S. (1974) Scanning electron microscopy of *Verticillium albo-atrum* in xylem vessels of tomato plants. *Physiological Plant Pathology* 4: 443-446.

Cooper, R. M. and Wood, R. K. S. (1980) Cell wall degrading enzymes of vascular wilt fungi. III. Possible involvement of endo-pectin lyase in Verticillium wilt of tomato. *Physiological Plant Pathology* 16: 285-300.

Daayf, F., Nicole M., Boher, B., Pando A. and Geiger, J. P. (1997) Early vascular defense reactions of cotton roots infected with a defoliating mutant strain of *Verticillium dahliae*. *European Journal of Plant Pathology* 103: 125-136.

Daebeler, F., Amelung, D. and Zeise, K. (1988) *Verticillium*-Welke an Winterraps- Auftreten und Bedeutung. *Nachrichtenbl. Pflanzenschutz DDR* 42: 71-73.

Dan, H., Ali-Khan, S. T. and Robb, J. (2001) Use of Quantitative PCR diagnostics to identify tolerance and resistance to *Verticillium dahliae* in potato. *Plant Disease* 85: 700-705.

Debode, J., Declercq, B. and Höfte, M. (2005) Identification of cauliflower cultivars that differ in susceptibility to *Verticillium longisporum* using different inoculation methods. *Journal of Phytopathology* 153: 257-263.

Debode, J., Hemelrijck W. v., Baeyen, S., Creemers, P., Heungens, K. and Maes M. (2009) Quantitative detection and monitoring of *Colletotrichum acutatum* in strawberry leaves using real-time PCR. *Plant Pathology* 58: 504-514.

Debode, J., Poucke, K. V., França, S. C., Maes, M., Höfte, M. and Heungens, K. (2011) Detection of multiple *Verticillium* species in soil using density flotation and real-time PCR, Plant Disease 95: 1571-1580.

Delauney, A. J. and Verma, D. P. S. (1993) Proline biosynthesis and osmoregulation in plants. *The Plant Journal* 4: 215-223.

Diepenbrock, W. (2000) Yield analysis of winter oilseed rape (*Brassica napus* L.): a review. *Field Crops Research* 67: 35-49.

Dixelius, C., Happstadius, I., Berg, G. (2005) *Verticillium* wilt on Brassica oil crops - a swedish perspective. *Journal of the Swedish Seed Association* 115: 36-48.

Dixon, G. R. and Pegg, G. F. (1969) Hyphal lysis and tylose formation in tomato cultivars infected by *Verticillium albo-atrum*. *Transactions of the British Mycological Society* 53: 109-118.

Dunker, S. (2006) Untersuchungen zur Schadwirkung von *Sclerotinia sclerotiorum* (Lib. de Bary) und *Verticillium longisporum* (comb. nov. Karapapa) in Winterraps (*Brassica napus*) Dissertation, Universität Göttingen.

Dunker, S., Keunecke, H., Steinbach, P. and von Tiedemann, A. (2008) Impact of *Verticillium longisporum* on yield and morphology of winter oilseed rape (*Brassica napus*) in relation to systemic spread in the plant. *Journal of Phytopathol*ogy 156: 698-707.

Eibel, P., Wolf, G., and Koch, E. (2005) Development and evaluation of an enzyme-linked immunosorbent assay (ELISA) for the detection of loose smut of barley (*Ustilago nuda*). *European Journal of Plant Pathology* 111: 113-124.

Elgersma, D. M., MacHardy, W. E. and Beckman, C. H. (1972) Growth and distribution of *Fusarium oxysporum* f. sp. *lycopersici* in near-isogenic lines of tomato resistant or susceptible to wilt. *Phytopathology* 62: 1232-1237.

Eurostat: http://epp.eurostat.ec.europa.eu/portal/page/portal/eurostat/home/; visited: 18 May 2010

Evert R. F. (2006) Esau's Plant Anatomy: Meristems, Cells, and Tissues of the Plant Body: Their Structure, Function, and Development. John Wiley & Sons, Inc., Publication, New Jersey, third edition.

Eynck, C. (2008) Identification of resistance sources and characterization of resistance factors in *Brassica* species to *Verticillium longisporum*. Dissertation, Universität Göttingen.

Eynck C., Koopmann B., Grunewaldt-Stöcker G., Karlovsky P. and Tiedemann, A. v. (2007) Differential interactions of Verticillium longisporum and Verticillium dahliae with *Brassica napus* detected with molecular and histological techniques. *European Journal of Plant Pathology* 118: 259-274.

Eynck, C., Koopmann, B., Karlovsky, P. and Tiedemann, A. v. (2009) Internal resistance in winter oilseed rape inhibits systemic spread of the vascular pathogen *Verticillium longisporum*. *Phytopathology* 99: 802-811.

Eynck, C., Koopmann, B. and Tiedemann, A. v. (2009) Identification of *Brassica* accessions with enhanced resistance to *Verticillium longisporum* under controlled and field conditions. *Journal of Plant Diseases and Protection* 116: 63-72.

Fahleson, J., Hu. Q. and Dixelius, C. (2004) Phylogenetic analysis of *Verticillium* species based on nuclear and mitochondrial sequences. *Archives of Microbiology* 181: 435-442.

Flegler, S., Heckman, J. W. and Klomparens, K. L. (1995) Elektronenmikroskopie-Grundlagen, Methoden, Anwendungen. From the American: Marita Blankenhagel, Spektrum Akademischer Verlag, Heidelberg, first edition.

Floerl, S., Druebert, C., Majcherczyk, A., Karlovsky, P., Kues, U. and Polle, A. (2008) Defence reactions in the apoplastic proteome of oilseed rape (*Brassica napus* var. *napus*) attenuate *Verticillium longisporum* growth but not disease symptoms. *BMC Plant Biology* 8: 129-144.

Friedt, W., Christen, O. (2007) Winterraps: Das Handbuch für Profis. DLG Verlag, first edition.

Fravel, D. R. and Larkin, R. P. (1997) Effect of Sublethal Stresses on Microsclerotia of *Verticillium dahliae*. In: Tjamos, E. C., Rowe, R. C., Heale, J. B., Fravel, D. R. Advances in *Verticillium*: Research and disease management. *Proceedings of the Seventh International Verticillium Symposium*, APS Press, St. Paul, Minnesota, pp. 301-306.

Gayoso, C., de Ilárduya, O. M., Pomar, F. and de Cáceres, F. M. (2007) Assessment of real-time PCR as a method for determining the presence of *Verticillium dahliae* in different *Solanaceae* cultivars. *European Journal of Plant Pathology* 118: 199-209.

Gladders, P., Smith, J. A., Kirkpatrick, L., Clewes, E., Grant, C., Barbara, D., Barnes, A. V. and Lane, C. R. (2011) First record of *verticillium* wilt (*Verticillium longisporum*) in winter oilseed rape in the UK. *New Disease Reports* 23 (8).

Gödecke, R. (2007) Einfluss von Wurzelexudaten bei der wirtsspezifischen Induktion der Mikrosklerotienkeimung von *Verticillium longisporum,* Master thesis Universität Göttingen.

Gold, J., Robb J. (1995) The role of coating response in Craigella tomatoes infected with *Verticillium dahliae*, races 1 and 2. *Physiological and Molecular Plant Pathology* 47: 141-157.

Grimault, V., Gélie B., Lemattre M., Prior P. and Schmit J. (1994) Comparative histology of resistant and susceptible tomato cultivars infected by *Pseudomonas solanacearum*. *Physiological and Molecular Plant Pathology* 44: 105-123.

Günzelmann, H. and Paul, V. H. (1990) Zum Auftreten und zur Bedeutung der Verticillium-Welke an Raps in der Bundesrepublik Deutschland in 1989. *Raps* 8 (1): 23-25.

Heale, J. B., and Karapapa, K. V. (1999) The *Verticillium* threat to Canada's major oilseed crop: Canola. *Canadian Journal of Plant Pathology* 21:1-7.

Häffner, E., Karlovsky, P. and Diederichsen, E. (2010) Genetic and environmental control of the *Verticillium* syndrome in *Arabidopsis thaliana*. *BMC Plant Biology* 10: 235.

Happstadius L., Ljunberg A., Kristiansson B., Dixelius C. (2003) Identification of *Brassica oleracea* germplasm with improved resistance to *Verticillium* wilt. *Plant Breeding* 122: 30–34.

Harrison, N. A. and Beckman, C. H. (1982) Time/space relationships of colonization and host response in wilt-resistant and wilt-susceptible cotton (*Gossypium*) cultivars inoculated with *Verticillium dahliae* and *Fusarium oxysporum* f. sp. *vasinfectum*. *Physiological Plant Pathology* 21: 193-207.

Hartung, W., Sauter, A. and Hose, E. (2002) Abscisic acid in the xylem: where does it come from, where does it go to? *Journal of Experimental Botany* 53: 27 -32.

Heinz, R., Lee, S. W., Saparno, A., Nazar, R. N. and Robb, J. (1998) Cyclical systemic colonization in *Verticillium*-infected tomato. *Physiological and Molecular Plant Pathology* 52: 385-396.

Heseker, N. (2009) Charakterisierung der Aggressivität von *Verticillium longisporum* Isolaten verschiedener Herkunft gegenüber *Brassica napus*, Bachelor thesis Universität Göttingen.

Hornig, H. (1986) Krankhafte Abreife – Spätschäden durch *Phoma lingam* und/oder *Verticillium dahliae*? *Raps* 4(2): 83-85.

Hornig, H. (1987) Weitere Untersuchungen und Erkenntnisse zur Krankhaften Abreife. *Raps* 1: 27-30.

Hu, X., Nazar, R. N., Robb, J. (1993) Quantification of *Verticillium* biomass in wilt disease development. *Physiological and Molecular Plant Pathology* 42: 23–36.

Inderbitzin, P., Davis, R. M., Bostock, R. M. and Subbarao, K. V. (2011) The Ascomycete *Verticillium longisporum* is a hybrid and a plant pathogen with an expanded host range. *PLoS ONE* 6, no. 3.

Ishiguro, T., Saitoh, J., Yawata, H., Yamagishi, H., Iwasaki, S. and Mitoma, Y. (1995) Homogeneous Quantitative Assay of Hepatitis C Virus RNA by Polymerase Chain Reaction in the Presence of a Fluorescent Intercalater. *Analytical Biochemistry* 229: 207-213.

Janská, A., Zelenková, S., Klíma, M., Vyvadilová, M. and Prášil, I. T (2010) Freezing tolerance and proline content of in vitro selected hydroxyproline resistant winter oilseed rape. *Czech Journal of Genetics and Plant Breeding* 46: 35-40.

Jones, E. B. G. (1994) Fungal adhesion. *Mycological Research* 98: 961-981.

Karapapa, V. K., Bainbridge, B. W. and Heale, J. B. (1997) Morphological and molecular characterization of *Verticillium longisporum* comb. nov., pathogenic to oilseed rape. *Mycological Research* 101: 1281-1294.

Kemmochi, I., Kobayashi, I., Tsuchiya, M., Sakai, H. and Shimizu, M. (2000) Breeding materials for resistance to *Verticillium* wilt in Japanese cabbage (*Brassica oleracea* L. var. *capitata*). *Journal of the Japanese Society for Horticultural Science* 69: 483-491.

Keunecke, H. (2009) Einfluss von Kohlfliegenbefall auf die Infektion und Schadwirkung von *Verticillium longisporum* und *Phoma lingam* an Raps. Dissertation Universität Göttingen.

Kpémoua, K., Boher, B., Nicole, M., Calatayud, P. and Geiger, J. P. (1996) Cytochemistry of defense responses in cassava infected by *Xanthomonas campestris* pv. *manihotis*. *Canadian Journal of Microbiology* 42: 1131-1143.

Kroeker G (1970) Vissnesjuka på raps och rybs i Skåne orsakad av *Verticillium*. Svensk Frötidning 19: 10–13.

Laermann, H. T. (1972) Die Wirkung von Terbutryn und Methabenzthiazuron auf Wintergerste in Abhängigkeit von verschiedenen Bodeneigenschaften und Umweltbedingungen, Dissertation Universität Göttingen.

Larsen, R. C., Vandemark, G. J., Hughes, T. J. and Grau, C. R. (2007) Development of a real-time polymerase chain reaction assay for quantifying *Verticillium albo-atrum* DNA in resistant and susceptible alfalfa. *Phytopathology* 97: 1519-1525.

Lancashire, P. D., Bleiholder, H., Boom, T. Van Den, Langelüddeke, P., Stauss, R., Weber, E. and Witzenberger, A. (1991) A uniform decimal code for growth stages of crops and weeds. *Annals of Applied Biology* 119: 561-601.

Lee, S. W., Nazar R. N., Powell D. A. and Robb J. (1992) Reduced PAL gene suppression in *Verticillium*-infected resistant tomatoes. *Plant molecular biology* 18: 345-352.

Li, K.-N., Rouse, D. I., German, T. L. (1994) PCR primers that allow intergeneric differentiation of ascomycetes and their application to *Verticillium* spp. *Applied and Environmental Microbiology* 60: 4324-4331.

Lievens, B., Brouwer, M., Vanachter, A. C. R. C., Cammue, B. P. A. and Thomma, B. P. H. J. (2006) Real-time PCR for detection and quantification of fungal and oomycete tomato pathogens in plant and soil samples. *Plant Science* 171: 155-165.

Lindhout, P. (2002) The perspectives of polygenic resistance in breeding for durable disease resistance. *Euphytica* 124: 217-226.

Ma, Z. and Michailides, T. J. (2007) Approaches for eliminating PCR inhibitors and designing PCR primers for the detection of phytopathogenic fungi. *Crop Protection* 26: 145-161.

Markakis, E., Tjamos, S.E., Antoniou, P. P., Paplomatas E. J. and Tjamos, E. C. (2009) Symptom development, pathogen isolation and Real-Time QPCR quantification as factors for evaluating the resistance of olive cultivars to *Verticillium* pathotypes. *European Journal of Plant Pathology* 124: 603-611.

Masoud Sinaki, M. J., Majidi Heravan, E., Shirani Rad, H., Noormohammadi, G. and Zarei, G.H. (2007) The effects of water deficit during growth stages of canola (*Brassica napus* L.). *American Eurasian Journal of Agricultural Environ*mental Sciences 2: 417-422.

McElrone, A. J. and Forseth, I. N. (2004) Photosynthetic responses of a temperate liana to *Xylella fastidiosa* infection and water stress. *Journal of Phytopathology* 152: 9-20.

Mercado-Blanco, J., Collado-Romero, M., Parrilla-Araujo, S., Rodríguez-Jurado, D. and Jiménez-Díaz, R. M. (2003) Quantitative monitoring of colonization of olive genotypes by *Verticillium dahliae* pathotypes with real-time polymerase chain reaction. *Physiological and Molecular Plant Pathology* 63: 91-105.

Mol L. and Riessen, H. W. v. (1995) Effect of plant roots on the germination of microsclerotia of Verticillium dahlia. *European Journal of Plant Pathology* 101: 673-678.

Moreau, M., Catesson, A., Péresse, M. and Czaninski, Y. (1978) Dynamique comparée des réactions cytologiques du xylème de l'Oeillet en présence de parasites vasculaires. *Journal of Phytopathology* 91: 289-306.

Morrison, T. B., Weis, J. J. and Wittwer, C. T. (1998) Quantification of low-copy transcripts by continuous SYBR Green I monitoring during amplification. *BioTechniques* 24: 954-958, 960, 962.

Naderikharaji, R., Pakniyat, H. and Biabani, A. R. (2008) Effect of drought stress on photosynthetic rate of four rapeseed (*Brassica napus*) cultivars. *Journal of Applied Sciences* 8: 4460-4463.

Nahimana, A., Francioli, P., Blanc, D. S., Bille, J., Wakefield, A. E. and Hauser, P. M. (2000) Determination of the copy number of the nuclear rDNA and beta-tubulin genes of *Pneumocystis carinii* f. sp. *hominis* using PCR multicompetitors. *The Journal of Eukaryotic Microbiology* 47: 368-372.

Nazar, R. N., Hu, X., Schmidt, J., Culham, D. and Robb, J. (1991): Potential use of PCR-amplified ribosomal intergenic sequences in the detection and differentiation of *Verticillium* wilt pathogens. *Physiological and Molecular Plant Pathology* 39: 1-11.

Newcombe, G. and Robb, J. (1988) The function and relative importance of the vascular coating response in highly resistant, moderately resistant and susceptible alfalfa infected by *Verticillium albo-atrum*. *Physiological and Molecular Plant Pathology* 33: 47-58.

Newcombe, G. and Robb, J. (1989) The chronological development of a lipid-to-suberin response at *Verticillium* trapping sites in alfalfa*. Physiological and Molecular Plant Pathology* 34: 55-73.

Nicholson, R. L. and Hammerschmidt, R. (1992) Phenolic compounds and their role in disease resistance. *Annual Review of Phytopathology* 30: 369-389.

Niederleitner, S., Zinkernagel V. and Bartscherer H.-C. (1991) Untersuchungen zur Pathogenese von *Verticillium dahliae* an *Impatiens balsamina* und *Brassica napus*. *Journal of Plant Diseases and Protection* 98: 484-489.

Ohashi, Y., Nakayama, N., Saneoka, H. and Fujita, K. (2006) Effects of drought stress on photosynthetic gas exchange, chlorophyll fluorescence and stem diameter of soybean plants. *Biologia Plantarum* 50: 138-141.

Olbrich, A. (2005) Korrelative licht- und elektronenmikroskopische Untersuchungen zu Tonoplast intrinsischen Proteinen als Merkmale verschiedener Vakuolentypen. Dissertation, Universität Heidelberg.

Olsson, S. and Nordbring-Hertz, B. (1985) Microsclerotial germination of *Verticillium dahliae* as affected by rape rhizosphere. *FEMS Microbiology Letters* 31: 293-299.

Ouellette, G.B., Baayen R.P, Simard M.and Rioux D. (1999) Ultrastructural and cytochemical study of colonization of xylem vessel elements of susceptible and resistant *Dianthus caryophyllus* by *Fusarium oxysporum* f.sp. *dianthi*. *Canadian Journal of Botany* 77: 644-663.

Ouellette, G. B. (2006) Histopathology of Fusarium wilt of staghorn sumac (*Rhus typhina*) caused by *Fusarium oxysporum* f. sp*. callistephi* race 3. III. Host cell and tissue reactions. *Phytoprotection* 87: 17-27.

Palmer, C. S., Saleeba, J. A. and Lyon, B. R. (2005) Phytotoxicity on cotton ex-plants of an 18.5 kDa protein from culture filtrates of *Verticillium dahliae*. *Physiological and Molecular Plant Pathology* 67: 308-318.

Pedras, M. S. C., Nycholat C. M., Montaut S., Xu, Y. and Khan A. Q. (2002) Chemical defenses of crucifers: elicitation and metabolism of phytoalexins and indole-3-acetonitrile in brown mustard and turnip. *Phytochemistry* 59: 611-625.

Pegg, G. F. and Brady, B. L. (2002) *Verticillium* Wilts. Wallingford, UK: CAB Publishing

Pennypacker, B. W., Leath, K. T. and Hill, R. R. (1991) Impact of drought stress on the expression of resistance to *Verticillium albo-atrum* in alfalfa. *Phytopathology* 81: 1014-1024.

Pennypacker, B. W. and Leath, K. T. (1993) Anatomical response of resistant alfalfa infected with *Verticillium albo-atrum*. *Phytopathology* 83: 80-85.

Qing-Ming, Q., Vallad, G. E, Wu, B. M. and Subbarao, K. V. (2006) Phylogenetic analyses of phytopathogenic isolates of *Verticillium* spp. *Phytopathology* 96: 582-592.

Ratzinger, A., Riediger, N., Tiedemann, A. v. and Karlovsky, P. (2009) Salicylic acid and salicylic acid glucoside in xylem sap of *Brassica napus* infected with *Verticillium longisporum*. *Journal of Plant Research* 122: 571-579.

Richards, R. A. and Thurling, N. (1978) Variation between and within Species of Rapeseed (*Brassica campestris* and *B. napus*) in Response to Drought Stress. I Sensitivity at Different Stages of Development. *Australian Journal of Agricultural Research* 29: 469-477.

Riediger, N. (2008) Beteiligung systemischer Signale an der Symptomauslösung bei *Brassica napus* nach Infektion mit *Verticillium longisporum* und *V. dahliae*. Dissertation, Universität Göttingen.

Rioux, D., Nicole, M., Simard, M. and Ouellette, G. B. (1998) Immunocytochemical evidence that secretion of pectin occurs during gel (gum) and tylosis formation in trees. *Phytopathology* 88: 494-505.

Robb, J. (2007) *Verticillium* tolerance: resistance, susceptibility, or mutualism? *Canadian Journal of Botany* 85: 903-910.

Robb, J., Smith A., Brisson, J. D. and Busch, L. (1979a) Ultrastructure of wilt syndrome caused by *Verticillium dahliae*. VI. Interpretive problems in the study of vessel coatings and tyloses. *Canadian Journal of Botany* 57: 795-821.

Robb, J., Brisson, J. D., Busch, L. and Lu, B. C. (1979b) Ultrastructure of wilt syndrome caused by *Verticillium dahliae*. VII. Correlated light and transmission electron microscope identification of vessel coatings and tyloses. *Canadian Journal of Botany* 57: 822-834.

Robb, J., Douglas, A. P. and Street, P. F. S. (1987) Time course of wall-coating secretion in *Verticillium*-infected tomatoes. *Physiological and Molecular Plant Pathology* 31: 217-226.

Robb, J., Powell, D. A. and Street, P. F. S. (1989) Vascular coating: a barrier to colonization by the pathogen in *Verticillium* wilt of tomato. *Canadian Journal of Botany* 67: 600-607.

Robb, J., Moukhamedov, R., Hu, X., Platt, H., Nazar, R. N. (1993) Putative subgroups of *Verticillium albo-atrum* distinguishable by PCR-based assays. *Physiological and Molecular Plant Pathology* 43: 423-426.

Robb, J., Hu, X., Platt, H. and Nazar, R. (1994): PCR-based assays for the detection and quantification of *Verticillium* species in potato. In: Schots, A., Dewey, F. M. and Oliver, R. P. (eds.) Modern assays for plant pathogenic fungi: identification, detection and quantification. CAB International, Wallingford, UK, pp. 83-90.

Rygulla, W. (2008) Verbesserung der Resistenz von Winterraps (*Brassica napus* L.) gegen *Verticillium longisporum*. Dissertation Universität Gießen.

Rygulla, W., Snowdon, R. J., Eynck, C., Tiedemann, A. v., Lühs, W. and Friedt, W. (2007a) Broadening the genetic basis *of Verticillium longisporum* resistance in *Brassica napus* by interspecific hybridisation. *Phytopathology* 97: 1391-1396.

Rygulla, W., Friedt, W., Seyis, F., Lühs, W., Eynck, C., Tiedemann, A. v. and Snowdon, R. J. (2007b) Combination of resistance to *Verticillium longisporum* from zero erucic acid *Brassica oleracea* and oilseed *Brassica rapa* genotypes in resynthesized rapeseed (*Brassica napus*) lines. *Plant Breeding 126*: 596-602.

Rygulla, W., Snowdon, R. J., Friedt, W., Happstadius, I., Cheung, W. Y. and Chen, D. (2008) Identification of quantitative trait loci for resistance against *Verticillium longisporum* in oilseed rape (*Brassica napus*). *The American Phytopathological Society* 98: 215-221

Sangtarash, M. H., Qaderi, M. M., Chinnappa, C. C. and Reid, D. M. (2009) Differential sensitivity of canola (*Brassica napus*) seedlings to ultraviolet-B radiation, water stress and abscisic acid. *Environmental and Experimental Botany* 66: 212-219.

Schena, L., Nigro, F., Ippolito, A. and Gallitelli, D. (2004) Real-time quantitative PCR: a new technology to detect and study phytopathogenic and antagonistic fungi. *European Journal of Plant Pathology* 110: 893-908.

Schnathorst (1981) Life cycle and Epidemiology of Verticillium. In: Mace, M. E., Bell, A. A. and Beckman, C. H. Fungal wilt diseases of plants: 81- 111, Academic Press, London.

Shaner, G. and Finney, R. E. (1977) The Effect of nitrogen fertilization on the expression of slow-mildewing resistance in knox-wheat*. Phytopathology* 67: 1051-1056.

Shao, H., Chu, L., Jaleel, C. A., Manivannan, P., Panneerselvam, R. and Shao, M. (2009) Understanding water deficit stress-induced changes in the basic metabolism of higher plants - biotechnologically and sustainably improving agriculture and the ecoenvironment in arid regions of the globe. *Critical Reviews in Biotechnology* 29: 131-151.

Smirnoff, N. and Cumbes, Q. J. (1989) Hydroxyl radical scavenging activity of compatible solutes. *Phytochemistry* 28: 1057-1060.

Smit, F. and Dubery, I. A. (1997) Cell wall reinforcement in cotton hypocotyls in response to a *Verticillium dahliae* elicitor. *Phytochemistry* 44: 811-815.

Spurr, A. (1969) A low-viscosity epoxy resin embedding medium for electron microscopy. *Journal of Ultrastructure Research* 26: 31-43.

Stadler, M. (2010) Entwicklung eines Verfahrens zum biologischen Abbau des Inokulums strohbürtiger pilzlicher Pathogene im Getreide- und Rapsanbau auf Basis des pilzlichen Antagonisten Microsphaeropsis ochracea. Dissertation Universität Göttingen.

Stark, C. (1961) Das Auftreten der *Verticillium*-Tracheomykosen in Hamburger Gartenbaukulturen. *Gartenbauwissenschaft* 26: 493-528.

Steinbach, P., Kreye, H. and Wolf, G. A. (2005) Bundesweites *Verticillium*-Monitoring: Bewertung von Diagnosesicherheit und Risikofaktoren. *Raps* 1, 20-26.

Steventon, L. A., Fahleson, J., Hu, Q. and Dixelius, C. (2002) Identification of the causal agent of *Verticillium* wilt of winter oilseed rape in Sweden, *V. longisporum*. *Mycological Research* 106: 570-578.

Talboys, P. W. (1958) Association of tylosis and hyperplasia of the xylem with vascular invasion of the hop by *Verticillium albo-atrum*. *Transactions of the British Mycological Society* 41: 249-260.

Talboys, P. W. and Busch, L. V. (1970) Pectic enzymes produced by *Verticillium* species. *Transactions of the British Mycological Society* 55: 367-381

Tebbe, C. C. and Vahjen, W. (1993) Interference of humic acids and DNA extracted directly from soil in detection and transformation of recombinant DNA from bacteria and a yeast. *Applied Environmental Microbiology* 59:2657–2665.

Tjamos, E. C. and Smith, I. M. (1974) The role of phytoalexins in the resistance of tomato to *Verticillium* wilt. *Physiological Plant Pathology* 4: 249-254.

Tjamos, E. C. and Smith, I. M. (1975) The expression of resistance to *Verticillium albo-atrum* in monogenically resistant tomato varieties. *Physiological Plant Pathology* 6: 215-222.

Vance, C. P., Kirk, T. K. and Sherwood, R. T. (1980) Lignification as a mechanism of disease resistance. *Annual Review of Phytopathology* 18: 259-288.

VanderMolen, G. E., Beckman C. H. and Rodehorst, E. (1977) Vascular gelation: a general response phenomenon following infection. *Physiological Plant Pathology* 11: 95-100.

VanderMolen, G. E., Beckman C. H. and Rodehorst, E. (1987) The ultrastructure of tylose formation in resistant banana following inoculation with *Fusarium oxysporum* f.sp. *cubense*. *Physiological and Molecular Plant Pathology* 31: 185-200.

Verbruggen, N. and Hermans, C. (2008) Proline accumulation in plants: a review. *Amino Acids* 35: 753-759.

Veronese, P., Narasimhan, M. L., Stevenson, R. A, Zhu, J., Weller, S. C., Subbarao, K. V., and Bressan, R. A. (2003) Identification of a locus controlling *Verticillium* disease symptom response in *Arabidopsis thaliana*. *The Plant Journal: For Cell and Molecular Biology* 35: 574-587.

Vidhyasekaran P. (2008) Fungal Pathogenesis in plants and crops - Molecular biology and host defense mechanisms. 2nd edition/CRC Press/Taylor and Francis Group.

Wallis, F. M. and Truter, S. J. (1978) Histopathology of tomato plants infected with *Pseudomonas solanacearum*, with emphasis on ultrastructure. *Physiological Plant Pathology* 13: 307-310.

Weber, E. and Bleiholder, H. (1990) Erläuterungen zu den BBCH-Dezimal-Codes für die Entwicklungsstadien von Mais, Raps, Faba-Bohne, Sonnenblume und Erbse - mit Abbildungen. *Gesunde Pflanzen* 42: 308-321.

Wiese, M. V., DeVay, J. E. and Ravencroft, A. V. (1970) Relationship between polygalacturonase activity and cultural characteristics of *Verticillium* isolates pathogenic in cotton. *Phytopathology* 60: 641-646.

Williams, J. S. and Cooper, R. M. (2003) Elemental sulphur is produced by diverse plant families as a component of defence against fungal and bacterial pathogens. *Physiological and Molecular Plant Pathology* 63: 3-16.

Williams, J. S., Hall, S. A, Hawkesford, M. J., Beale, M. H. and Cooper, R. M. (2002) Elemental sulfur and thiol accumulation in tomato and defense against a fungal vascular pathogen. *Plant Physiology* 128: 150-159.

Zeise, K. (1992) Gewächshaustest zur Resistenzprüfung von Winterraps (*Brassica napus* L. var. *oleifera* Metzger) gegen den Erreger der Rapswelke *Verticillium dahliae* Kleb. Nachrichtenblatt Deutscher Pflanzenschutzdienst 44: 125-128.

Zeise, K. and Seidel, D. (1990) Zur Entwicklung und Schadwirkung der *Verticillium*-Welkekrankheit am Winterraps. *Raps* 8: 20-22.

Zeise, K. and Steinbach, P. (2004) Schwarze Rapswurzeln und der Vormarsch der Verticillium-Rapswelke. *Raps* 4: 170-174.

Zeise, K. and Tiedemann, A. v. (2001) Morphological and physiological differentiation among vegetative compatibility groups of *Verticillium dahliae* in relation to *V. longisporum*. *Journal of Phytopathology* 149: 469-475.

Zeise, K. and Tiedemann, A. v., (2002a) Host Specialization among vegetative compatibility groups of *Verticillium dahliae* in relation to *Verticillium longisporum*. *Journal of Phytopathology* 150: 112-119.

Zeise, K. and Tiedemann, A. v. (2002b) Application of RAPD-PCR for virulence type analysis within *Verticillium dahliae* and *Verticillium longisporum*. *Journal of Phytopathology* 150: 557-563.

Zhou, L., Hu, Q., Johansson, A., and Dixelius, C. (2006) *Verticillium longisporum* and *V. dahliae*: infection and disease in *Brassica napus*. *Plant Pathology* 55: 137-144.

Zielinski, D. and Sadowsky, C. (1998) Effect of temperature on infestation and development of *Verticillium dahliae* Kleb. on winter oilseed rape. IOBC Bulletin 21 (5): 41-47.

Appendix

Table A 1 Agronomic practices of the field trial season 2008/09 (Große Breite, Göttingen)

Measurement	Date	
Pre-crop	3 July 2008	Harvest of winter barley
Tillage	13 Aug 2008	Plow with packer
Seedbed preparation	13 Aug 2008	Roller and Rotary Harrow
Incorporation of *Verticillium* inoculum	14 Aug 2008	Rotary Harrow
Sowing	14 Aug 2008	50 seeds/m^2 Seed coating: Cruiser OSR
N-Fertilization N_{min} 1st application (Ammonium sulfate) 2nd application (Urea ammonium nitrate solution) 3rd application (Urea ammonium nitrate solution) N_{total} (incl. N_{min})	 3 March 2009 3 March 2009 17 March 2009 2 April 2009 	 13.1 kg N/ha GS 18: SSA (170 kg ha^{-1}) = 35.7 kg N ha^{-1} GS 28: 80.0 kg N ha^{-1} GS 51: 80.0 kg N ha^{-1} 208.8 kg N ha^{-1}
S-Fertilization	3 March 2009	GS18: SSA (170 kg ha^{-1}) = 40.8 kg S ha^{-1}
Herbicides 1st herbicide 2nd herbicide	15 Aug 2008	 Before germination: 2.5 l ha^{-1} Nimbus GS 16: 0.5 l ha^{-1} Agil S
Growth regulators 1st growth regulator 2nd growth regulator	 16 Sept 2008 6 April 2009	 0.7 l ha^{-1} Caramba 1 l ha^{-1} Folicur
Fungicides 1st fungicide	 28 April 2009	 0.5 kg ha^{-1} Cantus
Insecticides 1st insecticide 2nd insecticide 3rd insecticide	 8 Sept 2008 6 April 2009 16 April 2009	 GS 16: 0.15 l ha^{-1} Sumicidin Alpha GS GS 50: 0.1 l ha^{-1} Fastac Super GS 59: 0.3 l ha^{-1} Biscaya
slug pellets	20 Aug 2008	about 6 kg ha^{-1} Spiess Urania
rodenticides		
Harvest	27 July 2009	

Table A 2 Agronomic practices of the field trial season 2009/10 (Dragoneranger, Göttingen)

Measurement	Date	
Pre-crop	16 July 2009	Harvest of winter barley
Tillage	14 Aug 2009	Plow with packer
Seedbed preparation	18 Aug 2009	Roller and Rotary Harrow
Incorporation of *Verticillium* inoculum	19 Aug 2009	Rotary Harrow
Sowing	20 Aug 2009	50 seeds/m^2 Seed coating: Cruiser OSR
N-Fertilization N_{min} 1st application (Ammonium sulfate) 2nd application (Urea ammonium nitrate solution) 3rd application (Urea ammonium nitrate solution) N_{total} (incl. N_{min})	 8 March 2010 10 March 2010 18 March 2010 9 April 2010	 40.9 kg N/ha GS 18: SSA (170 kg ha^{-1}) = 35.7 kg N ha^{-1} GS 18: 80.0 kg N ha^{-1} GS 50: 80.0 kg N ha^{-1} 236.6 kg N ha^{-1}
S-Fertilization	10 March 2010	GS18: SSA (170 kg ha^{-1}) = 40.8 kg S ha^{-1}
Herbicides 1st herbicide 2nd herbicide	 22 Aug 2009 17 Sept 2009	 Before germination: 3.5 l ha^{-1} Colzor Trio GS 14: 0.5 l ha^{-1} Agil S
Growth regulators 1st growth regulator 2nd growth regulator	 28 Sept 2009 8 April 2010	 GS 16: 0.6 l ha^{-1} Caramba GS 50: 0.8 l ha^{-1} Folicur
Fungicides 1st fungicide	 10 May 2010	 GS 65/67: 0.5 kg ha^{-1} Cantus
Insecticides 1st insecticide 2nd insecticide 3rd insecticide 4th insecticide 5th insecticide	 17 Sept 2009 28 Sept 2009 8 April 2010 20 April 2010 27 April 2010	 GS 14: 0.10 l ha^{-1} Fastac Super GS 16: 0.05 l ha^{-1} Karate Zeon GS 50: 0.20 l ha^{-1} Trebon GS 55/57: 0.30 l ha^{-1} Biscaya GS 59/61: 0.30 l ha^{-1} Biscaya
slug pellets	26 Aug 2009	FCS approx. 6 kg ha^{-1}
Harvest	31 July 2010	

Selected resistance screenings of *B. napus* accessions of the collaborating breeders

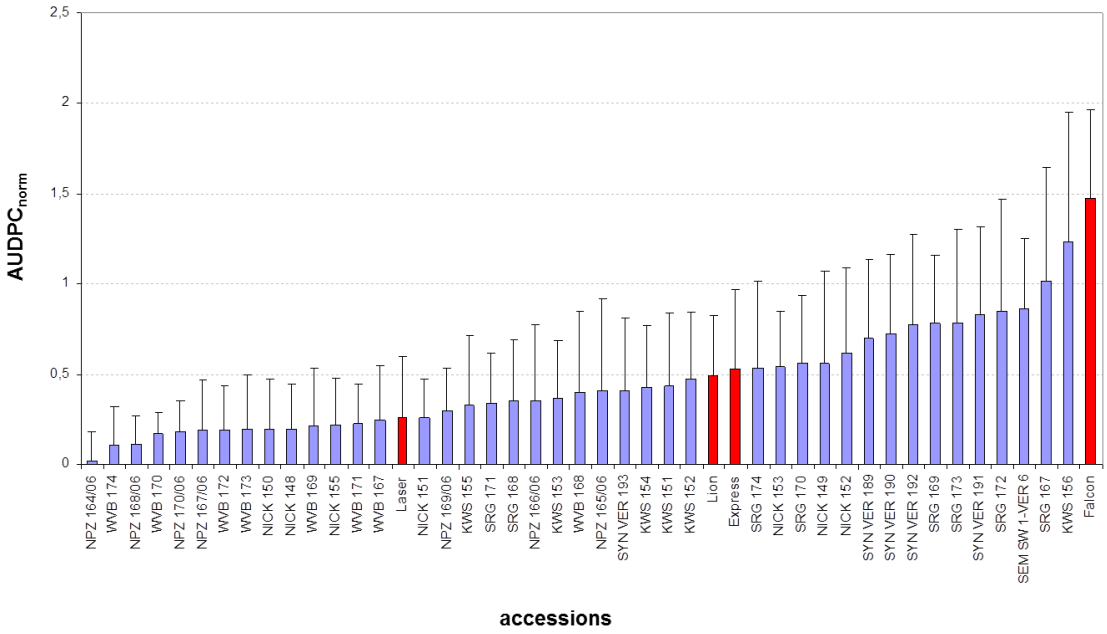

Figure A 1. Means (n = 20) of normalized area under disease progress curve values ($AUDPC_{norm}$) with standard deviations of 42 accessions screened in the period from 25.03. to 1.05.2008. Red bars represent reference cultivars.

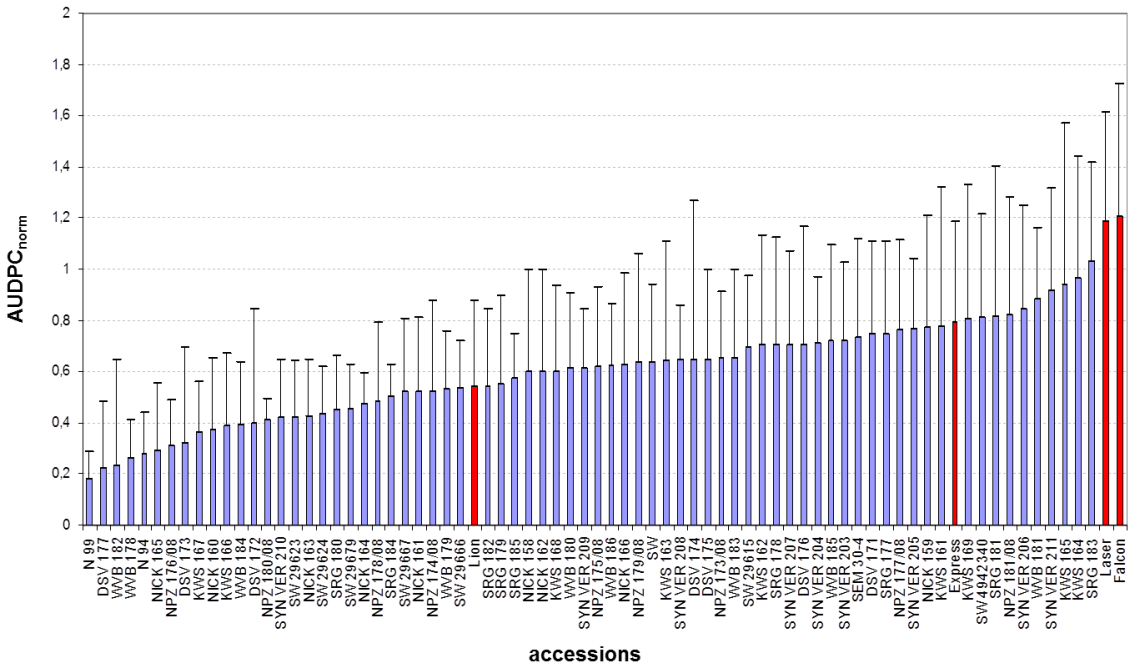

Figure A 2 Means (n = 20) of normalized area under disease progress curve values ($AUDPC_{norm}$) with standard deviations of 72 accessions screened in the period from 20.04.2009 to 29.05.2009. Red bars represent reference cultivars.

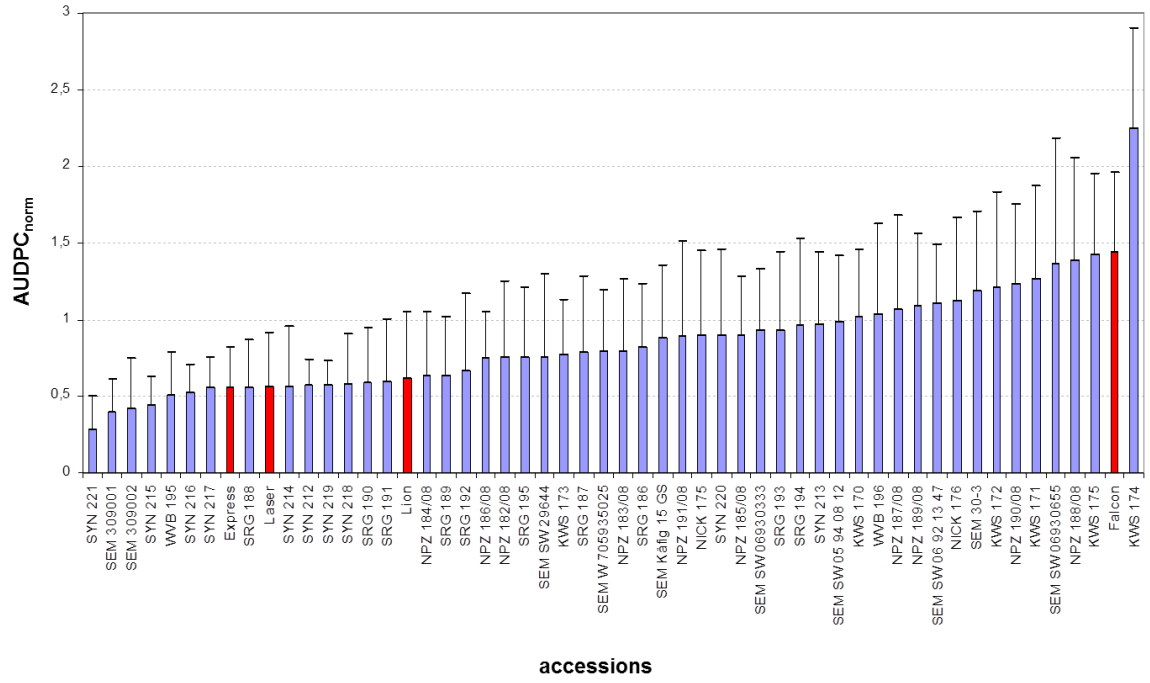

Figure A 3. Means (n = 20) of normalized area under disease progress curve values ($AUDPC_{norm}$) with standard deviations of 49 accessions screened in the period from 26.10.2009 to 4.12.2009. Red bars represent reference cultivars.

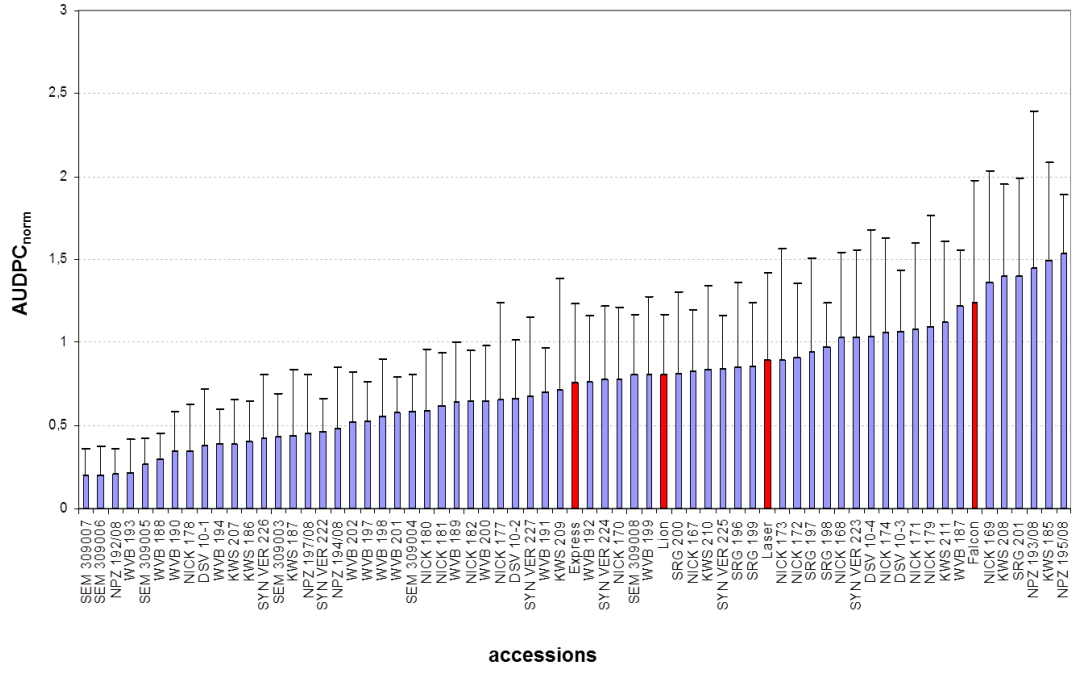

Figure A 4. Means (n = 20) of normalized area under disease progress curve values ($AUDPC_{norm}$) with standard deviations of 63 accessions screened in the period from 7.12.2009 to 14.01.2010. Red bars represent reference cultivars.

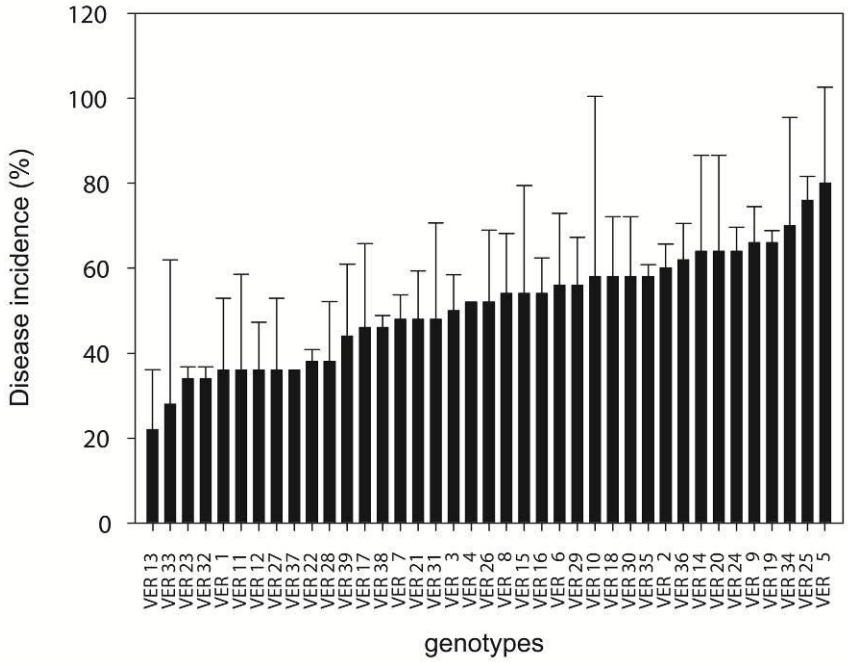

Figure A 5 Disease Incidence (DI) of winter rapeseed stubbles of 39 accessions in the season 2008/09 (Göttingen). Samples were collected shortly after harvest and screened for abundance of microsclerotia. Data are means (± s.d) of two replicates.

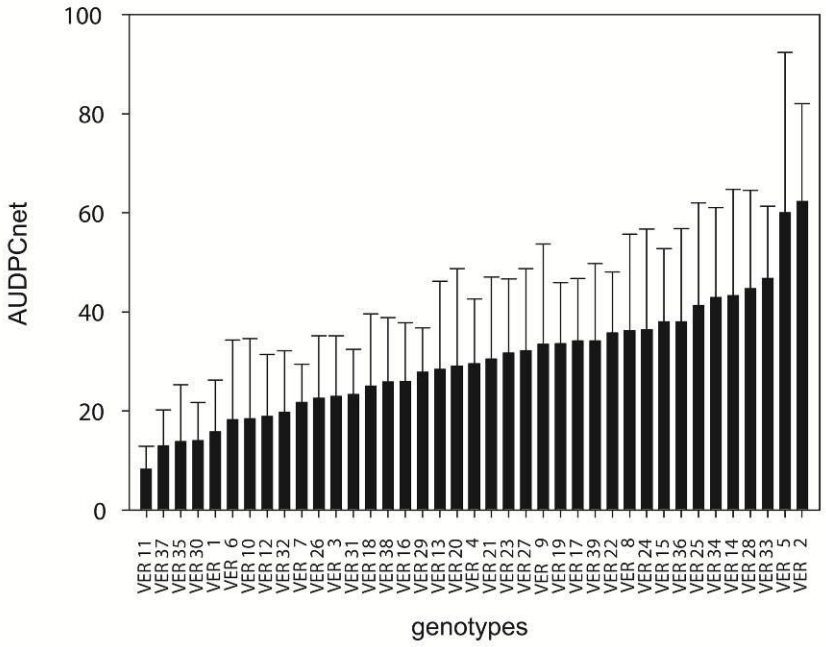

Figure A 6 Mean net AUDPC values and standard deviations of 39 accessions inoculated by *V. longisporum* in the greenhouse and screened over a period of four weeks. Data are means (± s.d) of 20 replicates.

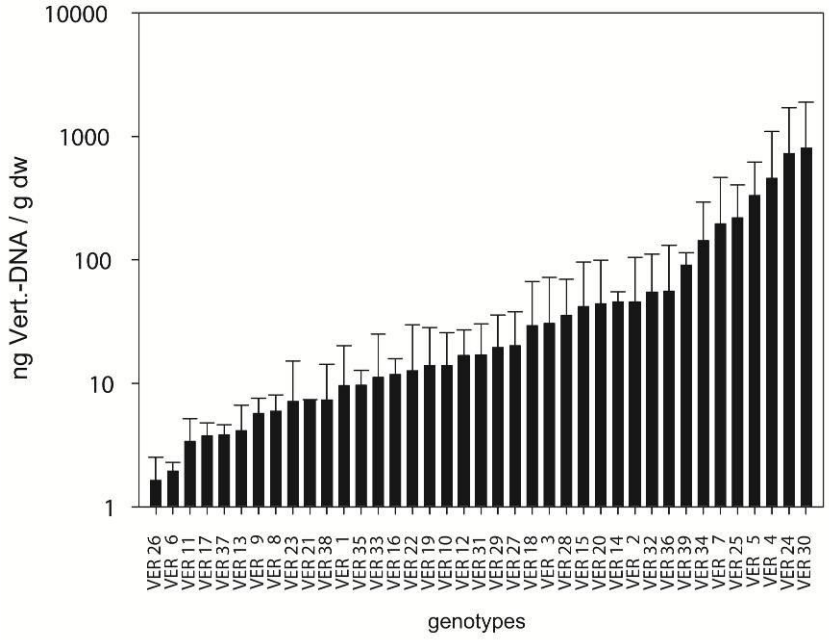

Figure A 7 Content of *Verticillium*-DNA detected by qPCR with ITS primers in stem tissue of 39 accessions at growth stage GS 80 in field season 2008/09 in Göttingen. Data are means (± s.d) of two replicates.

Table A 3 Phenological growth stage assessment by BBCH identification key

Oilseed rape Weber and Bleiholder, 1990; Lancashire et al., 1991

Phenological growth stages and BBCH-identification keys of oilseed rape
(*Brassica napus* L. ssp. *napus*)

Code	Description
Principal growth stage 0: Germination	
00	Dry seed
01	Beginning of seed imbibition
03	Seed imbibition complete
05	Radicle emerged from seed
07	Hypocotyl with cotyledons emerged from seed
08	Hypocotyl with cotyledons growing towards soil surface
09	Emergence: cotyledons emerge through soil surface
Principal growth stage 1: Leaf development[1]	
10	Cotyledons completely unfolded
11	First leaf unfolded
12	2 leaves unfolded
13	3 leaves unfolded
1 .	Stages continuous till . . .
19	9 or more leaves unfolded
Principal growth stage 2: Formation of side shoots	
20	No side shoots
21	Beginning of side shoot development: first side shoot detectable
22	2 side shoots detectable
23	3 side shoots detectable
2 .	Stages continuous till . . .
29	End of side shoot development: 9 or more side shoots detectable
Principal growth stage 3: Stem elongation[2]	
30	Beginning of stem elongation: no internodes ("rosette")
31	1 visibly extended internode
32	2 visibly extended internodes
33	3 visibly extended internodes
3 .	Stages continuous till . . .
39	9 or more visibly extended internodes

[1] Stem elongation may occur earlier than stage stage 19; in this case continue with stage 20
[2] Visibly extended internode n develops between leaf n and leaf n+1

Code	Description
Principal growth stage 5: Inflorescence emergence	
50	Flower buds present, still enclosed by leaves
51	Flower buds visible from above ("green bud")
52	Flower buds free, level with the youngest leaves
53	Flower buds raised above the youngest leaves
55	Individual flower buds (main inflorescence) visible but still closed
57	Individual flower buds (secondary inflorescences) visible but still closed
59	First petals visible, flower buds still closed ("yellow bud")
Principal growth stage 6: Flowering	
60	First flowers open
61	10% of flowers on main raceme open, main raceme elongating
62	20% of flowers on main raceme open
63	30% of flowers on main raceme open
64	40% of flowers on main raceme open
65	Full flowering: 50% flowers on main raceme open, older petals falling
67	Flowering declining: majority of petals fallen
69	End of flowering
Principal growth stage 7: Development of fruit	
71	10% of pods have reached final size
72	20% of pods have reached final size
73	30% of pods have reached final size
74	40% of pods have reached final size
75	50% of pods have reached final size
76	60% of pods have reached final size
77	70% of pods have reached final size
78	80% of pods have reached final size
79	Nearly all pods have reached final size
Principal growth stage 8: Ripening	
80	Beginning of ripening: seed green, filling pod cavity
81	10% of pods ripe, seeds dark and hard
82	20% of pods ripe, seeds dark and hard
83	30% of pods ripe, seeds dark and hard
84	40% of pods ripe, seeds dark and hard
85	50% of pods ripe, seeds dark and hard
86	60% of pods ripe, seeds dark and hard
87	70% of pods ripe, seeds dark and hard
88	80% of pods ripe, seeds dark and hard
89	Fully ripe: nearly all pods ripe, seeds dark and hard
Principal growth stage 9: Senescence	
97	Plant dead and dry
99	Harvested product

Danksagung

Mein besonderer Dank gilt Herrn Prof. Dr. Andreas von Tiedemann für die Bereitstellung des interessanten Themas, die Hilfe und Unterstützung bei der Durchführung dieser Arbeit und die Korrektur der Arbeit.

Herrn Prof. Dr. Petr Karlovsky danke ich für die interessanten Diskussionen, die hilfreichen methodischen Tipps und die Übernahme des Korreferates.

Ich möchte mich bei Dr. Birger Koopmann bedanken für die intensive Hilfe und Betreuung bei molekularbiologischen Fragen und anderen Fragestellungen rund um das Thema Verticillium.

Bei Jutta Schaper bedanke ich mich herzlich für die Hilfe bei der Durchführung der Gewächshaus-Screenings, die Unterstützung im Labor und im Feld und für die angenehme Atmosphäre bei unseren „Ausflügen“ in den Norden.

Ich danke Frau Prof. Dr. Andrea Polle für die Kollaboration bei den TEM-Untersuchungen. Besonders danke ich Frau Dr. Andrea Olbrich für die Hilfestellung bei der Erlernung von Probenvorbereitungen für TEM und für die Hilfe am Elektronenmikroskop.

Bei Dr. Michael Hoppert möchte ich mich für die Messung der Proben am TEM bedanken und bei allen Fragen rund um die Elektronenmikroskopie.

Evelin Vorbeck und Dagmar Tacke danke ich für die immer währende Unterstützung im Labor.

Bei Eugen Hodyl möchte ich mich für die Hilfe bei Gewächshausfragen und die Rundum-Betreuung von den Rapspflanzen bedanken.

Ein großes Dankeschön geht an Hubertus Reintke; deine Hilfe und Unterstützung waren goldwert und ich habe noch viel neues dazu gelernt.

Bei Daniel Lopisso möchte ich mich für die Durchführung des Trockenstress-Experimentes und die Korrektur bedanken.

Bei Heike Rollwage möchte ich mich für die Hilfe bei der real-time PCR Analyse bedanken.

Zahlreiche helfende Hände machten es möglich, dass die Stoppelprobenahme und -bonitur erfolgreich durchgeführt werden konnte. Ich möchte mich besonders bei Claudia Nordmann, Kirsten Steinke, Anna Pilot, Stefan Bucher und Victoria Wende für die Hilfe bedanken.

Mein besonderer Dank gilt Nazanin Zamani-Noor, die immer ein offenes Ohr für alle möglichen Fragen hatten und mir oft bei molekularbiologischen Fragestellungen weiterhelfen konnte. Ich möchte mich auch für die Durchsicht der Arbeit bedanken.

Bei Mark Winter möchte ich mich für die Hilfe bei allen möglichen Fragen bedanken. Und-
Mit deinem Humor hast du den Arbeitsalltag etwas bunter gemacht hat!

Tobias Wulf danke ich für die Unterstützung bei statistischen Fragen jeglicher Art und natürlich für die unterhaltsamen Fahrten zu den Projekttreffen.

Magdalena Siebold danke ich für die anregenden Gespräche rund um das Thema Verticillium und für die nette Atmosphäre in unserem Ecklabor.

Mein Dank geht auch an Isabella Lubig für die Unterstützung bei den molekularbiologischen Arbeiten.

Ich bedanke mich bei Frau Bode für die Hilfe bei allen administrativen Problemen und bei Herrn Gremmes für die Unterstützung bei technischen Fragen.

Ich bedanke mich für die finanzielle Unterstützung bei der Fachagentur Nachwachsender Rohstoffe (FNR) des Bundesministeriums für Ernährung, Landwirtschaft und Verbraucherschutz (BMELV) und der Gemeinschaft zur Förderung der privaten deutschen Pflanzenzüchtung e. V. (GFP).

Ich danke den am Projekt beiteiligten Züchtern Herrn Hauska, Herrn Horn, Frau Kaliff, Herrn Abel, Herrn Gierke, Herrn Stiewe, Herrn Pleines, Herrn Duchscherer, allen weiteren beteiligten Züchtern und Herrn Lütke Entrup für die gute Kooperation und Zusammenarbeit und die interessanten jährlichen GFP-Treffen mit anregenden Diskussionen.

Ein großer Dank gilt unseren Projektpartnern an der Universität Gießen (Institut für Pflanzenzüchtung), namentlich Herrn Prof. Dr. Wolfgang Friedt, Herrn Dr. Obermeier und Herrn Dr. Snowdon für die ergebnisreiche Zusammenarbeit.

Beim Institut für Pflanzenzüchtung der Universität Göttingen (Arbeitsgruppe Prof. Dr. Heiko Becker) möchte ich mich für die Bereitstellung von Pflanzenmaterial bedanken.

Ich danke allen Kollegen in unserer Abteilung für die nette Zusammenarbeit, die entgegengebrachte Unterstützung und die motivierende, oft heitere Arbeitsatmosphäre.

Abschließend danke ich meiner Familie, die mich immer in meinen Vorhaben unterstützt hat.

Mein großer Dank geht an Arjen Jakobi für die Durchsicht der Arbeit.

Dank je wel dat je er altijd voor me bent!

CURRICULUM VITAE

Personal

Name:	Jessica Knüfer
Date and place of birth:	24.08.1981 in Wiesbaden

Education

1988-1992	Primary school Breithard
1992-1994	Grammar school: Marienschule, Limburg
1994-1998	Grammar school: Gerhart-Hauptmann-Gymnasium Wiesbaden
1998-2001	Grammar school: Carl-von-Ossietzky-Schule, Wiesbaden University Entrance Qualification (Abitur) 2001

University Education

10/2001 - 08/2007	Studies of Biology at Johannes Gutenberg University Mainz
01/2004 - 12/2004	ERASMUS Student Exchange (Department of Biology, Århus University, Denmark)
08/2007	Diploma in Biology (title of thesis: *Comparative studies on substrate specificity of native and recombinant xanthophyll deepoxidases*)
10/2007-12/2007	Research internship at the department of Phytopathology, Wageningen (Netherlands)
Since 01/2008	PhD student at the Department of Crop Sciences, Section of General Plant Pathology and Crop Protection, University Göttingen

Eidesstattliche Erklärung

Hiermit erkläre ich, die vorliegende Arbeit selbstständig und ohne unerlaubte Hilfe angefertigt zu haben.

Göttingen, im Mai 2011